2006

A PROTEOMICS APPROACH TOWARDS BIOMARKERS OF PREECLAMPSIA

Aaron T. Booy
Western University

A PROTEOMICS APPROACH TOWARDS BIOMARKERS OF PREECLAMPSIA

(Spine title: A Proteomic Approach to Preeclampsia)

(Thesis format: Monograph)

by

Aaron T. Booy

Graduate Program in Biochemistry

A thesis submitted in partial fulfillment
of the requirements for the degree of
Master of Science

Faculty of Graduate Studies
The University of Western Ontario
London, Ontario, Canada

THE UNIVERSITY OF WESTERN ONTARIO
FACULTY OF GRADUATE STUDIES

CERTIFICATE OF EXAMINATION

Supervisor	Supervisory Committee
Dr. Gilles Lajoie	Dr. Ken Yeung
Co-Supervisor	Dr. Lina Dagnino
Dr. Victor Han	Examiners
	Dr. Susan Meakin
	Dr. Harvey Goldberg

The thesis by

Aaron Timothy Booy

entitled:

A PROTEOMICS APPROACH TOWARDS PREECLAMPTIC BIOMARKERS

is accepted in partial fulfilment of the
requirements for the degree of
Master of Science

Date_____

_____
Chair of the Thesis Examination Board

ABSTRACT

Preeclampsia (PE) is a pregnancy specific disease that affects 5-8% of all pregnancies worldwide, and is one of the leading causes of maternal and neonatal morbidity and mortality. While the cause of PE is still unknown, clinical evidence unequivocally points to placenta as the site of pathophysiology. It is widely accepted that impaired cellular invasion during placental development and a lack of proper development of the decidual spiral arteries account for the development of PE. Despite considerable research, the factor(s) that ultimately cause PE have not been fully characterized. Through the use of 2D SDS-PAGE and LC MS/MS, control and PE placental samples were compared at the proteomic level. This study identifies 12 differentially expressed proteins in PE. Many of these proteins are functionally related and point to several biological pathways or processes involved in the pathology of PE, suggesting a potential starting point for further biomarker discovery.

KEY WORDS

Preeclampsia, Proteomics, Biomarker Discovery, Mass Spectrometry, 2D SDS-PAGE, Chorionic Villi, Protein Validation, Fatty Acid Metabolism, Oxidative Stress.

DEDICATION

For my parents, who taught me to think on my own.

"Education is learning what you didn't even know you didn't know."
- *Daniel J. Boorstin*

ACKNOWLEDGEMENT

Without the continued support and guidance of many people, my experience during my time in graduate school would not have been as colorful as it was.

I would like to thank my supervisors, Drs. Gilles Lajoie, and Victor Han for the opportunity to be part of their labs and for the pleasure of working on the preeclampsia project. The training and experience I received over the years will, without a doubt, serve as a solid foundation in which to further build my career on. Thank you to my committee members, Drs. Ken Yeung and Lina Dagnino for your input and suggestions.

To the members of the Han lab, thank you, especially those who were awake at all hours of the night collecting placentas for me. The biggest thank you goes to the members of the Lajoie lab for making my experience in Grad school as good as it could be. Jennifer, Larry, Paula, Heidi, Amanda, Dustin, Suya, Cunje, and Greg, thanks for the great times and impeccable technical support.

To Sean, I am honored to have spent the last five years working beside you. You are an incredible inspiration, a patient teacher, and a good friend. Thank you.

TABLE OF CONTENTS

LIST OF TABLES

Chapter 2

Chapter 4

Appendix 3

Appendix 4

LIST OF FIGURES

Chapter 4 Continued

Chapter 5

Appendix 1

Appendix 2

Appendix 2 Continued

LIST OF APPENDICES

LIST OF ABBREVIATIONS

°C	Degrees Celsius
µg	Microgram
µL	Microliter
2D SDS-PAGE	Two Dimensional Sodium Dodecyl Polyacrylamide gel Elctrophoresis
Å	Angstrom
ANOVA	Analysis of Variation
BPD	Basal Plate Decidua
BSA	Bovine Serum Albumin
CAPG	Macrophage Capping Protein
CapLC	Capillary Liquid Chromatography
CHAPS	3-[(3-cholamidopropyl)-dimethylammonio]propanesulfonate
cm	Centimeter
CRH	Plasma Corticotropin-Releasing Hormone
CSH1	Placental Growth Hormone
CV	Chorionic Villi
DDA	Data Directed Analysis
dL	Deciliter
DNA	Deoxyribonucleic Acid
DTT	Dithiothreitol
ECH1	Enoyl CoA Hydratase
ECHS1	Δ3,5-Δ 2,4-dienoyl-CoA isomerase
EDTA	Ethylenediaminetetraacetic Acid
EFW	Estimated Fetal Weight
FABP4	Fatty Acid Binding Protein 4
g	Gram
GO	Gene Ontology
h	Hour
hCG	Human Chorionic Gonadotropin
HPLC	High Performance Liquid Chromatography
HRPO	Horse Radish Peroxidase
HSD17B1	Estradiol 17-beta-dehydrogenase
HSP27	Heat Shock Protein β-1
IEF	Isoelectric Focusing
IPG	Immobilized pH Gradient
IUGR	Intra Uterine Growth Restriction
KDa	Kilodalton
LC MS/MS	Liquid Chromatography Mass Spectrometry/Mass Spectrometry
LPC1	Lipocortin
m/z	Mass to Charge Ratio

MALDI ToF	Matrix Assisted Laser Desorption Ionization Time of Flight
mg	Milligram
mm	Millimeter
mM	Millimolar
MS	Mass Spectrometry
MS/MS	Mass Spectrometry/Mass Spectrometry
MSAFP	Maternal Serum Fetoprotein
MudPIT	Multidimensional Protein Identification Technology
MW	Molecular Weight
nG	Nanogram
NL	Non-linear
nm	Nanometer
oxLDL	Oxidized Low Density Lipoprotein
PA2G4	Proliferation-associated Protein 2G4
PE	Preeclampsia
Per6	Peroxiredoxin 6
PGDH1	Prostaglandin Dehydrogenase 1
PGF	Placental Growth Factor
pH	Potential of Hydrogen
pI	Isoelectric Point
PMSF	Phenylmethylsulphonylfluoride
PVDF	Polyvinylidene Fluoride
qToF	Quadrupole Time of Flight
RNA	Ribonucleic Acid
ROM	Rupture of Membranes
ROS	Reactive Oxygen Species
RT-PCR	Reverse Transcription Polymerase Chain Reaction
SCX	Strong Cation Exchange
SD	Standard Deviation
SDS	Sodium Dodecyl Sulfate
sFlt1	Soluble fms-like Tyrosine Kinase
SILAC	Stable Isotope Labeling with Amino Acids in Cell Culture
SOD	Super Oxide Dismutase
TBST	Tris Buffered Saline Tween
TIC	Total Ion Chromatograph
V	Volt
v/v	Volume per Volume
VEGF	Vascular Endothelial Growth Factor
Vhr	Volt Hour
w/v	Weight per Volume

Chapter 1
Introduction

1.1 An Introduction to Preeclampsia

Among the many diseases that can influence the successful outcome of pregnancy, preeclampsia is one of the most detrimental and yet, most poorly understood. This disease, which is specific only to pregnancy, is the leading cause of maternal and perinatal deaths worldwide [1]. It has been shown that this disease affects 3-10% of all pregnancies regardless of socioeconomic status or geographical location [1]. While the incidence of preeclampsia does not vary with race or ethnicity, the severity of the disease shows considerable variation amongst different racial or ethnic groups [2]. Despite considerable research efforts, the factor, or factors, that ultimately cause the onset of preeclampsia have yet to be identified. Over the last several decades, many theories have been put forward that speculate on the causative agent of preeclampsia. However, none of the molecules studied have been directly linked to this disease, either as a direct agent or a predictive biomarker. The abundance of unsubstantiated theories that have been proposed with regards to the causes of preeclampsia has lead to this disease being dubbed "the disease of theories" [3]. To date, there are no reliable diagnostics or biomarkers that can accurately predict the onset of preeclampsia. While the exact cause of this disease is unknown, clinical evidence unequivocally points to the placenta as the site of pathophysiology [4].

Preeclampsia is a multisystemic disease of the maternal endothelium that manifests itself in a variety of ways. Symptoms of this disease affect nearly every maternal organ system with profound pathophysiological effects [5]. Diagnostics used to determine if a pregnancy is preeclamptic or not depend on a broad range of traditionally measurable factors, as well as close observation of physical and neurological symptoms. Currently, the diagnosis of preeclampsia is made based on certain clinical criteria. The presence of hypertension, (a sustained blood pressure elevation of greater than 140/90 mmHg over the past 20 weeks of pregnancy in women who were previously normotensive), and

proteinurea (the excretion of protein in the urine exceeding 300 mg over a 24 hour period) are the two most important criteria [6]. As this disease is now recognized as a maternal endothelial disorder of pregnancy, generalized vasoconstriction, platelet activation, activation of the coagulation cascade and edema are also characteristics observed in women who have developed preeclampsia [7, 8]. In addition to these easily measured and well defined clinical characteristics of preeclampsia, several other symptoms are believed to accompany this disease, such as neurological symptoms that range from auditory and visual disturbances to headaches or complete paralysis [9-11]. As many of these symptoms are manageable on their own, it is the combined affect of these symptoms and generalized endothelial dysfunction that ultimately becomes a problem during the pregnancy. If the pregnancy is left to continue the disease will progress from preeclampsia to eclampsia, which is characterized by maternal seizures, coma and potential mortality [12].

Although very little is known about which factors ultimately cause the onset of preeclampsia, it is known that the development and sustainability of this disease are entirely dependent on the presence of the placenta and not the fetus [4]. In preeclamptic pregnancies that have been ended prematurely by the delivery of the fetus, the failure to remove the entire placenta from the uterus of the preeclamptic mother results in the continued manifestation of this disease. Once the entire placenta has been removed, the symptoms and pathology of this disease are completely reversed within 24-48 hours [13]. Since preeclampsia affects women in the late second and third trimester of pregnancy, the premature delivery of the placenta, and hence premature delivery of the fetus, is clearly not desirable. Additional supporting evidence linking this disease with the presence of a placenta is given by the observance of preeclampsia in women who carry molar pregnancies, a pregnancy by which a sperm fertilizes an empty egg, and a placenta develops in the absence of a fetus [14]. This abnormal and aggressive growth of the placenta puts these women at risk of contracting severe preeclampsia even though a fetus is not present. As in the case of a normal pregnancy affected by preeclampsia, the reversal of the symptoms of

preeclampsia comes only upon the delivery of the entire placenta. The fact that women who carry molar pregnancies are still susceptible to developing this disease supports the theory that the placenta is essential for the development of preeclampsia.

1.2 The Pathophysiology of Preeclampsia

1.2.1 An Introduction to Placental Structure

Although not traditionally thought of as a fetal organ, the placenta is one of the earliest and most critical organs to form early in pregnancy. It is responsible for the exchange of blood gases, nutrients, and metabolic wastes between the fetus and the mother. It is critical that this organ function with high fidelity for the successful continuation of a pregnancy. Figure 1.1 shows the gross location and general structure of a typical full term placenta relative to the developing fetus.

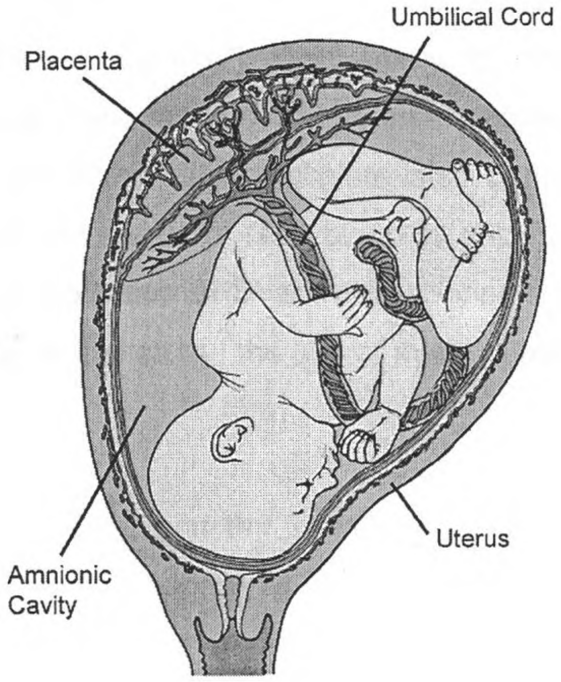

Figure 1.1: Cutaway view of a normal full term uterus showing a typical orientation of the placenta within the amniotic cavity. Image adapted from online resource [15].

The correct functioning of the placenta depends on the cooperative and accurate coordination of both maternal and fetal physiology. After fertilization and implantation, specialized cells called trophoblasts arise from the trophectoderm of the blastocyst and adhere to the uterus. These trophoblasts invade the decidua of the myometrium and begin to form the placenta. During this process, several different lineages of trophoblasts develop, with each type of trophoblast serving a very specific function [16]. To fully appreciate the complexity of the placenta as the link between the mother and the developing fetus, a closer look at the gross morphology of the placenta and chorionic villi (CV) is needed.

The placenta can be thought of as a sandwich comprised of the maternal aspect (made up of the basal plate decidua (BPD)), the fetal aspect (made up of the chorionic plate), and the space between these two membranes where the chorionic villi are located, as shown in Figure 1.2. The BPD serves as the anchoring point for the maternal aspect of the placenta to the uterus and houses the maternal spiral arteries which are known to play a key role in the pathophysiology of preeclampsia [17]. Conversely, the chorionic plate comprises the fetal aspect of the placenta and serves as an anchoring point for the umbilical cord. The membranes of the chorionic plate also contain the fetal veins and arteries that facilitate the transfer of fetal blood to and from the chorionic villi of the placenta. While both the BPD and the chorionic plate make up a large portion of the placenta, in this study, the site of interest was the chorionic villi.

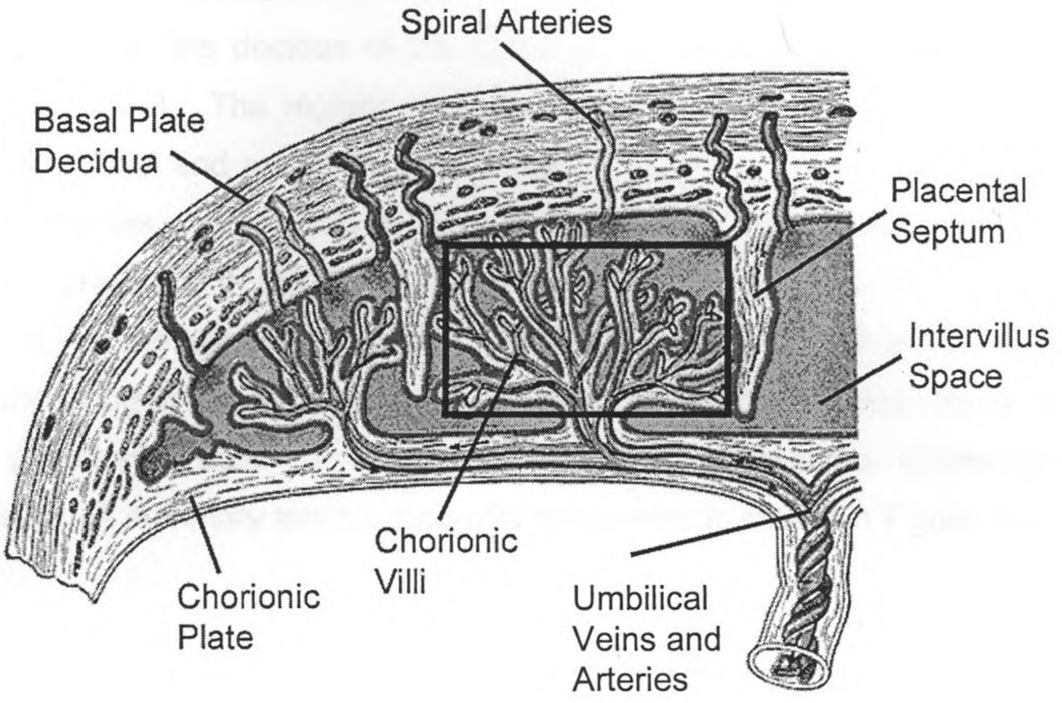

Figure 1.2: The coarse structure of a fully developed human placenta. The maternal aspect and location of the placental attachment point to the uterus is the basal plate decidua. The fetal aspect of the placenta, location of the placental fetal veins and arteries and the umbilical cord attachment point is the chorionic plate. The chorionic villi are situated in the intervillous spaces and are bathed in maternal blood arising from the spiral arteries. Image adapted from online resource. [18]

1.2.2 The Chorionic Villi

Chorionic villi are finger-like projections that form from the fetal membranes of the placenta and allow for the uninhibited transfer of nutrients, blood gases, and metabolic wastes between the mother and the fetus. To understand the cells that make up the walls and anchoring sites of the CV, we must take a closer look at the different lineages of trophoblasts that exist within the placenta. Two major lineages of trophoblasts exist in the placenta, the syncytiotrophoblast and the invasive trophoblast [16]. In addition, there is a sub-population of trophoblastic stem cells, called villous cytotrophoblasts, that reside within the CV [19].

The walls of the CV are made up of a thin layer of syncytiotrophoblasts that facilitates the transfer of blood gases and nutrients between the mother and

fetus. In addition, the syncytiotrophoblast is responsible for the production of many placental hormones and growth factors [20]. The tree-like structure of the CV is attached to the decidua of the placenta through anchoring points called anchoring villi [21]. The regions in between the individual CV are called the intervillous spaces and are continually bathed in maternal blood circulating from the spiral arteries. In addition to syncytiotrophoblast, there is a population of interstitial extravillous trophoblasts, which arise from the tip of the anchoring villi and invade into the decidua [19]. These extravillous trophoblasts play a key role in the remodeling of the maternal spiral arteries. Extravillous trophoblasts adhere to the endothelial cells of the spiral arteries and become endovascular trophoblasts. A summary and location of these events is shown in Figure 1.3.

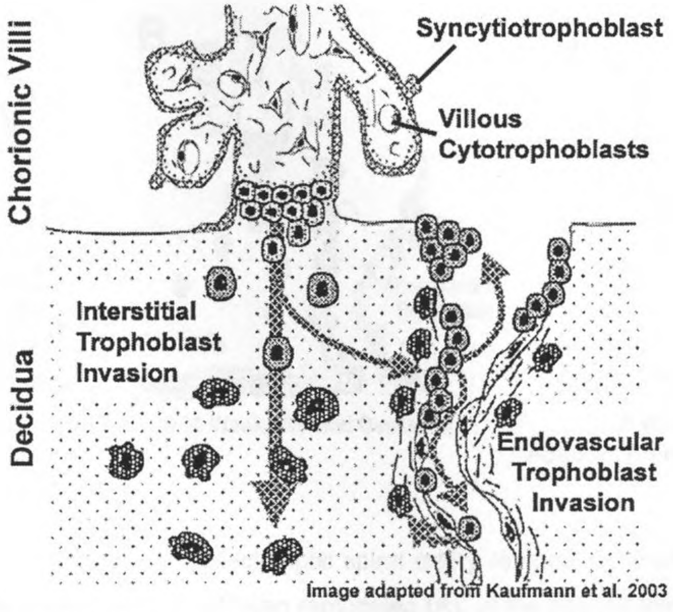

Figure 1.3: Cell types making up the walls of the chorionic villi (syncytiotrophoblast and villous cytotrophoblasts) are shown. Invasive interstitial trophoblast arise from the cell column at the attachment point of the chorionic villi to the decidua. Invasive interstitial trophoblast responsible for decidual remodeling migrate into the decidua. Invasive interstitial trophoblast that remodels the maternal spiral arteries becomes invasive endovascular trophoblast [17].

The remodeling of the spiral arteries is a key factor in the successful development and functioning of a normal placenta. A lack of this remodeling process has been implicated with early pathophysiology of a preeclamptic pregnancy [17, 22].

1.2.3 Spiral Artery Remodeling

The spiral arteries of the uterus are continually formed and shed on a monthly cycle until successful blastocyst implantation, trophoblast invasion, and early development of a placenta prevent this from occurring. Part of the trophoblast invasion process is remodeling of the maternal spiral arteries. Figure 1.4 illustrates the differences between a normal healthy pregnancy and a preeclamptic pregnancy in terms of spiral artery remodeling events.

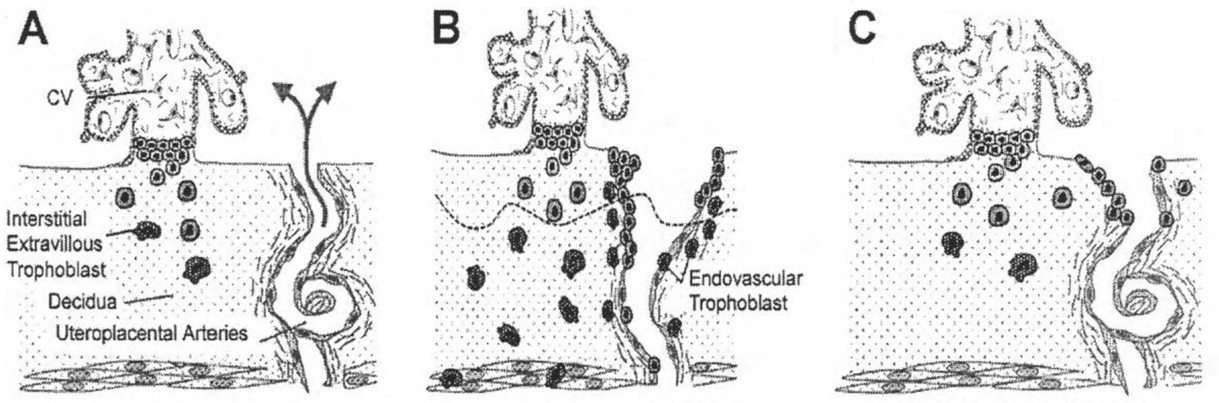

Figure 1.4: A comparison of normal and preeclamptic spiral artery remodeling. Early in the first trimester, the spiral uteroplacental arteries have not yet been remodeled (A). In the second trimester, extravillous and endovascular trophoblast remodel the spiral arteries allowing for uninhibited placental perfusion (B). In the preeclamptic placenta, spiral artery remodeling does not occur to its full extent and a hypoxic condition is created in the placenta (C) [17].

Early on in the development of the placenta, the uteroplacental arteries (spiral arteries) are in a tightly coiled form. The smooth muscle that makes up the walls of the spiral arteries are under maternal control at this point. In order for the placental bed to be perfused to an extent that will allow for the necessary volume of maternal blood to circulate through the intervillous space, it is critical that these spiral arteries are remodeled by the invasive trophoblast. As this invasion occurs, the smooth elastic muscle that lines the spiral arteries is replaced by endovascular trophoblast. This invasion process remodels the tight elastic spiral arteries into high throughput, flaccid vessels that are markedly dilated compared to their pre-invasion state. With this remodeling of the spiral arteries in the decidua, maternal blood is allowed to flow unimpeded between the mother and the intervillous spaces of the placenta. It is critical that successful remodeling occurs at this point for the continuation of a normal pregnancy to proceed. Defects in this remodeling process cause impaired perfusion, or reduced blood flow to the placenta resulting in placental ischemia [17].

The emergence of a hypoxic condition within the placenta presents a detrimental situation for the developing fetus. Several studies have shown that reduced blood flow results in oxidative stress within the placenta [23]. Of critical significance in the context of this study, hypoperfusion of the placenta due to impaired trophoblast invasion with a lack of spiral artery remodeling presents as the pathological root of preeclamptic pregnancies. Hence, this has become a topic of intense research to determine what causes the defective invasion of the spiral arteries by extravillous trophoblast in preeclamptic pregnancies.

Since preeclampsia manifests as a maternal disease with placental origins, the search for a secreted factor (or factors) from the hypoperfused CV into the maternal circulation has been extensively studied [24] [8, 25-28]. As the CV serves as the site of materno-fetal exchange of small molecules, it is hypothesized in this study that this particular location would be the most likely site for the identification of molecules associated with preeclampsia.

1.3 Current Theories of PE; Causation and Detection of Preeclampsia

1.3.1 The Two Part Theory of PE

The development of preeclampsia as a disease occurs because of many physiological changes that occur within the decidua, CV, and ultimately, within the maternal endothelium. Hence, it has been proposed that this disease can be thought of as a case study in two parts: the consistently observed and known changes in placental morphology and structure, and the manifestation of this disease within the mother.

Stage one of preeclampsia is the defective remodeling of the maternal spiral arteries, as described above. As a direct result of this defective trophoblastic invasion and lack of spiral artery remodeling, the placenta is subjected to abnormally low maternal blood flow, giving rise to placental ischemia and subsequently placental hypoxia. Current theories suggest the release of vasoactive or endothelial targeted factor(s) from the hypoperfused placenta into the maternal blood stream [26, 29, 30]. Stage two is a direct result of this hypoperfusion and consists of the widespread systematic maternal endothelial dysfunction seen in the onset of preeclampsia. It is at this stage that the symptoms of preeclampsia manifest themselves in the mother and the disease becomes symptomatic. The effects of preeclampsia on the maternal epithelium are so profound and widespread that there are only a few organ systems that are left unaffected by this disease. In women who have progressed to eclampsia, the very serious and final stage of preeclampsia, all of their organ systems exhibit severe damage consistent with extreme organ hypoperfusion [5, 31].

With the two-stage model of the development of preeclampsia in place, this disease can be viewed as two distinct events: the physical placental defect(s) due to incomplete spiral artery remodeling and the ensuing maternal endothelial dysfunction. While little is known about what causes each of these stages to progress in their own respect, the real question, and subject of intensive research, is what factor or factors link these two stages. If this link can

be found, then potential avenues for early detection and therapeutic treatment of preeclampsia can be developed.

1.3.2 "The Disease of Theories": Current Theories as to What Causes Preeclampsia

It is now widely accepted that the pathological defect at the root of preeclampsia is the lack, or impairment of spiral artery remodeling. However, there are many different theories proposed which claim to offer insight into the specific causes and mechanisms of preeclampsia. These theories focus on such aspects as immunological or genetic insufficiency, infection, or nutritional defects [32, 33]. Although many of these theories were explored in the past, no individual theory has proven to be definitive as to the cause of preeclampsia.

It has been shown that there is a familial or genetic risk factor in the development of preeclampsia. Women whose mother and/or sister(s) have had preeclamptic pregnancies show an increased susceptibility to the development of this disease [34]. It has also been shown that the probability of a pregnancy becoming preeclamptic is greatest in the first pregnancy and then diminishes with each subsequent pregnancy [35]. Interestingly, this risk factor also seems to have a paternal element, in that, when a woman who has had several children with the same partner changes partners, her chances of having a preeclamptic pregnancy return to a level consistent with her first pregnancy [35].

Although many of the theories that attempted to describe the pathological root or cause of preeclampsia have been abandoned in favor of the "insufficient spiral artery remodeling" theory, research on preeclampsia has failed to uncover the exact cause of this remodeling deficiency. While no single molecule or pathway has been proven to be the direct cause of preeclampsia, much of the current research related to this disease has been directed at diagnostic biomarker discovery [28]. While the discovery of a preeclamptic biomarker may not uncover the physiological defect at the root of preeclampsia, it would prove to be an extremely useful clinical diagnostic for the prediction or assessment of this disease.

1.3.3 Current Knowledge of Potential Biomarkers of Preeclampsia

As none of the above theories have given rise to biomarkers that were useful in the detection of preeclampsia, current research is focused on the identification of readily accessible, soluble preeclamptic biomarkers in the maternal blood stream or amniotic fluid. As a result of the low positive predictive values and significant patient to patient variation seen in maternal plasma-based biomarkers, current studies showing limited promise in the diagnosis of preeclampsia have gone largely unnoticed. The following is a summary of some of the potential biomarkers involved in the diagnosis of this disease and the work that has been done to prove their predictive value as a diagnostic. While not each and every molecule that has been studied or assessed as a maternal biomarker in preeclampsia will be addressed, the major studies and molecules that show the most promise are summarized.

The biomarkers that have been studied in the past, or are in the process of being assessed, for their diagnostic capabilities for preeclampsia can be loosely grouped into two categories. The first category is reserved for suspected preeclamptic biomarkers that have been abandoned because they showed no promise as a diagnostic for reasons such as low positive predictive value, low specificity, or low sensitivity. The second group, and much more clinically relevant group, is comprised of suspected preeclamptic biomarkers that either show promise as a diagnostic marker, or are in the process of being assessed to this end.

In order for a biomarker to be of real use it needs to be a reliable diagnostic tool early on in the pregnancy. Proving that a pregnancy is preeclamptic once the symptoms are fully developed in the third trimester is of little use for prophylactic clinical screening. Two possible preeclamptic biomarkers examined in the past were dismissed for this reason. Fibronectin was shown to be increased in the maternal serum very early on in a preeclamptic pregnancy. While it initially showed promise as an early diagnostic biomarker, further studies proved that this difference really only manifested later in the third

trimester and it was summarily dismissed as a potential biomarker [36, 37]. The second biomarker was based on the fact that women who will develop preeclampsia are much more susceptible to vasoactive compounds, like angiotensin II. Vasoactive sensitivity assays, which test for susceptibility to these compounds, presented a formidable clinical and cost-related challenge. In addition, it was shown that this sort of test only became significant in the third trimester after the onset of preeclampsia [38]. Both fibronectin and the vasoactive compound susceptibility testing were dismissed as diagnostic tools, not because of their irrelevance to this disease condition, but for the apparent lack of utility as early biomarkers due to their effectiveness only within the third trimester [38].

Low positive predictive value is also a major hurdle in the assessment of a molecule as a successful biomarker. Both homocysteine and human chorionic gonadotrophin (hCG) were initially identified as reliable preeclamptic biomarkers [39, 40]. Unfortunately, further studies proved that their positive predictive value was much too low to be considered for this purpose [39, 40]. In the case of homocysteine, it was found that multiple factors, such as environmental, genetic, and nutritional fluctuations, influenced the metabolism of this molecule in a manner unrelated to the preeclamptic disease state [41].

Taking a hypothesis-driven approach towards the discovery of biomarkers has also been shown to have some pitfalls. The danger of this approach is that depending on the patient sample size used and the statistics applied in the analysis, there is inherent bias introduced into the studies. If a molecule is hypothetically predetermined to be, or suspected to be, a preeclamptic biomarker, there is a tendency to attempt to prove its reliability as a marker in any way possible. Plasma corticotrophin-releasing hormone (CRH), maternal serum α-fetoprotein (MSAFP) and a host of different signaling molecules, like plasma interleukin-12, TNF-α and interleukin 6, were all proved and then disproved as viable preeclamptic biomarkers that were selected through a hypothesis-driven approach [27, 42-44]. Although these molecules may play a role in the pathology of preeclampsia, it is unlikely that they are the initial cause

of this disease, but rather down-stream responses to an unknown, underlying dysfunction.

To date, there have been dozens of molecules that were studied as possible maternal serum biomarkers. However, most of these biomarkers were abandoned as viable candidates for reasons stated in the preceding text. While there have been some setbacks, several molecules have been identified in maternal serum that hold promise as diagnostic biomarkers, facilitating the early detection of preeclampsia or supporting other more traditional diagnostics. Some of these molecules include placental growth factor (PGF), inhibin-A, activin-A, vascular endothelial growth factor (VEGF), leptin, neurokinin B, P-selectin, transforming growth factor-β1, and serum soluble fms-like tyrosine kinase (sFlt1) [28, 42, 45]. Amongst these molecules, sFlt1 has received the greatest amount of attention. Current research has shown that the infusion of sFlt1 into the bloodstream of rats induces severe endothelial dysfunction with symptoms that mimic preeclampsia [46]. It has also been shown that sFlt1 is significantly up-regulated in the plasma of preeclamptic women [47]. While no one single molecule has been shown to be an effective biomarker for the onset or susceptibility of preeclampsia in a clinical setting, it is much more likely that a panel of biomarkers will ultimately facilitate the early diagnosis of this disease in women who will go on to develop preeclampsia.

The benefits of using a biomarker discovery approach that does not rely on a hypothesis-driven approach is that no inherent bias is given towards any one molecule of interest. Technologies that aim to analyze the broadest possible range of proteins as potential preeclamptic biomarkers not only allow for a global approach for the discovery of proteins related to this disease, but also eliminate the bias associated with working on molecules of known identification. While the causative agent of preeclampsia may be a lipid, steroid or hormone, each of these molecules will cause perturbations on the protein level and thus the CV protein component was examined. Additionally, there is no rule that says the molecule or molecules that play a role in preeclampsia have to be well characterized or even implicated in any previous disease state. Thus, the

analysis of a broad range of proteins allows for the possibility that the unknown causative factor in preeclampsia may, in fact, be a molecule that would never have been suspected had it been targeted from a hypothesis-driven approach.

There are many different proteomic approaches that can be taken in the analysis of a complex biological sample, such as chorionic villi. All of these proteomic approaches have their benefits and shortcomings. The following is a summary of current proteomic tools that are currently being applied in biomarker discovery initiatives for complex biological systems.

1.4 Proteomic Techniques for the Analysis of Complex Samples

Without a doubt, one of the most challenging issues facing the field of proteomics is the separation and prefractionation of complex biological samples. Of particular interest, and substantial complexity, is the separation and identification of proteins that are either up- or down-regulated in diseased tissue samples. While the mass spectrometry-based identification of proteins is well established and highly effective, the ability to resolve proteins present in a sample that show no change in expression from differentially expressed proteins remains a challenge [48]. There are several mainstream techniques that aim to separate proteins in a manner that allows for the quantitation and identification of differentially expressed proteins. Many of these techniques are complementary to one another and each one has its own particular strengths and weaknesses. Frequently, the accurate detection and analysis of differentially expressed proteins takes advantage of several of these proteomic techniques.

Perhaps the most widely used and earliest developed method to look at changes at the proteomic level is analysis by two dimensional sodium dodecyl sulfate polyacrylamide gel electrophoresis (2D SDS-PAGE). This technique consists of a 1^{st} dimensional separation based on proteins' isoelectric points and a 2^{nd} dimensional separation based on proteins' molecular weight. The quantitation of proteins between different samples is achieved by the software-based comparison of gel images, which allows the identification of differentially

regulated proteins. While it is not the most modern tool used to examine differences at the proteome level, 2D SDS-PAGE has several distinct advantages, including its relative speed of operation, its high sample loading capacity per single run, its cost effectiveness, and the fact that differentially regulated proteins, and not the entire proteome, can be carefully selected and identified from individual spots by mass spectrometry. Unfortunately, there are several disadvantages that limit the utility of this technique. Since all of the proteins in a successful 2D SDS-PAGE sample must be soluble, membrane proteins and proteins that are near their solubility limit tend to be a problem in obtaining high resolution, streak-free gel images. In addition to solubility issues at the sample preparation level, the fact that proteins are least soluble at their isoelectric point may cause proteins to precipitate during isoelectric focusing in the first dimension of the 2D SDS-PAGE. As well as solubility becoming an issue in the separation of proteins by this technique, it should be noted that this system is adversely affected by endogenous salts, DNA, and lipids that are present in the sample. By carefully controlling the sample preparation and running conditions, this limitation can be overcome and reproducible high resolution images can be produced across an entire sample set. Although 2D gels allow for high sample loading, samples containing high abundance proteins or extremely complex protein samples may require other techniques, such as immunodepletion, in order to effectively separate these protein samples.

As an alternative to 2D gels, a gel-free HPLC/mass spectrometry based approach can be employed. One such technique is termed multidimensional protein identification technology, or MudPIT. This methodology uses both strong cation exchange (SCX) and reverse phase HPLC columns as the first and second dimension, respectively [49]. As opposed to the 2D SDS-PAGE methodology of whole proteins being separated, analyzed, selectively digested and identified by mass spectrometry, MudPIT utilizes tryptic digests of sample proteins, separates these peptides in two dimensions by HPLC, elutes the separated sample peptides directly into the mass spectrometer and identifies each peptide by MS. Protein quantification between different samples depends

on the highly reproducible separation and elution of peptides from the HPLC column. By cataloguing the retention time, mass to charge ratio and intensity of the peptides observed by the mass spectrometer, an *in silico* 2D map of the peptides present can be developed [50]. Plotting each peptide's retention time versus mass to charge ratio, and indicating its relative abundance by the intensity of the spot on this graph, creates a visual map of all of the proteins present in a sample. Using software to compare differences in spot locations and intensities between these *in silico* 2D maps allows for the detection of differentially regulated proteins between different samples. While this technique allows for a more comprehensive and sensitive analysis of proteins present in a sample, it still has its disadvantages. The high reproducibility in HPLC retention time prior to MS presents a formidable hurdle. Additionally, the software needed to detect differences in this manner is not commercially available and depends on the production of in-house technologies to analyze these data sets. As well, the identification of peptides eluting from the HPLC into the mass spectrometer is limited by the short elution period of the peptide from the HPLC column, the complexity of the peptide digest being analyzed, and the fixed duty cycle of the mass spectrometer which may prevent every peptide that gets eluted from being identified. As a means to separate peptides in a time resolved manner so the mass spectrometer has more time to analyze each peptide, a more comprehensive SCX elution profile can be used and an extended reverse phase gradient can be employed. Even with an extremely long MudPIT run, not all peptides will have time to be analyzed in one experiment. To overcome this limitation, successive runs of the same sample are often analyzed, with ions identified in previous runs excluded from being subjected to analysis again in each subsequent run.

There are many other approaches that can be employed in the quantitative analysis of complex proteomes that take advantage of specific properties or functional groups of the proteins being separated. Different quantification reagents have been employed that target specific functional moieties, such as sulfhydryl, amine, lysine, carboxyl, or sugar residues [51]. In

order to quantitate the levels of proteins in a sample at the peptide level by mass spectrometry, a plethora of different methodologies or techniques has been developed. Peptides from enzymatic digestions can be isotopically labeled at the N- or C-terminus, or at cysteine or lysine residues [51]. The incorporation of a different isotopic tag in each of the protein samples being analyzed, coupled with enzymatic digestion with trypsin and mixing of the samples at the peptide level, allows for the quantification of protein expression levels by mass spectrometry. A more comprehensive review of this technology can be found in Gygi et al. (1999) and Smolka et al. (2001) [52, 53]. Alternatively, isotopically labeled amino acids can be added directly to growth media, a method termed stable isotope labeling with amino acids in cell culture (or SILAC), which allows for the differentiation of control- and experimental-protein components at the mass spectrometry level [54]. While this is not an exhaustive list of quantitation approaches by any means, a more comprehensive review of these techniques can be found in Leitner et al. (2004) [55]. The utility of these approaches are all valid, but each separate technology has its own drawbacks. Frequently the cost of special reagents, use of proprietary software for data analysis, and limited compatibility of certain brands of mass spectrometer make these approaches less desirable than traditional protein quantitation approaches.

Like the wide range of proteomic analysis methodologies mentioned above, there are many different types of mass spectrometers available, each with its own advantages and disadvantages. The simplest and fastest type of mass spectrometer is a matrix assisted laser desorption ionization time of flight, or MALDI ToF. Although this type of mass spectrometer is fast, it lacks a collision cell for the fragmentation of peptides and cannot determine the sequence of each peptide fragment analyzed. Identification of proteins by MALDI ToF depends on peptide mass fingerprinting, which is the comparison of sample peptides against an in silico database, as described by Thiede and Jungblut (2005)[56]. Peptide analyses performed with MALDI ToF instruments dependent on the ionization efficiency of the peptides from the sample matrix, and real time separation (i.e., on-line LC separations) of sample peptides prior to mass analysis are not

available. Another commonly used mass spectrometer is a triple quadrupole mass spectrometer. In contrast to MALDI ToF instruments, triple quadrupole mass spectrometers are amenable to sample separation by LC prior to mass analysis, the selective analysis of single peptide masses, and the sequencing of peptides by MS/MS Fragmentation. Sequencing of peptides by MS/MS fragmentation is facilitated by the quadrupole based separation of a single peptide m/z followed by collisionally-induced dissociation of the peptide in a collision cell. Peptide fragments are generated by very specific cleavages of the peptide backbone in the collision cell. As this fragmentation takes place randomly, at regular intervals along the peptide backbone, a population of peptide fragments are generated that allows for the parent ion sequence determination. The downsides of this technology are that it is of limited sensitivity and mass accuracy compared to the ToF [57]. A more robust and sensitive technology is a hybrid instrument that combines the benefits of both ToF and triple quadrupole mass spectrometers: a quadrupole time of flight, or qTof. These instruments allow for the real time chromatographic separation of sample peptides prior to mass analysis, the isolation of single peptide masses, and the sequencing of the peptides by MS/MS. The LC MS/MS capabilities, high sensitivity, high resolution, and high mass accuracy of the qToF instrument yields quality data conducive to the identification of low-level protein samples such as those examined in this study. As technology advances in the field of mass spectrometry, new instruments are constantly being developed that serve to separate and identify proteins, peptides or small molecules in a diverse manner. A much more complete discussion of these instruments, and the instruments discussed above can be found in Glish and Vachet (2003) [58], and Aebersold and Mann (2003) [48].

As there are many different targeted or selective approaches that can be taken in the analysis of a proteome, the initial assessment of the proteins that are present in a sample should begin with the broadest and simplest possible approach. A logical approach would begin by first looking for coarse changes in higher abundance proteins, then only later hunting for all of the low abundance

proteins that are present in the sample. As proteins that are present in lower concentrations are often molecules involved in cell signaling, protein phosphorylation, or act as hormones or growth modulators, it is often tempting to try an approach that attempts to cover both high and low abundance proteins. Looking at low abundance proteins presents a substantial hurdle due to the fact that proteins present in the sample at a much higher concentration have an unfortunate way of completely eclipsing those proteins that are present at low concentrations. This highly desirable approach that aims to cover both high and low abundance proteins is simply not feasible due to the huge dynamic range of protein concentrations in the cell which can range by up to ten orders of magnitude [59]. As a result of the substantial infrastructure costs involved with isotopic mass spectrometry-based proteomic approaches, and the desire to examine easily separated high abundance proteins as a first pass analysis, 2D gels have been, and still are, the traditional standard for first pass proteomic approaches that seek to find differentially expressed proteins.

1.5 Dimensional Gel Electrophoresis.

1.5.1 What is Two Dimensional Gel Electrophoresis?

Two dimensional gel electrophoresis is one of the most widely used and robust methods for the differential analysis of proteomic samples. Although 2D gel methodology is well established as a first pass proteomic tool, the final preparation and running conditions seldom follow a standard protocol. There are several standard methods that are commonly used as an initial starting point in developing a method for the separation of a specific tissue or cell type. While many factors vary between specific running protocols, only two things remain constant between all 2D gels; a first dimension separation by isoelectric focusing (IEF) and second dimension separation by molecular weight using SDS-PAGE.

As a first step in the preparation of a 2D gel, all proteins in a sample are separated based on their isoelectric points. The isoelectric point (pI) of a protein is the pH at which the net charge of a protein is zero. Proteins are amphoteric

molecules, which, depending on the pH of their environment, may carry a positive, negative or net charge of zero. This net charge is based on the sum of all the positively and negatively charged amino acid side chains, as well as the charges arising from the carboxyl and amino termini at a given pH. A protein that is in a pH environment that is below its pI will be positively charged, while a protein that is in a pH environment that is above its pI will be negatively charged. This type of separation takes advantage of the multiplicity of charges on different proteins and the fact that proteins carrying a net charge will move within an electric field until they reach their pI, at which point the absence of net charge prevents further migration. It follows from this that the isoelectric point of a protein is the point within a pH gradient in which the net charge, and hence electric mobility, of protein is zero. The pI-based separation of proteins by isoelectric focusing is the basis for the first dimensional separation of the 2D electrophoresis procedure.

In order for this type of separation to occur, a stable and reproducible immobilized pH gradient (IPG) needs to be established. Many different pH ranges of IPG strips can be prepared and the pH range of each separation can be tailored to fit the application. Although IPG strips were traditionally manufactured in house, reproducibility and quality control issues have made commercially available IPG strips the industry standard. An IPG strip consists of a plastic backing with a linear (or non-linear) immobilized ampholyte pH gradient within an acrylamide layer bound to the plastic backing. Sample proteins are applied by absorption in a suitable rehydration buffer directly to the dehydrated acrylamide IPG strip. Once rehydration and sample entry into the acrylamide/ampholyte IPG strip has occurred, an electrical current is applied. As time progresses, individual proteins within the electric field migrate to their isoelectric point in the IPG strip. Figure 5 illustrates this principle for a simplified theoretical sample consisting of a single protein.

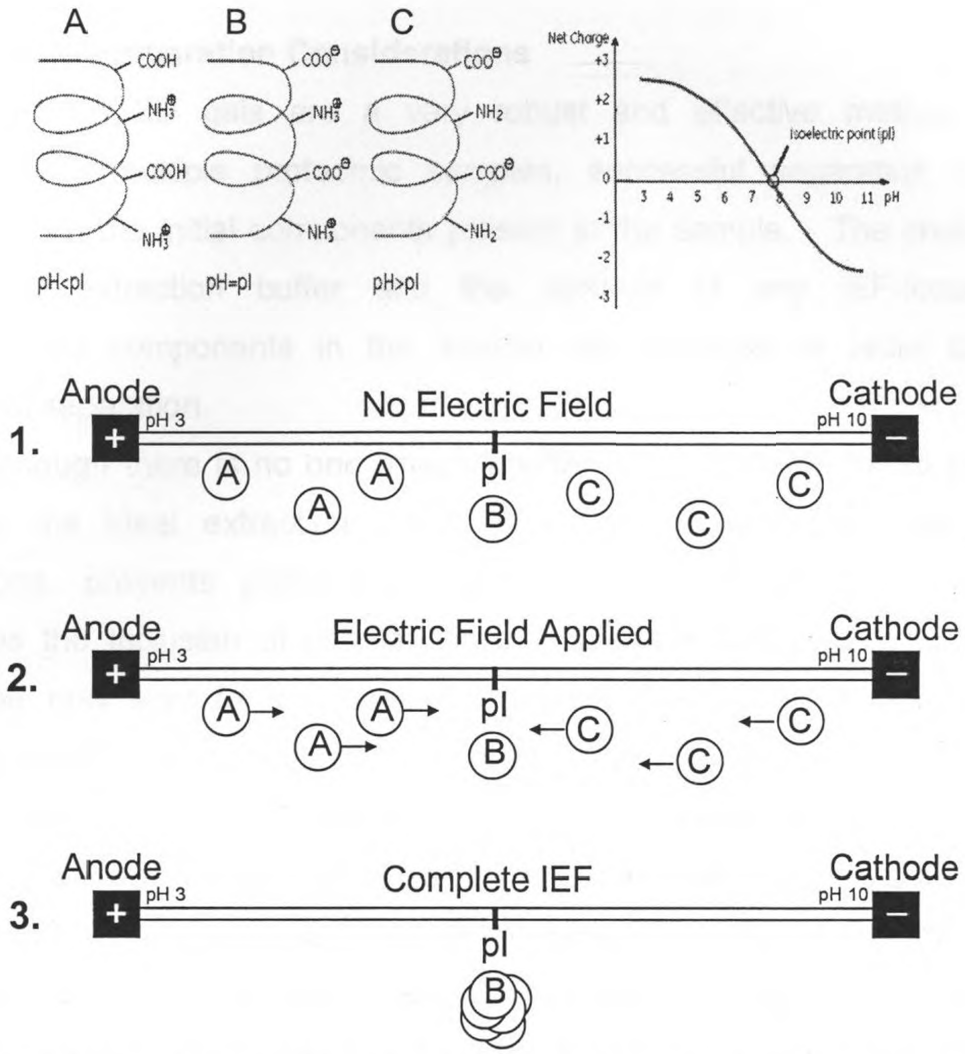

Figure 1.5: The isoelectric focusing of a single protein within the IEF strip. Three charge species of this protein are shown: A) the protein in a pH environment below its pI where the net charge of the protein is positive, B) the protein at its isoelectric point with a net charge of zero, and C) the protein in a pH environment above its pI where the net charge of the protein is negative. The IEF progress of this protein is shown under three conditions. 1) The rehydrated IEF strip under no electric field showing all three species of the protein. 2) The IEF strip under an electric field showing the net movement of positively charged species moving towards the cathode, negatively charged species moving toward the anode, and molecules with a net charge of zero at the isoelectric point of this protein staying stationary. 3) Complete IEF with all of the molecules at the isoelectric point.

Once the proteins in the sample have been separated by their isoelectric points, the IPG strip is loaded on a large format SDS-PAGE gel and the second dimension of the 2D electrophoresis protocol is run. This dimension runs perpendicular to the direction of IEF separation within the IPG strip and separates the isoelectrically focused proteins with respect to their molecular weight. A more elaborate reference covering each aspect of the 2D SDS-PAGE methodologies can be found in Görg et al. (2000) [60].

1.5.2 Sample Preparation Considerations

Although 2D gels are a very robust and effective method for the separation of multiple proteomic samples, successful separation is highly dependent on the initial components present in the sample. The choice of an appropriate extraction buffer and the removal of any IEF-incompatible contaminating components in the sample are essential in order to obtain successful separation.

Although there is no one "magic" buffer that is suitable for all proteomic samples, the ideal extraction buffer is one that disrupts all non-covalent interactions, prevents proteolytic digestion of the extracted proteins, and minimizes the inclusion of substances that interfere with isoelectric focusing. Often the only way to determine the correct concentrations of detergents, reducing agents, chaotropes and ampholytes used in an extraction is through repeated trial and error. In general, a good initial recipe for a cell lysis/protein extraction buffer should contain 1-2% CHAPS or another non-ionic or zwitterionic detergent, 1% dithiothreitol (DTT), sufficient protease inhibitors, 2M thiourea, 7M urea, and 0.5% carrier ampholytes. Perhaps the greatest hurdle in the successful separation of proteins by 2D gel is the removal of contaminants that adversely affect the IEF.

As proteins are separated in an electric field based on their pI in the IPG strip, contaminating components in the sample that are charged will greatly affect the resolution of the IEF step. The main interfering components that present a problem in 2D gel electrophoresis are salts, nucleic acids, lipids, and polysaccharides [61]. With respect to the overall quality of the IEF, salts pose the biggest problem and should be kept to an absolute minimum. Migration of the proteins to their isoelectric points depends on the electric current acting on them. Charged species, such as interfering salts, serve to increase the electrical current across the IPG strip and impede the focusing of proteins in the sample. Additionally, the inclusion of nucleic acids in the sample can cause staining artifacts in the high molecular weight region of the gel. By treating the IEF

sample with nucleases to degrade nucleic acids and reduce the viscosity of the cell lysate and by removing or limiting salts in the sample, successful isoelectric focusing is facilitated. Endogenous proteases are also a problem when preparing high resolution 2D gels. While proteases do not adversely affect the running of the IEF step, they will create multiple spots in the second dimension through the degradation of individual proteins. This creates a level of complexity that makes relative quantitation impossible. In order to compare multiple gels accurately from a variety of samples, endogenous proteases must be effectively inhibited. Once again, the optimal concentrations of protease inhibitors needed to effectively prevent proteolysis of the sample are usually determined by trial and error. After running the SDS-PAGE second dimension and high resolution 2D gels are obtained, a suitable protein visualization procedure must be selected.

1.5.3 Protein Staining

There are four main categories of stains traditionally used to visualize proteins after a one, or two dimensional gel-based separation. These categories are: (1) coomassie blue-based stains, (2) silver stains, (3) zinc or copper stains, and (4) fluorescent stains. Coomassie blue-based stains are visible, cheap, fast and sensitive, but they lack selectivity and stain many other biomolecules (e.g., nucleic acids) other than proteins in the gel [62]. Silver stains are traditionally the most sensitive of protein stains; however, like coomassie blue stains, they lack selectivity. A further drawback of the silver stain is their lack of compatibility with down-stream analysis by mass spectrometry. Fortunately, slight modifications of the silver staining protocol that are mass spectrometry-friendly can be prepared [63]. Zinc- or copper-based protein stains are ideal for proteomics-based applications because they stain the background of the gel and leave the proteins in the gel unstained [64]. These "negative" stains are fast, specific, cost effective, and allow for unimpeded down-stream analysis due to the lack of stain bound to the proteins of interest. However, these stains are seldom used due to the thin nature of 2D gels, which do not allow for adequate background staining,

thus providing insufficient contrast for protein identification. Fluorescent stains encompass the benefits of silver stain in sensitivity, the selectivity of zinc or copper stains in specificity for proteins, and have a very large dynamic range, which makes them very effective when coupled to densiometric analysis techniques [65, 66]. The downsides to fluorescent stains are that they are costly, and gels are not easily visualized without the use of expensive imaging equipment. In this study, a fluorescent stain was used to visualize the separated proteins due to its sensitive and selective staining, and the dynamic range benefits of the stain.

1.6. Summary

A review of the current literature revealed that no specific proteins have been reliably identified or significantly implicated in the causation or onset of preeclampsia. Hence, an approach that employed 2D gel electrophoresis as a broad first pass examination was used in this study. This methodology allows for the separation and quantitation of the high abundance component of the chorionic villous proteome in a broad, fast, and effective manner in order to examine proteomic differences between the preeclamptic and control placental samples. As previously stated, the purpose of this approach is not to examine proteins at the lowest possible level of abundance, but to identify high abundance differentially regulated proteins during the first pass analysis of whole unfractionated CV. Moreover, as the CV are the sites from which preeclamptic placenta will produce disease-related proteins into the maternal circulation, it is hypothesized that the proteomic analysis of control and preeclamptic CV samples will subsequently yield a higher probability of detecting a molecule or molecules that are associated with preeclampsia. Through 2D SDS-PAGE analysis, the proteomic comparison of disease and control chorionic villi samples will provide an understanding of proteins involved in preeclampsia. While identifying proteins potentially responsible for the pathology of this disease, the proteins that are reliably linked to a preeclamptic pregnancy will be explored as potential biomarkers of preeclampsia.

Chapter 2
Experimental Design

2.1 Sample Collection

Between the years 2000 and 2006, a tissue repository of 275 clinical preeclamptic and control placental samples was created at the London St Josephs' Hospital and was based on the following inclusion criteria. For a pregnancy to be included in sampling for the preeclamptic tissue repository, the maternal blood pressure had to exceed a systolic measurement of 160 mm Hg or a diastolic measurement of 110 mm Hg, and show at least one of the secondary "Inclusion Criteria" listed in Table 2.1. Potential preeclamptic placental samples were rejected from this study if any of the "Exclusion Criteria" in Table 2.1 were met. For the purpose of this study, gestationally age-matched placentas that were used as controls were added to the tissue repository if neither inclusion or exclusion criteria were met, provided that the placental age exceeded 22 weeks gestation.

Table 2.1: Criteria used in the selection of placentas from preeclamptic and control pregnancies. For a placenta to be included in the preeclamptic sample group one of the two primary inclusion criteria must have been met as well as at least one of the secondary inclusion criteria. Preeclamptic placentas were not included in the preeclamptic sampling if any of the above exclusion criteria were met. Control placentas were collected if they exceeded 22 weeks gestation and the pregnancy showed neither inclusion nor exclusion preeclamptic criteria.

Inclusion Criteria	Exclusion Criteria
Pregnancies included in the preeclamptic placental sampling **MUST** have met one of the following primary inclusion criteria: • A maternal systolic blood pressure > 160 mmHg **OR** • A maternal diastolic blood pressure > 110 mmHg **AND** any one of the following secondary inclusion criteria:	Placentas were excluded from this study if **ANY** of the following exclusion criteria were met in the pregnancy: • ROM > 18 hours • Evidence of chorioamnionitis • Fetal congenital or genetic anomalies • Polyhydroamnios
Secondary Inclusion Criteria: • Proteinuria: > 3 g in 24 hours OR > 3+ by dipstick. • Platelets: < 100 x 10^9/L • IUGR: EFW < 5 percentile • Oliguria: < 500 ml in 24 hours • Cerebral or visual disturbances • Severe edema • Epigastric pain	

Collection of control or preeclamptic placentas meeting the inclusion criteria were sampled in the following manner. Immediately after delivery, 12-one centimeter by one centimeter cubes were excised from the placenta according to the sampling grid shown in Figure 2.1. The sampling grid used for the determination of the twelve collection sites insured an even and representative sampling of each placenta.

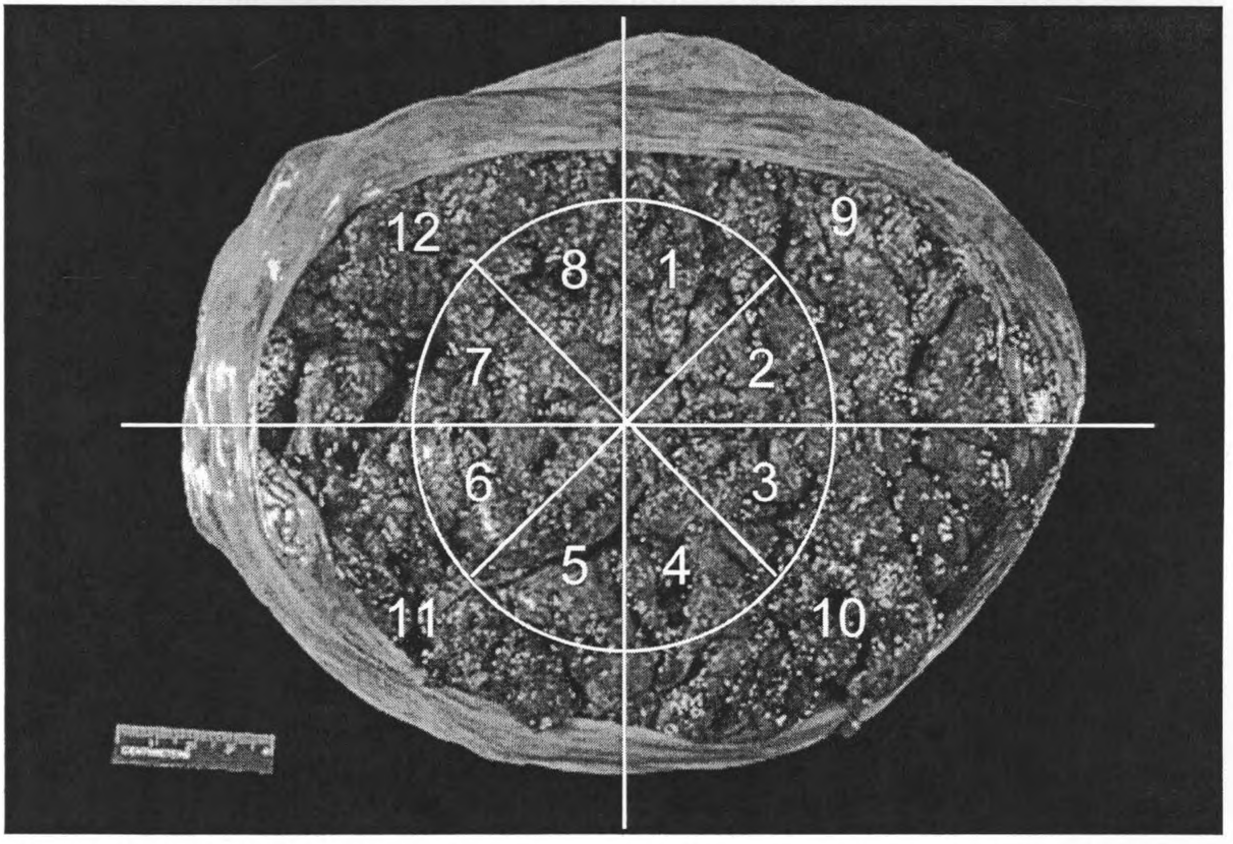

Figure 2.1: A typical full term human placenta presented with the maternal aspect facing up. For sampling of CV in both the preeclamptic and control placentas used in this study the superimposed sampling grid was used. A 1cm cube of tissue was removed from the center of each of the 12 sites shown and pooled as one sample to minimize location-based sampling variation. Image adapted from online resource [67].

Each sample then had the basal plate decidua (BPD) and chorionic plate cut away retaining only the CV. The twelve CV samples from each placenta were immediately snap frozen in liquid nitrogen and pooled in a sample collection bag to comprise one sample. One third of each of the twelve pieces was removed and pooled for proteomic analysis, while the remaining two thirds was retained for RNA analysis by microarray and reverse transcription-polymerase

chain reaction (RT-PCR). Additionally, three samples were removed from each control and preeclamptic placenta for the purpose of histological examination. Preeclamptic and control placentas meeting the above sampling criteria were added to the placental tissue repository.

From the tissue repository, an initial sample set of twenty four placentas was selected for analysis by 2D SDS-PAGE. Since this data set was used for the initial determination of differentially expressed proteins between the control and preeclamptic sample groups, it was termed the "discovery sample set". An additional sample set was selected from the tissue repository in order to validate proteomic differences obtained through the 2D gel analysis of the "discovery sample set". This group of samples was termed the "validation sample set". Table 2.2 summarizes the placental identification, experimental condition, and gestational age bracket for each of the CV samples in both the discovery and validation sample sets.

Table 2.2: A summary of the placentas used in this study. The first sample set, termed the discovery sample set, was subjected to 2D gel analysis with differentially regulated proteins being validated by western blotting. The second data set was used validate proteomic differences found in the discovery sample set and was termed the validation sample set. Placental identification number, condition of the pregnancy, and gestational age bracket are shown in this table.

Discovery Sample set							
Placental Sample number	Placenta ID	Experimental Condition	Gestational Age Bracket	Placental Sample number	Placenta ID	Experimental Condition	Gestational Age Bracket
1	21-99	Control	<28wks	13	39-01	PE	<28wks
2	59-01	Control	<28wks	14	17-99	PE	<28wks
3	188-04	Control	<28wks	15	117-02	PE	<28wks
4	46-01	Control	<28wks	16	174-03	PE	<28wks
5	118-02	Control	<28wks	17	137-03	PE	<28wks
6	87-02	Control	<28wks	18	189-04	PE	<28wks
7	28-00	Control	>28wks	19	3-00	PE	>28wks
8	89-02	Control	>28wks	20	159-03	PE	>28wks
9	23-99	Control	>28wks	21	145-03	PE	>28wks
10	5-99	Control	>28wks	22	141-03	PE	>28wks
11	151-03	Control	>28wks	23	58-01	PE	>28wks
12	34-01	Control	>28wks	24	103-02	PE	>28wks
Validation Sample set							
Placental Sample number	Placenta ID	Experimental Condition	Gestational Age Bracket	Placental Sample number	Placenta ID	Experimental Condition	Gestational Age Bracket
25	203-04	Control	<28wks	44	236-04	PE	<28wks
26	101-02A	Control	<28wks	45	135-03	PE	<28wks
27	206-04	Control	<28wks	46	202-04	PE	<28wks
28	250-05	Control	<28wks	47	254-05	PE	<28wks
29	149-03	Control	<28wks	48	241-05	PE	<28wks
30	219-04	Control	<28wks	49	39-01	PE	<28wks
31	19-98	Control	<28wks	50	90-02	PE	<28wks
32	238-04	Control	<28wks	51	17-96	PE	<28wks
33	229-04	Control	<28wks	52	82-01	PE	<28wks
34	260-03	Control	>28wks	53	225-05	PE	<28wks
35	232-04A	Control	>28wks	54	57-01	PE	>28wks
36	278-06	Control	>28wks	55	16-00	PE	>28wks
37	199-04	Control	>28wks	56	83-01	PE	>28wks
38	152-03A	Control	>28wks	57	91-02	PE	>28wks
39	213-04	Control	>28wks	58	215-04	PE	>28wks
40	211-04	Control	>28wks	59	49-01	PE	>28wks
41	261-05	Control	>28wks	60	163-03	PE	>28wks
42	73-01	Control	>28wks	61	142-03A	PE	>28wks
43	256-05	Control	>28wks	62	12-00	PE	>28wks
				63	25-99	PE	>28wks

2.2 Patient Demographics

Performing proteomic analysis on complex tissues from variable sources requires special attention to sample selection. In this study, the details of each pregnancy were carefully examined in order to ensure the closest possible gestational age and conditions of pregnancy within each test group. Table 2.3 summarizes the patient demographics for each test group used in this study. Note that the samples from the discovery data set and the validation data set have been merged as single groups for the purpose of patient demographics.

Table 2.3: Total Patient Demographics

Category	**< 28 weeks**		**> 28 weeks**	
	Control (n = 17)	PE (n = 16)	Control (n = 18)	PE (n = 16)
Non-twin Pregnancy (%)	82.35%	100%	83.33%	93.75%
Age (yrs)	24.76 +/- 5.84	28.5 +/- 5.88	27.71 +/- 5.75	26.13 +/- 5.55
First Pregnancy (%)	52.94%	62.5%	61.11%	62.5%
Gestational Age (wks)	26.07 +/- 1.54	25.98 +/- 1.3	33.23 +/- 1.95	33.68 +/- 2.07%
Severe PE (%)	N/A	75%	N/A	87.5%
PE + HELLP (%)	N/A	18.75%	N/A	12.5%
Antenatal Steroids (%)	70.59%	81.25%	55.56%	68.75%
Birth Weight* (g)	921.41 +/- 217.63	680.75 +/- 174.69	2247.4 +/- 568.70	1848.31 +/- 581.33
Placenta Weight** (g)	311.79 +/- 133.55	214.75 +/- 57.93	559.4 +/- 162.98	414.93 +/- 159.47***
Caesarean Section (%)	47.01%	62.5%	50%	68.75%

Value +/- Standard Deviation

* In twins pregnancy, the weight of baby A is chosen to calculate the mean

** The mean placental weight is for non-twin pregnancies only

*** The mean placenta weight of singleton pregnancy n = 14. One placenta weight is unknown.

2.3 Experimental design of the project

The "discovery sample set" was comprised of twenty four samples selected from the placenta tissue repository. These samples were split into two separate groups, the first of which included twelve placenta samples, all under 28 weeks of age. Six of the placenta samples were selected from preeclamptic pregnancies and the other six selected from gestationally age matched controls.

The second group was also comprised of twelve placentas (six PE and 6 controls), but these were from post 28 week deliveries. The cutoff of 28 weeks between the two sample sets was a time point that was set in the clinical environment.

The goal of this study was to examine and compare the proteomes of preeclamptic CV and age matched control CV at both below and above the 28 week cutoff. Hence, the under 28 week and over 28 week samples were analyzed separately. An additional group of placentas were selected for the purpose of validating proteomic differences seen in the 2D gel analysis of the "discovery sample set". The "validation sample set" was also comprised of two groups. The samples in the first group were all under 28 weeks gestation and were made up of 9 control and 10 preeclamptic samples. The second set was comprised of 10 control and 10 preeclamptic samples, all of which were above 28 weeks gestation. Once differentially regulated proteins were identified in the discovery sample set, the expression levels were validated by western blotting with an independent group of control and preeclamptic samples. Figure 2.2 shows the general design of the experimental approach taken in the analysis of the discovery data set. This figure outlines the analysis flow for the under 28 week discovery sample set.

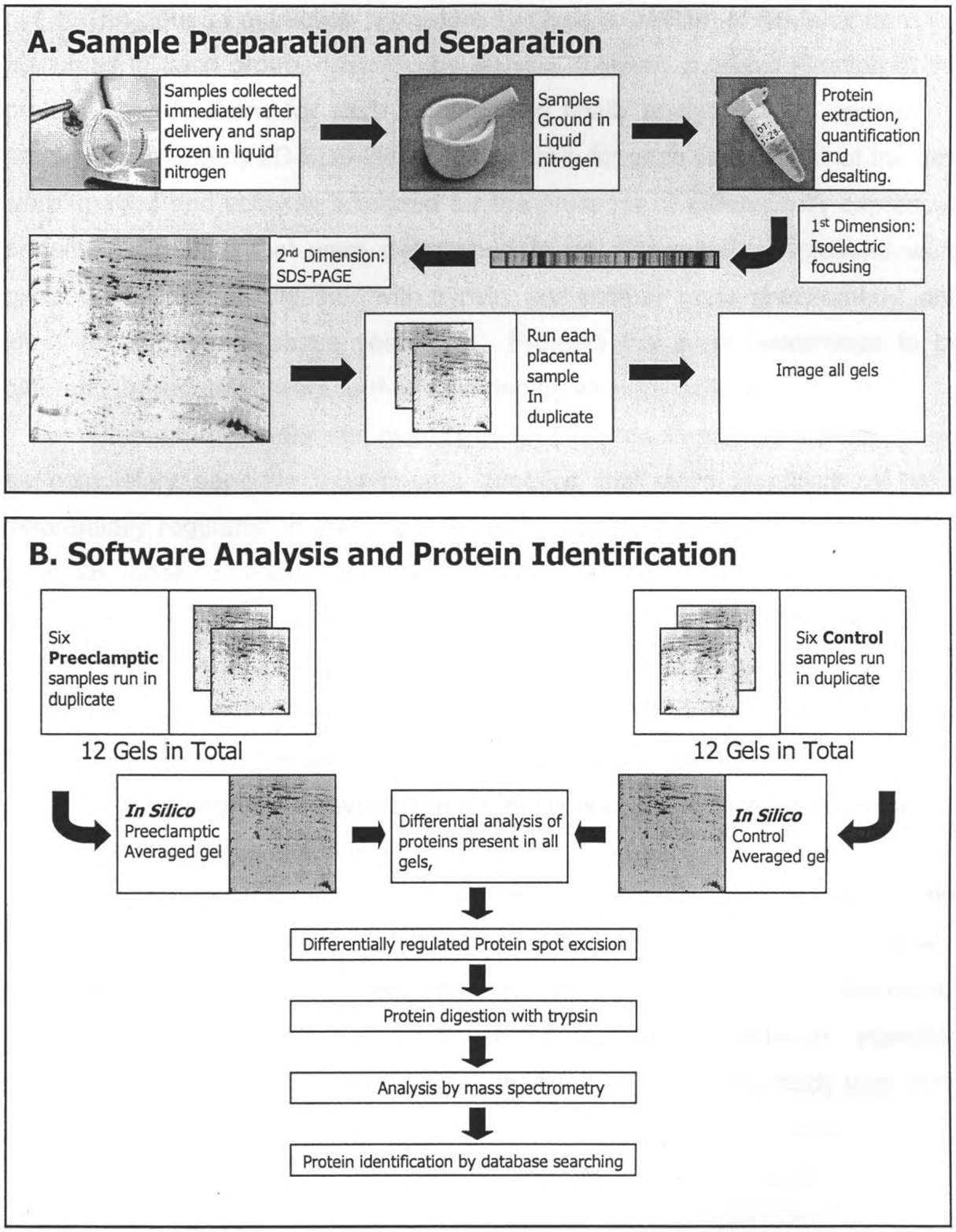

Figure 2.2: The general experimental design for the analysis of preeclamptic and control CV samples in the discovery data set. The experiment can be divided into initial sample preparation and separation (**A**) and software based differential analysis and protein identification (**B**). Details of each of these steps are given below in Section 2.4: Materials and Methods.

The general extraction procedure involved extraction of proteins from the placentas in each group, desalting by dialysis, followed by determination of the protein concentrations for each sample, and finally analysis of an appropriate amount of protein by 2D SDS-PAGE in duplicate for each sample. All of the gels were imaged and software analyzed for the presence of differentially expressed proteins. Proteins that were determined to be differentially expressed were excised from the gel, digested with trypsin, analyzed by mass spectrometry, and identified through database searching. Proteins that were determined to be differentially regulated were further validated by western blotting.

Although the under and over 28 week placenta sample sets were treated as completely separate experiments, proteins that were identified as being differentially regulated in the under 28 week samples were investigated in the over 28 week samples, and vice versa. By comparing the differentially expressed proteins between the two placental age groups, proteins of interest in each group were assessed with respect to their placental age specificity. This was done in order to determine if the increase or decrease in regulation of a specific protein was the same in the under or over 28 week gestation placental group, or if the expression level of the protein was confined to the gestational age of the placental group examined.

As stated above, the control and preeclamptic CV samples in the "discovery sample set" were split three ways. One third of each CV sample was subjected to 2D SDS-PAGE analysis, one third was subjected to microarray analysis, and the remainder was retained for future experimentation. Handling and treatment of all of the CV samples that were used in this study was done according to the following methodologies.

Chapter 3
Material and Methods

3.1 Sample Collection of the Chorionic Villi (CV)

Both preeclamptic and control placenta CV samples were collected in a timely manner immediately after delivery. Freshly delivered intact placenta was placed fetal aspect face down and a standardized sample collection grid was superimposed upon the placenta (Figure 2.1). Individual 1 cm x 1 cm tissue samples were excised from the center of each collection grid matrix, giving rise to 12 samples per placenta. The basal plate decidua and the chorionic plate were surgically removed from the CV and each sample was snap frozen in liquid nitrogen. All twelve samples from each individual placenta were pooled and stored at -80°C for further analysis.

3.2 Protein Extraction from the Chorionic Villi

For each individual placental protein extraction performed, a 100 µg portion of each of the 12 samples was chiseled off of the original 1 cm x 1 cm samples and pooled to give a sample of ~1 g (1.00 g - 1.29 g). The pooled CV samples remained frozen at all times while being ground under liquid nitrogen with a mortar and pestle. Once the CV was ground to a talcum powder-like consistency, a 200 µg aliquot of this homogenate was removed for protein extraction; the remaining tissue was stored at -80°C. To each 200 µg CV sample was added 435 µL of 2X PE extraction buffer [4% CHAPS (Sigma, St Louis, MO), 50mM ammonium bicarbonate (Sigma), 20 mM DTT (Sigma), 20 µL/mL Ettan protease inhibitor mix (GE Healthcare Bio-Sciences Corp. Piscataway, NJ), 5 mM EDTA (Fisher Biotech, NJ)]. Protein extraction was allowed to proceed on ice with vigorous shearing of the genomic DNA with a 30.5 gauge needle. To further extract the protein; an aliquot of 380 mg of urea (Sigma) and 139 mg of thiourea (Sigma) was added to the homogenate for a final concentration of 7 M urea, 2 M thiourea. Samples were subsequently dialyzed in Slide-A-Lyzers (Pierce, Rockford, IL) against 1 mM EDTA for 48 h. Protein concentrations of the

dialyzed samples were determined by Modified Micro-Bradford Assay (Bio-Rad, Hercules, CA). Extracted proteins were stored at -80°C for further analysis.

3.3 Two-Dimensional Polyacrylamide Gel Electrophoresis.

First dimension isoelectric focusing (IEF) was carried out as follows. Sufficient rehydration buffer [6 M urea, 2 M thiourea, 4% CHAPS, 0.4% DTT, 0.5% ampholytes (GE Healthcare), 10 uL/mL Ettan protease inhibitor mix, 10 mM EDTA, 1 mM PMSF(Sigma)] was added to 200 µg of protein to make a total volume of 450 µL. This solution was dispensed evenly across the trough in a reswelling tray and the IPG Immobiline Drystrip pH 3-10 NL (GE Healthcare) was added and covered with mineral oil to prevent evaporation during a 16 h rehydration. The rehydrated strips were focused in an Ettan IPGphor manifold with an Ettan IPGphor II isoelectric focusing apparatus (GE Healthcare). IEF was carried out by using the following voltage gradient: a constant 500 V for 1 h, a 1 h gradient to 1000 V, another 2 h gradient to 5500 V, and finally a constant 5500 V for 8 h, for a total of 99,000 Vh for complete IEF.

For the second dimension, the focused proteins were equilibrated, reduced, and alkylated in SDS equilibration buffer [2% SDS (Sigma), 6 M urea, 30% glycerol (FisherBiotech), 50 mM Tris-Cl pH 8.0 (Bioshop, Burlington, ON)] for 40 min just prior to use. The IPG strips were reduced in 10 mL SDS equilibration buffer with 1% w/v DTT for 20 min at room temperature. The free thiol groups of the proteins' cysteines were then *S*-carboxyamidomethylated by reaction with 2.5% w/v iodoacetamide (Sigma) for an additional 20 min in 10 mL of SDS equilibration buffer. Polyacrylamide slab gels (25.5 cm X 20.5 cm X 0.15 cm, 12% acrylamide) were cast in a PROTEAN® Plus Multi-casting chamber (Bio-Rad, Hercules, CA). The IPG strips bearing the reduced and alkylated proteins were sealed in place with agarose sealing solution (0.5% Agarose, 0.002% w/v bromophenol blue, 0.1% SDS). The gels were loaded, 12 at a time, into a PROTEAN® Plus Dodeca™ electrophoresis cell (Bio-Rad) and were stacked at a constant 100 V for 1h. This voltage was finally adjusted to 250 V for

6-7 h, or until the dye front had migrated to within 0.5 cm from the edge of the gel. In the second dimension, the SDS running buffer (25 mM Tris, 192 mM glycine, 0.1% (w/v) SDS, pH 8.3) was held at a constant 15°C throughout the entire run.

3.4 2D GE Gel Imaging, Image Analysis and Robotic Spot Picking.

Polyacrylamide gels were stained with the fluorescent stain Sypro Ruby (Molecular Probes, Eugene, OR) for 48 h following overnight fixation in a solution of 50% methanol, 7% acetic acid. In order to minimize background staining, destaining prior to gel image acquisition was carried out for 30 min in a solution of 10% methanol, 7% acetic acid, followed by 3 washes in milliQ dd H_2O. The Sypro Ruby stained gels were imaged on a ProXPRESS Proteomic Imaging System (Perkin-Elmer, Boston, MA) using top illumination with a solid black bottom tray and green acrylic sheet for flat field acquisition. The images were acquired at an excitation wavelength of 480 nm and emission wavelength of 620 nm. The scanned gels were analyzed using Phoretix 2D Expressions gel documentation software (Non-Linear Dynamics, Newcastle UK). Differentially regulated spots were selected for based on the following criteria: 1) the protein expression between the experimental and control gels had to exceed +/- 2-fold regulation to be considered differentially regulated; 2) the spot of interest needed to be present in all of the experimental and control gels; and 3) the spots selected must have been statistically significant as determined by an ANOVA (p-value <0.005). Spots meeting these criteria were excised from the gels by means of robotic spot excision into 96 well plates (Ettan spot picker, GE Healthcare).

3.5 Tryptic Digestion of Protein Samples for Mass Spectrometry

Previously excised 2D SDS-PAGE spots of interest were transferred to 1.5 mL microfuge tubes and destained with alternating washes of 50% (v/v) methanol / 5% (v/v) acetic acid and 20% (v/v) acetonitrile / 1M ammonium bicarbonate. The destained gel pieces were then dehydrated in 100%

acetonitrile, dried in a rotary Speed Vac concentrator (Savant, Hicksville, NY), and reduced for 1h by rehydration in 30 µL of 10 mM DTT/100 mM ammonium bicarbonate. The free thiol groups of the cysteines were alkylated after removing the DTT solution by aspiration and adding 30 µL of 100 mM iodoacetamide in 100 mM ammonium bicarbonate and incubating for 1 h. The gel pieces were then dried by Speed Vac concentrator and rehydrated with 30 µL of a solution containing 0.6 µg of sequencing grade modified trypsin (Promega, Madison, WI) in 50 mM ammonium bicarbonate. After 10 min of rehydration on ice, the excess trypsin solution was removed by aspiration and 5 µL of 50 mM ammonium bicarbonate was added. The tryptic digestion was allowed to proceed at 37 °C for 18 h. The tryptic peptides were extracted from the gel pieces by washing with 30 µL of 50 mM ammonium bicarbonate, followed by two 30 µL washes of 10% (v/v) formic acid, and a final 50 µL wash with 100% acetonitrile. The washes were pooled in a 500 µL microfuge tube and the volume reduced to dryness in a rotary Speed Vac concentrator (Savant, Hicksville, NY). Samples were stored at -80°C until analysis.

3.6 Mass Spectrometry

The samples analyzed by MS were brought up in 5% acetonitrile / 1% formic acid prior to sample injection. All MS analyses were performed on a Micromass Q-ToF Ultima Global (Waters, Milford, MA) running in positive ESI mode. Samples were injected in "µl pick up mode" into a nano-liquid chromatography system comprised of a Micromass Modular CapLC (Waters) using a 5 mm x 300 µm 100 Å PepMap C18 µ-precolumn (LC Packings, San Francisco, CA) and a 15 cm x 75 µm 100 Å PepMap C18 column (LC Packings). Peptides were loaded on-column in 0.1% formic acid and eluted into the MS by means of a 5-70% acetonitrile/0.1% formic acid gradient over 60 min. The data-dependent acquisition (DDA) method that was employed followed the following protocol. MS survey scans were run between *m/z* 400-1800 for 2.4 s and ions exceeding an intensity threshold of 25 counts per second were selected for MS/MS. MS/MS was performed using charge state recognition for the

assignment of collision energies on the gated ions for either 10 s or until the TIC rose above 10,000. Upon switching back to the survey scan, previously gated ions were excluded from being re-gated using real time exclusion for a period of 200 s. All samples were run sequentially with identical experimental parameters.

3.7 Database Searching

Protein identifications of the excised protein spots was done using three independent software packages: Protein Lynx Global Server II (Waters), Mascot (Matrix Science Inc, Boston, MA), and PEAKS (Bioinformatics Solutions, Waterloo, ON) Positive identification of the spots of interest were based on the following criteria: all three software packages had to arrive at the same protein identification, the spot on the gel had to match both the pI and MW of the putative protein identification, and the MS/MS sequence coverage of the protein had to meet or exceed 10%. If all of these criteria were met, the protein identification was taken as positive.

3.8 Preparation of Additional Preeclamptic and Control Placental Samples for Use in the Validation of Differentially Expressed Proteins.

Additional samples used for the validation of differentially expressed proteins were treated in the following manner. Approximately 50 mg of tissue was removed from each of the twelve 1cm x 1cm CV samples per placenta and were pooled together. The pooled CV tissue samples obtained from the placental tissue repository ranged from 240 – 710 mg. To each sample 1 ml of extraction buffer (2% SDS, 50 mM Tris pH 6.8) was added for each 500 mg of CV tissue being extracted. The CV was homogenized at "setting six" using a PowerGen 700 tissue homogenizer (Fisher Scientific). After complete homogenization of the sample, protein extraction was performed by placing the sample in a boiling water bath for 10 minutes. Nucleic acids liberated during cell lysis were sheared through repeated aspirations using a 30.5 gauge needle. After protein extraction and shearing of the nucleic acids, the samples were spun at 15,000 x g for 15 minutes at 15°C to clarify the sample. The protein extracts

were aspirated off of the pellet, aliquoted and stored at -80°C for further use. A 10 µL aliquot was removed from each of the protein extracts to be used in the determination of protein concentration by means of a modified micro-Bradford assay (Bio-Rad).

3.9 Validation of Differentially Expressed Proteins by Immunoblotting.

For validation of the differentially expressed proteins (FABP4 and Per6) in the individual CV samples, 10 µg of each placental protein extract described above was resolved by 12% 1D SDS-PAGE and electroblotted onto polyvinylidene fluoride membrane (PVDF) (Bio-Rad Laboratories). Electroblotting was performed at 25 V for 40 min in a Trans-Blot SD semi-dry apparatus (Bio-Rad Laboratories) using Tris/Gly transfer buffer (25 mM Tris, 192 mM glycine, 20% methanol). Blocking of the PVDF membrane was allowed to proceed overnight at room temperature in TBST (10 mM Tris pH 7.6, 150 mM NaCl, 0.1% Tween 20) with 5% skim milk powder. The primary antibodies used were rabbit anti-FABP4 (Cayman, Ann Arbor, MI) at a dilution of 1:200, and rabbit anti-peroxiredoxin 6 (Per6) (Abcam, Cambridge, MA) at a dilution of 1:2000. For FABP4 and Per6, an HRPO conjugated goat anti-rabbit IgG (Jackson Immunoresearch, West Grove, PA) was used as the secondary antibody at a dilution of 1:10,000. All antibodies were diluted in TBST with 5% skim milk powder. After addition of SuperSignal Dura chemiluminescent substrate (Pierce Chemical Company), the immunoblot was developed for 2 min, imaged on a ProXPRESS Proteomic Imaging System (Perkin-Elmer). The immunoreactive protein bands in each of the three immunoblots were quantified using Phoretix 2D Expressions gel documentation software (Non-Linear Dynamics). The loading control for each individual sample was monitored by the quantitation of actin. The primary mouse anti-actin antibody, Ab-5 (Lab Vision, Freemont, CA), was used at a concentration of 1:400 and an HRPO conjugated goat anti-mouse IgG (Jackson Immunoresearch) was used as the secondary antibody at a dilution of 1:10,000.

Chapter 4
Experimental Results

4.1 Protein Extraction

There is no one definitive procedure that can be used for the separation of complex biological samples by two-dimensional gel electrophoresis. The sheer complexities of most samples, the salt concentrations of the extraction buffers, and the concentrations of endogenous contaminating components, such as lipids and nucleic acids, make finding the optimal experimental conditions quite challenging. In the specific case of this research, chorionic villi (CV) are a heterogeneous mixture of different cell types, all of which are at physiological salt concentrations and contain many components that interfere with the successful running of 2D gels. Therefore, the successful separation of the CV proteome in this study by 2D SDS-PAGE depended on the careful preparation of salt-free protein extracts and the optimization of running buffer conditions, particularly those conditions pertaining to first dimensional isoelectric focusing.

As discussed previously, there are many different charged molecules, both endogenous and buffer-related, that adversely affect the quality of isoelectric focusing. As a first step in the analysis of the control and preeclamptic CV samples, a successful and robust protein extraction protocol needed to be developed that was compatible with analysis by 2D SDS-PAGE. As the proteins of the CV were of primary interest, it was initially considered that a brief washing of the freshly sampled CV with cold isotonic saline would help rid the CV samples of the interfering maternal and fetal plasma component. Plasma contains 10 proteins that account for approximately 95% of the total protein present in the plasma [59]. It was thought that by removing these dominant endogenous proteins, such as human serum albumin and IgG, the resolution and detection of CV proteins would be greatly enhanced. On further examination, the washing of the CV samples at the point of collection was abandoned because the molecule or molecules of specific interest to the onset or pathology of preeclampsia may in

fact be soluble molecules. Although a saline wash would help to eliminate the number of serum proteins that would have to be analyzed along with the CV proteome, washing the CV samples could potentially serve to eliminate possible proteins of interest from the analysis done in this study. In actuality, the plasma component of the CV did not pose a problem for the successful separation and resolution of the CV proteomes. Although placenta is a bloody organ, the plasma protein component within the CV was limited and the majority of the proteins separated were from the CV tissues alone. The analysis of CV revealed many plasma proteins; however their concentrations were not high enough to pose a problem resolving CV proteins.

In order to directly compare the proteomes of each placental sample, a highly reproducible, 2D gel-compatible buffer that would extract the highest possible number of sample proteins was needed. As SDS is not compatible with the isoelectric focusing step of the 2D analysis, a buffer containing CHAPS was prepared and optimized for the extraction of CV proteins. Tissue samples were individually ground under liquid nitrogen prior to extraction with this buffer in order to facilitate the shearing of tough placental tissues and to allow for maximal solvent accessibility into the sample. After the extractions of the CV proteins were complete, the endogenous salts, lipids and sheared nucleic acids that were co-extracted with the proteins needed to be removed. This was done by dialysis against a low salt buffer with subsequent re-concentration by speed vac. Roughly 250 mg of each liquid nitrogen ground sample was extracted according to the above procedure, dialyzed to remove salt contaminants, and the protein concentrations were determined by micro-Bradford assay. Table 4.1 summarizes the identification, experimental condition, mass of CV used in the protein extractions, and the resulting protein concentrations obtained for the discovery sample set.

Table 4.1: The results of the discovery sample set protein extractions. The mass of CV extracted ranged from 193-324 mg giving rise to protein concentrations that ranged from 2.42 – 8.98 µg/ul. All protein concentrations were determined using a modified micro-Bradford assay.

Discovery Sample Set						
Placental Sample number	**Placenta ID**	**Experimental Condition**	**Gestational Age Bracket**	**Total CV Obtained (g)**	**Total CV Extracted (µg)**	**Protein Concentration After Extraction (µg/µl)**
1	21-99	Control	<28wks	1	208	2.42
2	59-01	Control	<28wks	1.17	204	2.52
3	188-04	Control	<28wks	1.26	266.7	5.89
4	46-01	Control	<28wks	1	245.5	4.98
5	118-02	Control	<28wks	1.09	253.9	3.17
6	87-02	Control	<28wks	1.06	277	3.61
7	28-00	Control	>28wks	1	205	3.49
8	89-02	Control	>28wks	1.1	244.4	5.21
9	23-99	Control	>28wks	1.06	235.5	4.09
10	5-99	Control	>28wks	1.147	285	7.49
11	151-03	Control	>28wks	1.24	252.7	8.12
12	34-01	Control	>28wks	1.23	214.2	5.97
13	39-01	PE	<28wks	1	193	3.35
14	17-99	PE	<28wks	1.08	195	3.34
15	117-02	PE	<28wks	1.08	235.2	4.36
16	174-03	PE	<28wks	1.24	276.2	6.94
17	137-03	PE	<28wks	1.14	257.8	8.23
18	189-04	PE	<28wks	1.4	320.7	8.98
19	3-00	PE	>28wks	1.26	262.3	8.39
20	159-03	PE	>28wks	1.23	324.1	6.81
21	145-03	PE	>28wks	1.29	218	3.65
22	141-03	PE	>28wks	1.1	223.8	6.3
23	58-01	PE	>28wks	1.2	246.1	5.44
24	103-02	PE	>28wks	1.11	296.1	7.1

The extraction of proteins from samples in the validation sample set was done slightly differently than for the discovery sample set. Without the charged species limitations associated with the running IEF, the protein extractions of the validation sample set was not as technically challenging as with the discovery sample set. In this case, SDS could be used to extract the sample proteins and salt concentrations were not an issue. The protein extraction from the validation sample set samples was done by homogenization in hot SDS. The protein concentrations that were determined for each of the validation sample set samples are summarized in Table 4.2.

Table 4.2: The results of the validation sample set protein extractions. The mass of CV extracted ranged from 193-324 mg giving rise to protein concentrations that ranged from 2.42 – 8.98 µg/ul. All protein concentrations were determined using a modified micro-Bradford assay.

Validation Sample Set				
Placental Sample number	**Placenta ID**	**Experimental Condition**	**Gestational Age Bracket**	**Protein Concentration After Extraction (µg/µl)**
25	203-04	Control	<28wks	12.01
26	101-02A	Control	<28wks	12.95
27	206-04	Control	<28wks	12.54
28	250-05	Control	<28wks	9.14
29	149-03	Control	<28wks	13.03
30	219-04	Control	<28wks	12.7
31	19-98	Control	<28wks	8.92
32	238-04	Control	<28wks	11.51
33	229-04	Control	<28wks	10.16
34	260-03	Control	>28wks	15.22
35	232-04A	Control	>28wks	16.35
36	278-06	Control	>28wks	16.78
37	199-04	Control	>28wks	18.25
38	152-03A	Control	>28wks	15.82
39	213-04	Control	>28wks	15.59
40	211-04	Control	>28wks	15.90
41	261-05	Control	>28wks	15.22
42	73-01	Control	>28wks	13.31
43	256-05	Control	>28wks	14.13
44	236-04	PE	<28wks	12.88
45	135-03	PE	<28wks	12.27
46	202-04	PE	<28wks	12.07
47	254-05	PE	<28wks	11.88
48	241-05	PE	<28wks	13.03
49	39-01	PE	<28wks	11.61
50	90-02	PE	<28wks	12.46
51	17-96	PE	<28wks	9.1
52	82-01	PE	<28wks	8.72
53	225-05	PE	<28wks	12.61
54	57-01	PE	>28wks	18.76
55	16-00	PE	>28wks	17.55
56	83-01	PE	>28wks	16.73
57	91-02	PE	>28wks	19.26
58	215-04	PE	>28wks	19.36
59	49-01	PE	>28wks	18.92
60	163-03	PE	>28wks	18.19
61	142-03A	PE	>28wks	16.03
62	12-00	PE	>28wks	14.58
63	25-99	PE	>28wks	16.91

4.2 Running of the Two Dimensional Gels

While the reduction of the salt concentration by dialysis was successful, an initial MS-based examination of post-dialyzed proteins separated by 2D electrophoresis revealed an unwanted intense proteolytic degradation of the proteins on a wide scale. From the initial 2D gels that were run, 294 protein spots of the highest abundance and reproducibility were selected for identification by MS. This was done to assess sample integrity post-sample collection, the quality of separation by 2D SDS-PAGE, and the expected dynamic range of this analysis. Many of the proteins that were identified by MS appeared in the 2D gel at the incorrect (lower) molecular weight and pI. While slight variations in the molecular weights and pIs of proteins due to post-translational modifications are expected in a 2D gel experiment, this case was particularly unsatisfactory. Most of the proteins identified were at much lower molecular weights than theoretically expected, which is a good indication of proteolytic digestion. Figure 4.1 shows the distribution of all 294 high abundance protein spots selected from the gel. Of these, the majority of the protein spots were low mass proteolytic degradation products of proteins that should have been detected migrating at much higher molecular weights. Clearly, there were active proteases that were either (a) evading neutralization by the extraction buffer laden with protease inhibitor or (b) were refolding and regaining activity after the removal of high concentrations of the extraction buffer or protease inhibitors during dialysis. It was decided that the concentrations of protease inhibitors present in the extraction and IEF stages were not sufficient to prevent the proteolytic digestion of the sample and further optimization was required.

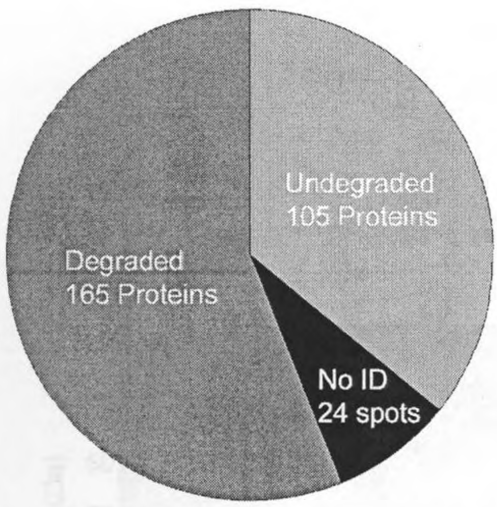

Figure 4.1: The breakdown of the 294 spots selected for assessment of sample integrity post sample collection, protein extraction, and separation by 2D SDS-PAGE. Clearly the majority of the proteins that were analyzed were degradation products.

Before further analysis of CV samples could be performed by 2D SDS-PAGE, it was essential we identify the stage at which the deleterious proteolytic digestion was occurring. If this degradation was occurring during delivery of the placenta, or collection of the CV immediately after delivery, this would lead to a critical re-evaluation of a protein-based approach for PE biomarker discovery. In order to probe for the stage of protein degradation, three samples were prepared. The first was a control sample comprised of liquid nitrogen-ground CV extracted in Laemmli buffer, the second sample was CHAPS-extracted CV prior to dialysis, and the third sample was CHAPS extracted CV post-dialysis. When the protein profiles of these three samples (Figure 4.2A) were compared to the protein profile obtained by 2D gel (Figure 4.2B), it became clear that degradation was occurring in either the rehydration or IEF step of the first dimensional separation. By comparing the proteins seen in Figure 4.2A to the proteins seen in Figure 4.2B, there is an apparent lack of high abundance, high molecular weight proteins seen in the 2D gel. Therefore, further efforts to prevent proteolytic digestion were focused on the rehydration and IEF step of the 2D gel analysis.

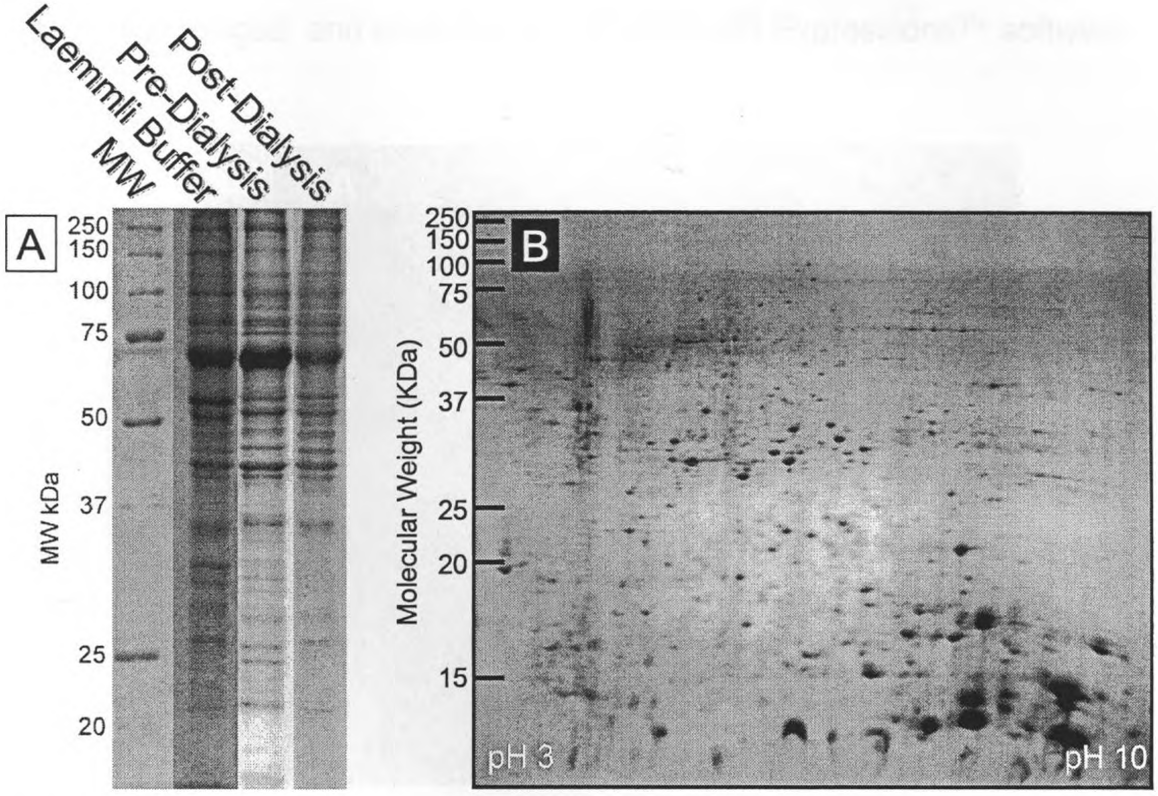

Figure 4.2: A) Three samples to assess proteolytic degradation in the CV samples. Retention of high mass proteins in the 1D gels across the Laemmli buffer, pre, and post-dialysis samples indicated that degradation was occurring in the IEF step of the analysis. B) Comparison of the proteins seen in A with the protein profile seen in B above clearly shows the widespread proteolysis taking place during IEF. All gels were run at 12% acrylamide.

After numerous different combinations of several protease inhibitor cocktails and many attempts at successful IEF runs, it was determined that an EDTA concentration of at least 5 mM was needed to inhibit the proteolysis initially seen during protein extraction. After this discovery, protein extraction of the samples was redone in 5 mM EDTA, with subsequent salt removal by dialysis performed against 1 mM EDTA. This resolved the proteolysis problem, as both the number of spots separated and the overall resolution of the gels increased. Figure 4.3 illustrates the striking difference between the pre-EDTA extracted samples and the optimized post-EDTA extracted samples in terms of overall gel quality.

With a robust and effective extraction procedure in place, each sample was then successfully separated by 2D SDS-PAGE. All gels were stained with Sypro ruby, imaged, and analyzed with Phoretix 2D Expressions™ software.

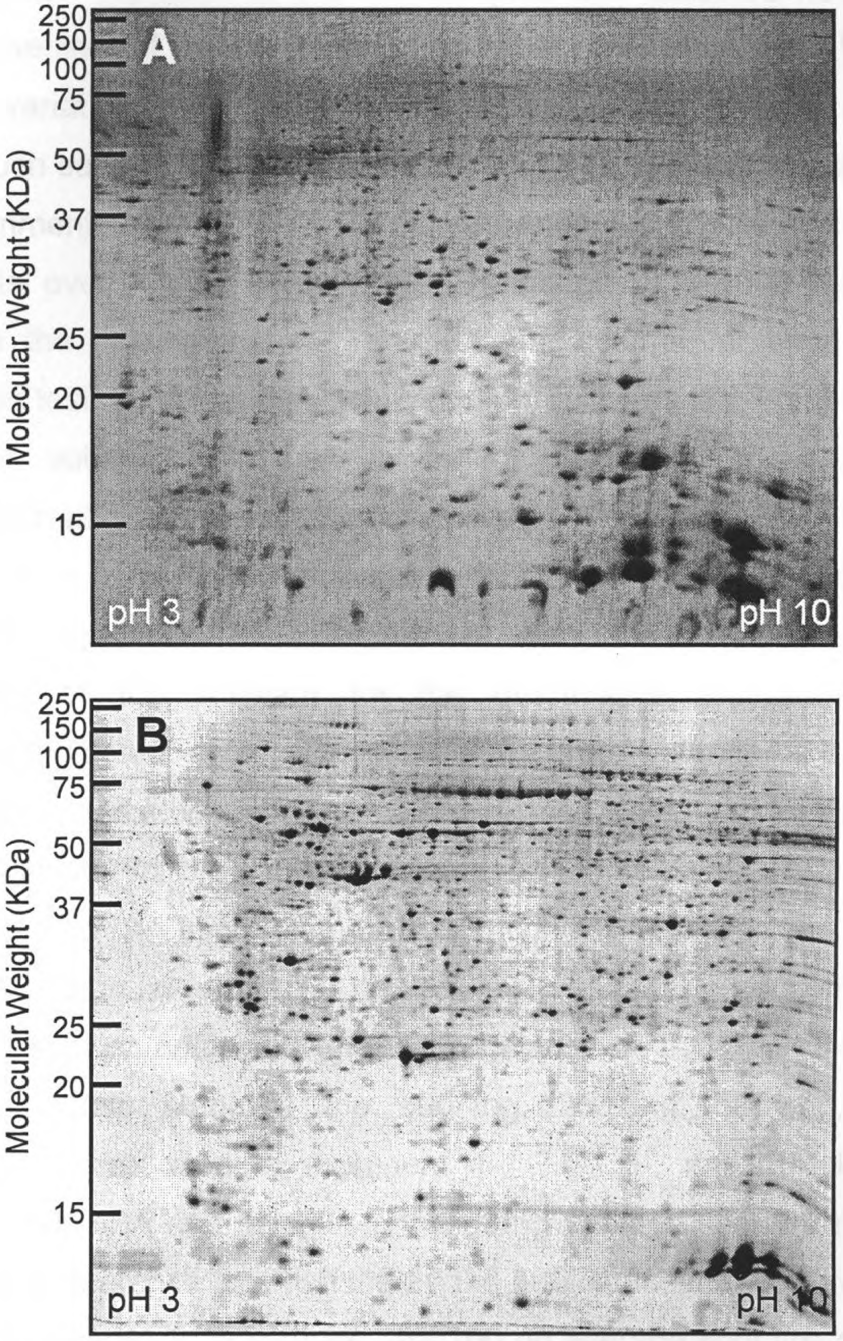

Figure 4.3: Comparison of the same CV sample run under identical conditions with the only exception being the use of an optimized protease inhibitor cocktail in gel B. The use of a standard protease inhibitor cocktail did not inhibit the proteolysis of proteins in gel A. Comparison of the high molecular weight proteins between gel A and gel B clearly shows the increase in protein species retained during separation in gel B.

4.3 Testing for Differential Analysis Software Fidelity

Successful differential display analysis of the samples used in this study depended on the accurate and reproducible software-based analysis of high quality 2D gels. As each of the CV samples was collected from a different patient, an element of patient-to-patient variability was expected. While we did not expect variation in the performance of the 2D gel analysis software, we tested for such sample-to-sample variability between identical standard samples. These experiments involved analyzing three protein standards, which were run in quadruplicate over a spot concentration range of 50 – 1000 ng. Table 4.3 summarizes the values obtained for the spot volume for each protein and concentration tested. It was found that all four replicates in a group showed very similar spot volumes with low standard deviations observed over the concentration replicates for each standard tested.

In addition to testing for replicate variability during 2D gel analysis with the Phoretix 2D Expressions™ software, we also assessed the linearity and reproducibility of the software for the quantitative analysis of artificially "differentially regulated" spots. The same three protein standards that were used to determine the variation among sample replicates were used for this evaluation; the values obtained for the sample replicate assessment were averaged in order to give a value for the spot volume of each concentration tested. For the BSA and myoglobin standards, the 50 ng, 100 ng and 250 ng concentrations were used to represent an artificial differential regulation of 1-, 2- and 5-fold. For the carbonic anhydrase standard the 100 ng, 250 ng, 500 ng, and 1 µg concentrations were used to represent 1-, 2.5-, 5-, and 10-fold differential regulations. For BSA and myoglobin the 50 ng average spot volume was used as the 1:1 ratio reference to which the 2- and 5-fold concentration averages were compared. For carbonic anhydrase, the 100 ng average spot volume was used as the 1:1 ratio reference to which the 2.5-, 5-, and 10-fold concentration averages were compared. Table 4.3 summarizes the values obtained for the theoretical regulation ratios and the observed experimental regulation ratios.

Figures 4.4A, 4.4B and 4.4C illustrate the replicate reproducibility of the different standards, as well as the correlation of theoretical and experimental regulation ratios. The replicate reproducibility and ratio correlation determined for this set of standards correlated with current published data [68].

BSA								
Protein Per Spot	Spot Volume				Replicate Average	Replicate Standard Deviation	Theoretical regulation	Actual regulation
	Replicate 1	Replicate 2	Replicate 3	Replicate 4				
250ng	90.67	90.5	94.25	91.4	91.7	1.74	1:5	1:3
100ng	54.26	43.06	54.01	48.93	50.07	5.27	1:2	1:1.6
50ng	27.42	32.63	31.96	34.47	31.62	2.99	1:1	1:1
Carbonic Anhydrase								
Protein Per Spot	Spot Volume				Replicate Average	Replicate Standard Deviation	Theoretical Regulation	Actual Regulation
	Replicate 1	Replicate 2	Replicate 3	Replicate 4				
1000ng	31.08	34.99	32.56	36.06	33.67	2.27	1:10	1:13
500ng	17.45	15.5	18.61	16.44	17	1.34	1:5	1:6.5
250ng	4.77	9.14	10.65	12.55	9.28	3.31	1:2.5	1:3.5
100ng	2.55	3.65	1.43	2.72	2.59	0.91	1:1	1:1
Myoglobin								
Protein Per Spot	Spot Volume				Replicate Average	Replicate Standard Deviation	Theoretical Regulation	Actual Regulation
	Replicate 1	Replicate 2	Replicate 3	Replicate 4				
250ng	89.26	102.15	125.97	118.14	108.88	16.41	1:5	1:3.4
100ng	44.31	47.38	61.63	58.67	52.99	8.44	1:2	1:1.7
50ng	29.27	27.1	37.41	35.36	32.29	4.89	1:1	1:1

Table 4.3: The three proteins used to determine the replicate reproducibility during analysis with the Phoretix 2D Expressions software. For BSA and myoglobin 50ng, 100ng, and 250ng of protein were run in quadruplicate. For the carbonic anhydrase standard 100ng, 250ng, 500ng, and 1µg of protein was run in quadruplicate. All four values obtained for spot volume at each concentration tested was averaged and the averaged values were compared to one another to mimic differential analysis.

BSA Standard

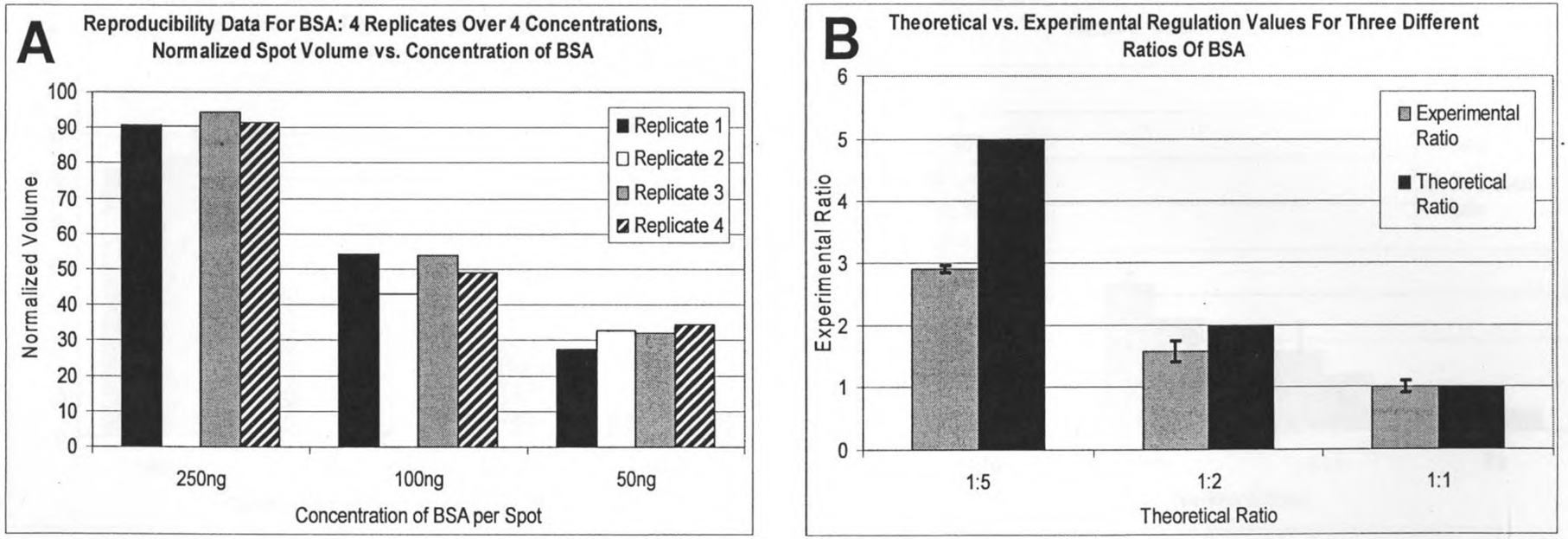

Figure 4.4A: Panel A shows the replicate reproducibility for each of the different test concentrations of bovine serum albumin (BSA). The average values for each set of replicates were used in assessing the reproducibility of differential regulation. Panel B illustrates the results of the artificially created differential regulation series.

Carbonic Anhydrase Standard

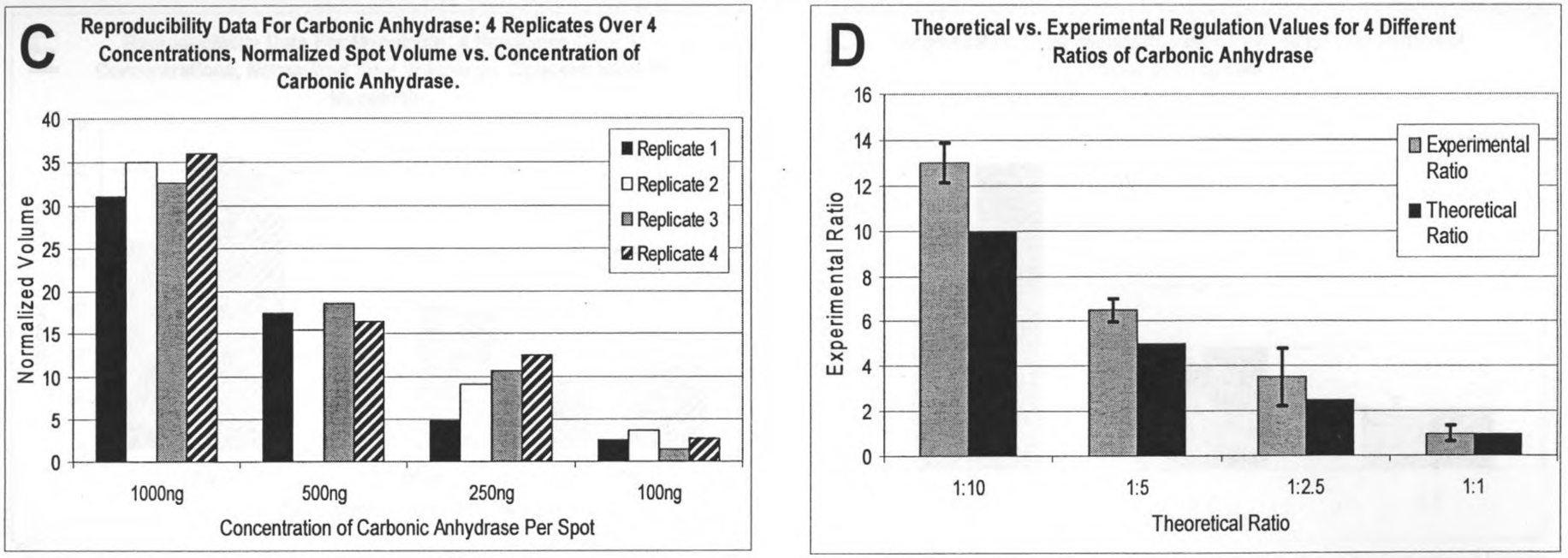

Figure 4.4B: Panel C shows the replicate reproducibility for each of the different test concentrations of carbonic anhydrase. The average values for each set of replicates were used in assessing the reproducibility of differential regulation. Panel D illustrates the results of the artificially created differential regulation series.

Myoglobin Standard

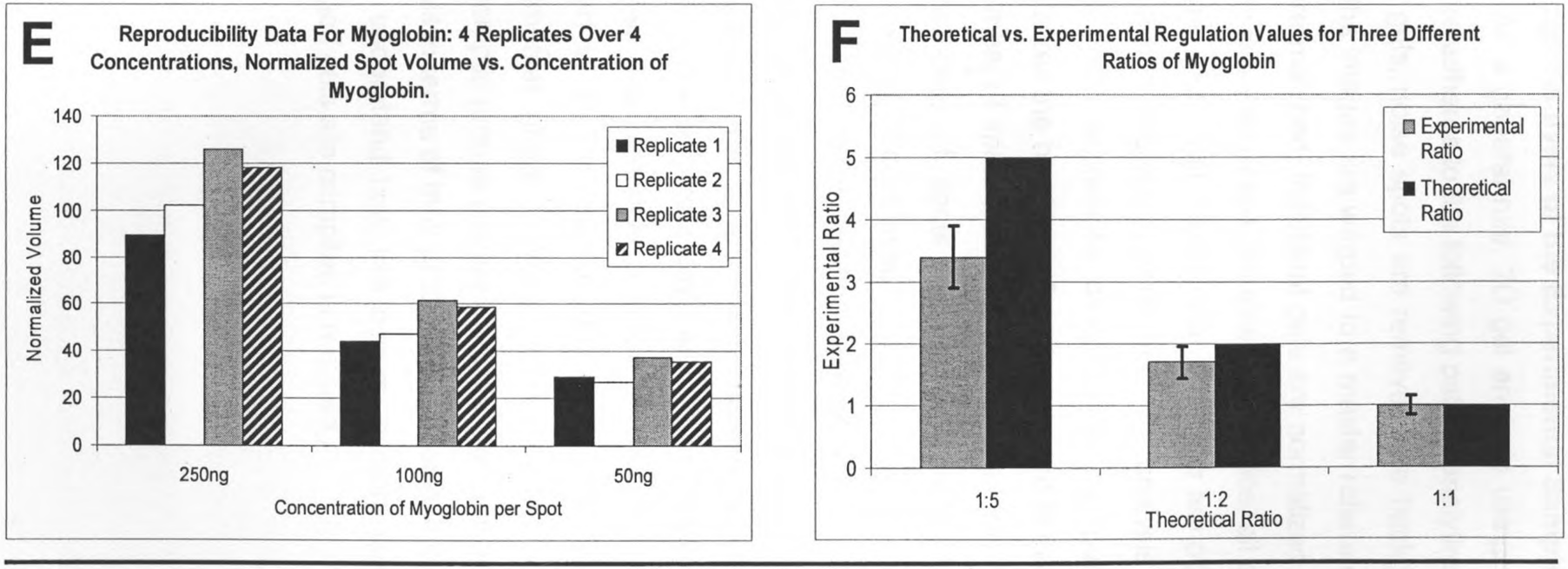

Figure 4.4C: Panel E shows the replicate reproducibility for each of the different test concentrations of myoglobin. The average values for each set of replicates were used in assessing the reproducibility of differential regulation. Panel F illustrates the results of the artificially created differential regulation series.

4.4 Image Analysis of the Experimental Samples

As a general rule, 2D gel analysis using the Phoretix 2D Expressions™ software adheres to the following path of analytical functions. Spots are detected in the gels, noise spots are removed, the background is subtracted from each spot, the images are warped to a master reference gel, spots between all of the gels are matched, individual gels are normalized and comparisons are made for differentially expressed proteins. In practice, all of these functions are essential; however, additional manual manipulations are occasionally required. A detailed description of the actual protocol for the analysis of the under-and over-28 week control and preeclamptic samples can be found in Appendix 1. Table 4.4 summarizes the numbers of spots detected in each of the experiments, including the number of spots matched, total differentially regulated protein spots, and the final numbers of spots that were found to be reproducibly detected at a statistically significant level.

Overall, fewer proteins were detected in the initial survey of the "over-28 weeks" experiment than in the "under-28 weeks" experiment. A possible reason for this is the rapid growth and metabolism of "under 28-week" placental samples as opposed to the more developed "over 28-week" placental samples. The rapid turn-over and varied expression of proteins in the under 28-week samples resulted in an increase of statistically differentially regulated proteins in this experimental group. The matching of the spots between the control and preeclamptic groups yielded a smaller data set due to subtle differences between the gels in terms of their protein constituents in the averaged gel sets. In order to better understand how this occurs, a more complete explanation of how the averaged gels are compiled is required.

Table 4.4: The total numbers of spots detected, detected as differentially regulated, and statistically differentially regulated in both the under and over 28 week experiments.

[1] Total spots detected refers to the number of spots that were present in the average gel for each group.

[2] Total spots matched refers to the number of spots that were matched between the control and preeclamptic average gels.

[3,4] Up regulated and down regulated spots are the total numbers of differentially regulated spots as determined by comparing the preeclamptic average gel spot values to the control average gel spot values.

[5,6] Up regulated and down regulated spots are the final numbers of spots that were reproducibly seen across all gels in the experiment and had an ANOVA p-value < 0.05.

Under 28 Weeks Gestation Experiment						
	Total Spots Detected[1]	Total Spots Matched[2]	Total Up Regulated Spots[3]	Total Down Regulated Spots[4]	Up Regulated Spots[5] (ANOVA p-Value < 0.05)	Down Regulated Spots[6] (ANOVA p-Value < 0.05)
Control Sample Group Average	1208	930	103	150	2	7
Preeclamptic Sample Group Average	1174					
Over 28 Weeks Gestation Experiment						
	Total Spots Detected[1]	Total Spots Matched[2]	Total Up Regulated Spots[3]	Total Down Regulated Spots[4]	Up Regulated Spots[5] (ANOVA p-Value < 0.05)	Down Regulated Spots[6] (ANOVA p-Value < 0.05)
Control Sample Group Average	960	810	32	25	3	0
Preeclamptic Sample Group Average	810					

To describe a simple case, the under-28 week control group will be considered here in describing the preparation of the under-28 week control averaged gel. A single gel in the rank of the under-28 week control sample replicates is selected as the "base gel" for the gel average for this group. After all of the spots are detected and matched within this group, spots are added to the computer-based average gel based on predetermined averaging parameters. In this case, spots had to be present in at least half of the sample replicates to be included in the average gel. Once the control- and preeclamptic-averaged gels

were compiled, the software used these spot catalogues to match proteins between the control and preeclamptic spot data sets. Proteins that were present only in the control average but not the preeclamptic average (or vice versa) were not included as matches and were examined independently. This resulted in a lower number of spots being matched between the gels compared to the total number of spots detected. After a closer examination of the spots that were not matched between the control and preeclamptic averages, it was determined that they were not statistically significant, due to extremely poor reproducibility and significant variation.

Upon further examination of the matched data between the control and preeclamptic averages, differentially regulated spot lists were extracted and subjected to further analysis. Each of the spots that were suspected as being differentially regulated was manually examined for presence in all of the gels within the experiment to confirm whether successful spot matching had occurred. After excluding spots that were not correctly matched, that were statistically insignificant in terms of differential expression (an ANOVA p-value of >0.05), or that were so complex that accurate spot values were impossible to obtain, a substantially smaller, but highly significant data set, was arrived at. The final numbers obtained from this filtering yielded two up-regulated and seven down-regulated proteins in the preeclamptic data set in the under-28 week experiment, and three up-regulated and zero down-regulated proteins in the preeclamptic data set in the over-28 week experiment.

4.5 Experimental Differential Regulation Analysis Results

After confirming the reproducibility and fidelity of the gel analysis software, both the under-28 week and over-28 week CV experimental groups were analyzed. The less than 28 week CV samples were analyzed with the Phoretix software using the previously stated parameters. Differentially regulated spots that were reproducibly observed in both the control and preeclamptic CV samples were excised and subjected to MS analysis. It should be noted that in

the case of the under-28 weeks samples, the sample size was limited to five control and five preeclamptic samples. Despite the use of an optimized 2D extraction and running protocol, one sample from each of the control and preeclamptic groups was unable to provide the resolution and proteolytic inhibition needed for successful 2D analysis. Sample integrity may have been compromised during delivery of the placenta or an extended CV sampling period that allowed proteolytic degradation to occur. Alternatively, these placentas might have greater levels of proteolytic enzymes present that would not be inhibited by the protease inhibitors. While increasing the concentration of EDTA in the extraction and running protocols may have corrected this problem, EDTA was used at the highest possible concentration that was determined to be compatible with the first dimensional isoelectric focusing step of the 2D analysis.

After extensive 2D gel analysis, nine proteins were identified reproducibly as being differentially regulated between the control and preeclamptic CV samples. For each of the under-28 week samples, the raw data and regulation values for every differentially regulated protein identified are tabulated in Appendix 2. Each of these proteins was excised and successfully identified by LC-MS/MS. Table 4.5 summarizes the differentially expressed proteins identified, the average normalized spot volumes of each identified protein, the statistical significance of the spot differences and the overall regulation difference between the under-28 week control and preeclamptic samples.

Each of the proteins that were identified in the under-28 week samples complied with the isoelectric point, molecular weight, MS/MS minimum peptide cutoff, and total protein coverage for the MS identification criteria previously described in Section 3.7. The details of the MS/MS and observed frequencies of each protein of interest amongst the samples tested are summarized in Table 4.6. Each of the proteins of interest had acceptable MS/MS coverage with adequate numbers of observed peptides with which to base the protein identifications. Additionally, each differentially regulated protein of interest was observed in each of the CV samples tested.

Table 4.5: Protein Identifications in the under-28 week analysis of five control and five preeclamptic pregnancies. The values for spot volumes are the averages of the five different CV samples run in duplicate (ten gels total). Ten values were averaged for the control samples and ten values averaged for the preeclamptic samples. Calculated standard deviations are shown in brackets for each average. Fold differences are the preeclamptic averages divided by the control averages. For raw data see Appendix 2.
* values displayed as: normalized spot volume (standard deviation)

Proteins Identified	Control Pregnancy Average Spot Volumes* (n=5)	Preeclamptic Pregnancy Average Spot Volumes* (n=5)	Fold Difference PE vs. Control	ANOVA p-value
Fatty Acid Binding Protein 4	0.057 (0.049)	0.213 (0.074)	3.7	<0.0001
Peroxiredoxin 6	0.093 (0.028)	0.250 (0.057)	2.7	<0.0001
Enoyl CoA Hydratase	0.116 (0.038)	0.060 (0.025)	-2	<0.005
Estradiol 17-beta-dehydrogenase	0.197 (0.050)	0.096 (0.031)	-2	<0.0001
Stathmin	0.080 (0.018)	0.038 (0.021)	-2.1	<0.0001
Human Placental Lactogen	0.239 (0.057)	0.097 (0.043)	-2.5	<0.0001
Lipocortin	0.063 (0.020)	0.026 (0.009)	-2.4	<0.0001
Proliferation-associated protein 2G4	0.052 (0.017)	0.019 (0.007)	-2.7	<0.001
Δ3,5-Δ2,4-dienoyl-CoA isomerase	0.132 (0.085)	0.038 (0.014)	-3.4	<0.005

Table 4.6: Protein Identification data for the under-28 week analysis. Each protein identified was present in all of the gels that were tested. LC-MS/MS yielded adequate numbers of peptides and sufficient coverage giving high confidence identifications for each protein analyzed. For raw data see Appendix 3.

Protein Identification	Number of Peptides observed	Mascot Score	Total Protein coverage	Number of Gels containing the Protein of Interest
Fatty Acid Binding Protein 4	6	374	48%	10/10
Peroxiredoxin 6	9	416	52%	10/10
Enoyl-CoA Hydratase	7	345	35%	10/10
Estradiol 17-beta-dehydrogenase	14	818	53%	10/10
Stathmin	4	169	28%	10/10
Human Placental Lactogen	5	316	29%	10/10
Lipocortin	6	437	21%	10/10
Proliferation-associated protein 2G4	5	186	12%	10/10
Δ3,5-Δ2,4-dienoyl-CoA isomerase	12	564	39%	10/10

The over-28 week control and preeclamptic CV samples were analyzed with an identical protocol as the under-28 week samples. Table 4.7 summarizes the three proteins that were reproducibly and statistically determined to be differentially regulated in the over-28 week samples. As per the under-28 week samples, the average normalized spot volume of each protein identified, the statistical significance of the spot differences, and the overall regulation difference between the control and preeclamptic samples are summarized. For each over-28 week sample, the raw data and regulation values for each differentially regulated protein can be seen in Appendix 2.

All three proteins of interest in the over-28 week samples followed the same MS-based identification criteria as the under-28 week samples. The over-28 week MS/MS results are shown in Table 4.8 and highlight the number of peptides seen, total MS/MS protein coverage, and observation frequency of each protein between the different samples of the over-28 week experiment. In general, there were far fewer proteins that were observed to be differentially regulated in the over-28 week sample set than in the under-28 week sample set.

Table 4.7: Protein Identifications in the over-28 week analysis of five control and six preeclamptic pregnancies. The values for spot volumes are the averages of the five different CV samples in duplicate. Ten values were averaged for the control samples and ten values averaged for the preeclamptic samples. Calculated standard deviations are shown in brackets for each average. Fold differences are the preeclamptic averages divided by the control averages. The raw data is provided in Appendix 2.

* values displayed as: normalized spot volume (standard deviation)

Protein Identification	Control Pregnancy Average Spot Volumes* (n=6)	Preeclamptic Pregnancy Average Spot Volumes* (n=5)	Fold Difference PE vs. Control	ANOVA p-value
Macrophage capping protein	0.020(0.013)	0.044(0.014)	2.2	<0.0005
Heat shock protein β-1	0.064(0.021)	0.129(0.060)	2	<0.005
Prostaglandin dehydrogenase 1	0.053 (0.029)	0.110 (0.035)	2	<0.0005

Table 4.8: Protein Identification data for the over-28 week analysis. Each protein identified was present in all of the gels that were tested. The LC-MS/MS analyses yielded adequate numbers of peptides and sufficient coverage giving high confidence identifications for each protein analyzed. The raw data is provided in Appendix 3.

Protein Identification	Number of Peptides Observed	Mascot Score	Total Protein coverage	Number of Gels containing the Protein of Interest
Macrophage capping protein	5	242	18%	11/11
Heat shock protein β-1	6	172	35%	11/11
Prostaglandin dehydrogenase 1	6	535	42%	11/11

Selecting and identifying the proteins that were determined to be differentially regulated yielded valuable information about proteins involved in the underlying process of preeclampsia. However, further validation of these results was required. After careful examination of the proteins that were determined to be differentially regulated in this study, several functional groups were identified. Functional groupings were assigned using the gene ontology (GO) database and GoMiner™, a comprehensive tool for the analysis of protein function [69]. After GoMiner™ analysis of the under and over-28 week data sets, differentially expressed proteins were functionally classified into the groups shown in Figure 4.5.

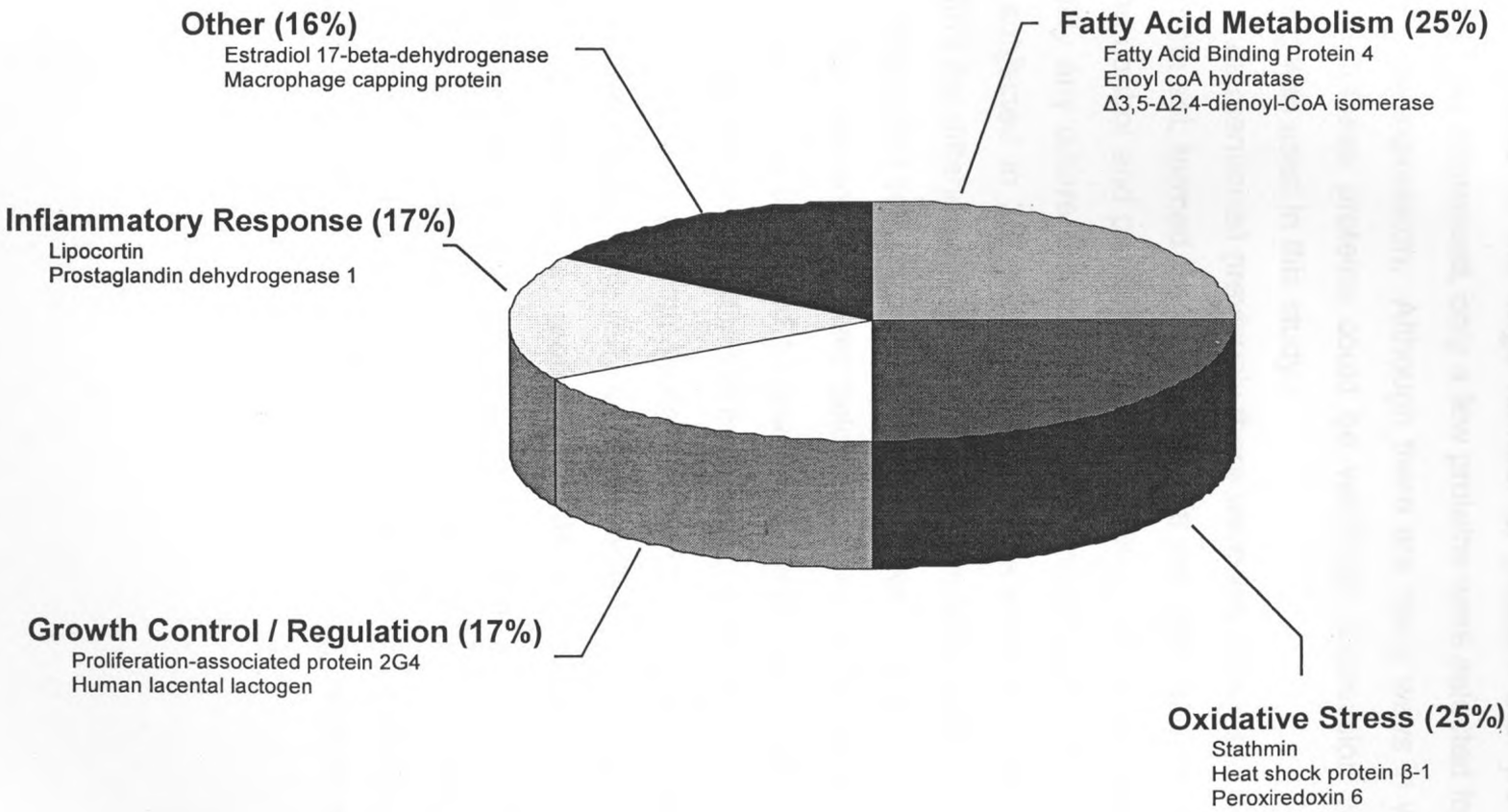

Figure 4.5: The breakdown of the proteins identified as being differentially expressed in either the over or under-28 week discovery sample sets.

4.6 Validation of Differentially Regulated Spots by Western Blotting

Because of the large number of proteins that were determined to be differentially expressed, only a few proteins were selected for further validation of differential expression. Although there are many ways in which the expression levels of these proteins could be validated, expression validation by western blotting was used in this study.

As mentioned previously there were two data sets used in this study. The first data set, termed the discovery data set, was used for the initial 2D analysis of the control and preeclamptic CV samples. These samples were employed to identify any differentially regulated proteins present. The second data set was not subjected to 2D gel analysis, but was instead used as a validation set to confirm the differential expression levels identified in the discovery data set. This secondary data set was termed the "validation data set".

For reasons discussed below, only two of the proteins showing differential regulation were subjected to analysis by western blotting in both the discovery and validation data set. One of the proteins that was assayed by western blotting is involved in fatty acid metabolism, while the other was involved in the mediation of oxidative stress. The fatty acid metabolism-related protein that was validated was fatty acid binding protein 4 (FABP4), and the protein involved in the mediation of oxidative stress was peroxiredoxin 6 (Per6). Initially the expression levels of these two proteins were validated in the discovery data set to confirm and support the differences in regulation seen in the 2D gel analysis. Figure 4.6 illustrates the results of the western blotting performed on the discovery data set samples.

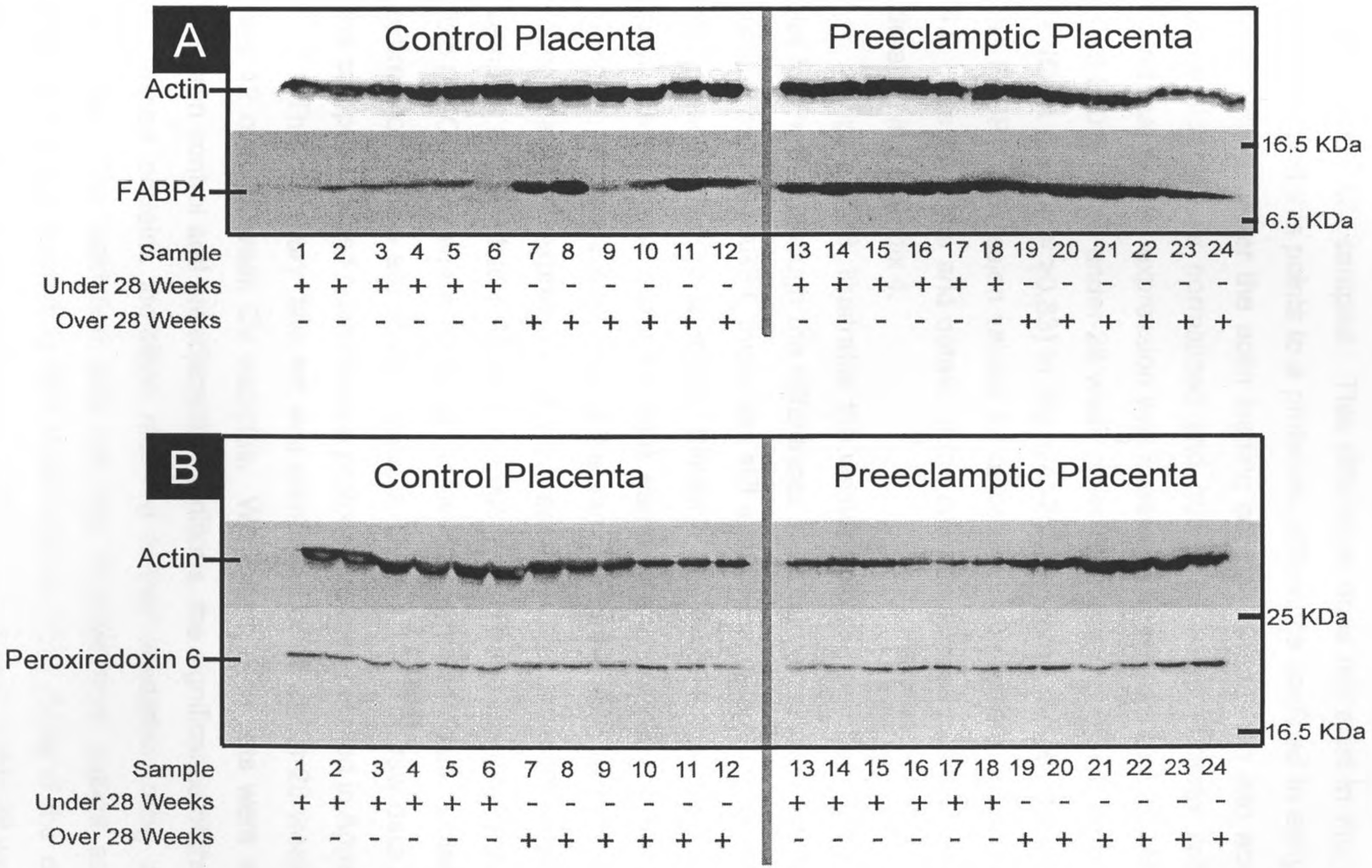

Figure 4.6: Western blotting results for FABP4 and Per6 in the discovery data set. FABP4 was determined to be upregulated in the under-28 week preeclampsia samples by 8.49 fold, while Per6 was upregulated in the under-28 week preeclampsia samples by 2.79 fold. Actin was used as the loading control in this experiment. Rabbit α-FABP4 was the primary antibody used in A, while rabbit α-Per6 was used as the primary antibody in B. In both the FABP4 and Per6 blots, the secondary antibody used was goat α-rabbit HRPO conjugate. The blots were visualized with SuperSignal® west pico.

By looking at the results in Figure 4.6A, it is clear that a substantial difference in FABP4 expression exists between the under-28 week control and preeclamptic CV samples. This difference does not exist in the over-28 week samples, and this points to a proteomic difference confined to early preeclamptic pregnancies. After the actin loading controls were taken into account and the expression values normalized and quantified using Phoretix software, it was found that FABP4 expression was increased by a factor of 8.49 (ANOVA p-value = <0.0001) in the under-28 week preeclamptic samples and by a factor of 1.06 (ANOVA p-value = >0.83) in the over-28 week preeclamptic samples. Details of the FABP4 expression values for discovery data set are shown below in Table 4.9. The raw data and details of the computer-based quantification protocol are detailed in Appendix 4.

Figure 4.6B. illustrates the western blotting results of the discovery data set for Per6. Although the differences in protein expression for Per6 are not as striking as with FABP4, there was still a statistical difference between the control and preeclamptic CV samples. Similar to the FABP4, the Per6 expression level only differed in the under-28 week samples and not differ in the over-28 week samples. After normalization of the samples to the actin loading controls, it was found that Per6 expression was increased in the under-28 week preeclamptic samples by 2.79 fold (ANOVA p-value =<0.01) and marginally decreased 0.69 fold (ANOVA p-value = >0.1) in the over-28 week samples. Details of the Per6 expression values are shown below in Table 4.10. The raw data and details of the computer-based quantification protocol are also detailed in Appendix 4.

The discovery data set was comprised of 10 under-28 week CV samples and 12 over-28 week CV samples. While both data sets were evenly divided between control and preeclamptic conditions, the significance of the differentially expressed proteins identified required further validation using a new set of samples. The validation data set was selected from patient samples in the placental tissue repository that were different from those of the discovery data set. This data set was comprised of 18 CV samples of under-28 weeks gestation and 20 CV samples of over-28 weeks gestation. Like the discovery data set,

each of these groups were evenly divided between control and preeclamptic experimental conditions. Figures 4.7 and 4.8 illustrate the results of the validation data set that was examined by western blotting for expression of both the FABP4 and Per6 proteins.

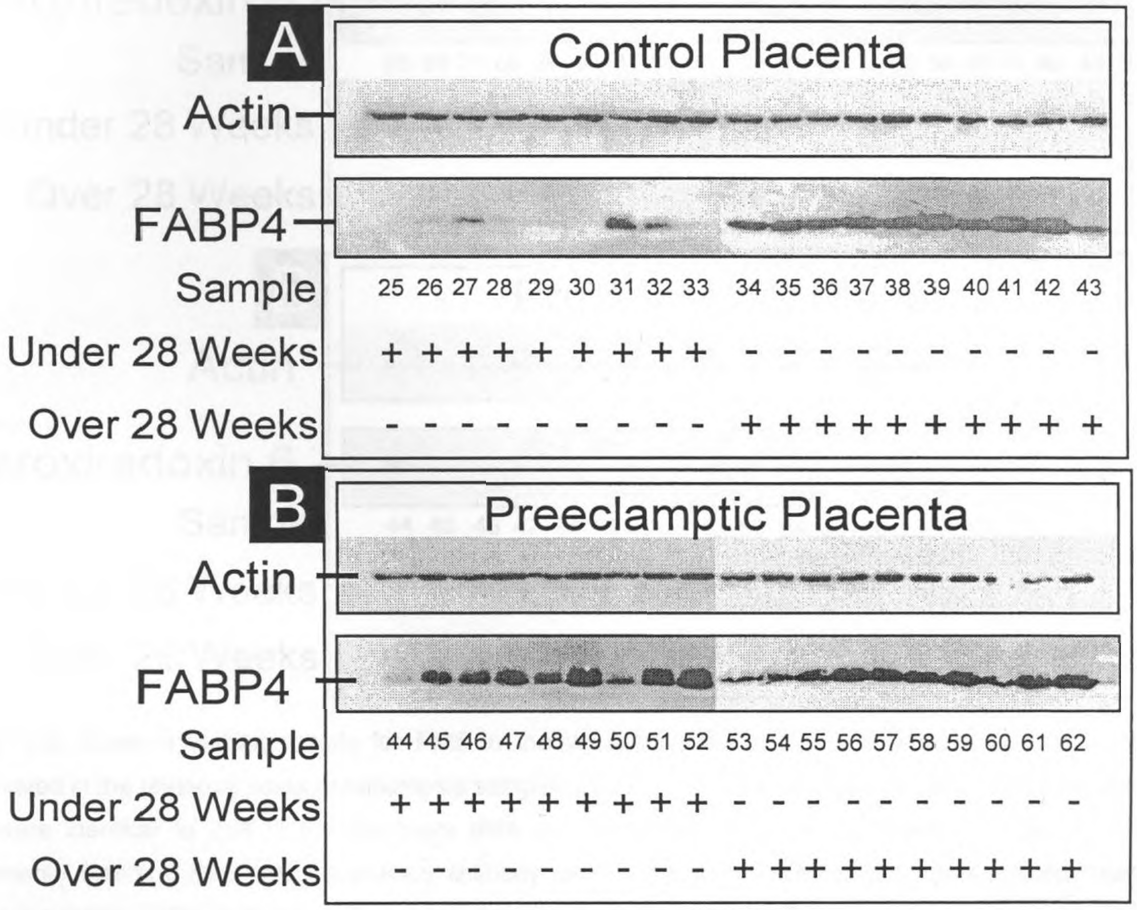

Figure 4.7: Western blotting results for FABP4 in the validation data set. FABP4 was determined to be upregulated in the under-28 week preeclampsia samples by 4.59 fold. All conditions used for these western blots were identical to that of the discovery data set. Actin was used as the loading control in this experiment. Rabbit α-FABP4 was the primary antibody used in A and B while the secondary antibody used was goat α-rabbit HRPO conjugate. Blots were visualized with SuperSignal® west pico.

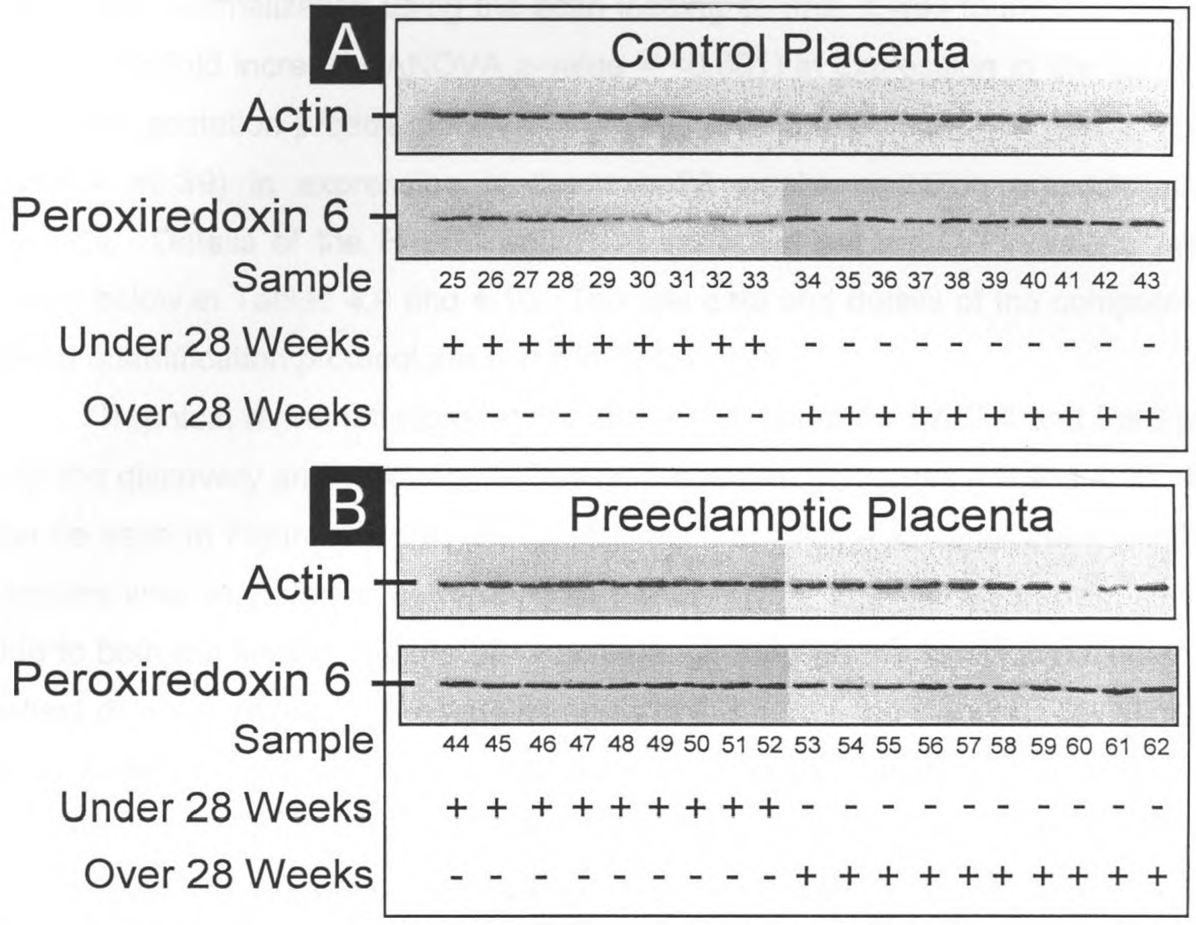

Figure 4.8: Western blotting results for Per6 in the validation data set. Per6 was determined to be upregulated in the under-28 week preeclampsia samples by 2.05 fold. All conditions used for these western blots were identical to that of the discovery data set. Actin was used as the loading control in this experiment. Rabbit α-Per6 was the primary antibody used in A and B while the secondary antibody used was goat α-rabbit HRPO conjugate. Blots were visualized with SuperSignal® west pico

The western blot results of the validation data set were very similar to that of the discovery data set, and this served to confirm the expression values observed in the 2D gel analysis. As with the discovery data set validation western blots, actin was used as the loading control for the validation data set. Once the loading controls were used to normalize the expression levels of FABP4 (Figures 4.7A and 4.7B), it was found that FABP4 expression was increased in the preeclamptic samples by 4.59 fold (ANOVA p-value = <0.001) in the under-28 week data set and by 1.13 fold (ANOVA p-value = >0.35) in the

over-28 week data set. In terms of Per6 expression levels (Figures 4.8A and 4.8B), after normalization using the actin loading control, it was found that there was a 2.05 fold increase (ANOVA p-value = <0.001) in expression in the under-28 weeks gestation preeclamptic samples and a 0.88 fold decrease (ANOVA p-value = >0.39) in expression in the over-28 weeks gestation preeclamptic samples. Details of the FABP4 and Per6 validation set regulation values are shown below in Tables 4.9 and 4.10. The raw data and details of the computer-based quantification protocol are given in Appendix 4.

Graphical representations of the expression levels for FABP4 and Per6 in both the discovery and validation data sets are shown in Figures 4.9 and 4.10. It can be seen in Figure 4.9 that the up-regulation of FABP4 in early preeclamptic samples was very similar between both the discovery and validation data sets. Due to both the limited number of samples analyzed and the inherent patient-to-patient diversity of placental tissue samples in this study, the standard deviations of each expression level reflect this level of expected variation. Since many proteins related to pregnancy are regulated in a gestational age related manner, the variation seen amongst different samples within each group may be due to the variety of different gestational ages in both the under- and over-28 week sample sets. As shown by the patient demographics in Table 2.3, every effort was taken to maintain the closest possible ranges in the gestational age of the placentas during sample selection. Despite considerable efforts in the selection and analysis of the sample sets, there remained notable variations in the regulations of the proteins that were identified as being differentially expressed in the sample sets. Although there were notable standard deviations associated with the results in Figures 4.9 and 4.10, it should be noted that the ANOVA scores summarized in Tables 4.9 and 4.10 showed that in the under-28 week samples, the regulation of both FABP4 and Per6 between the control and preeclamptic samples were statistically significant events. In terms of the over-28 week FABP4 and Per6 expression levels, it can be seen that no statistically significant differences existed as shown by the extremely high ANOVA p-values shown in Tables 4.9 and 4.10.

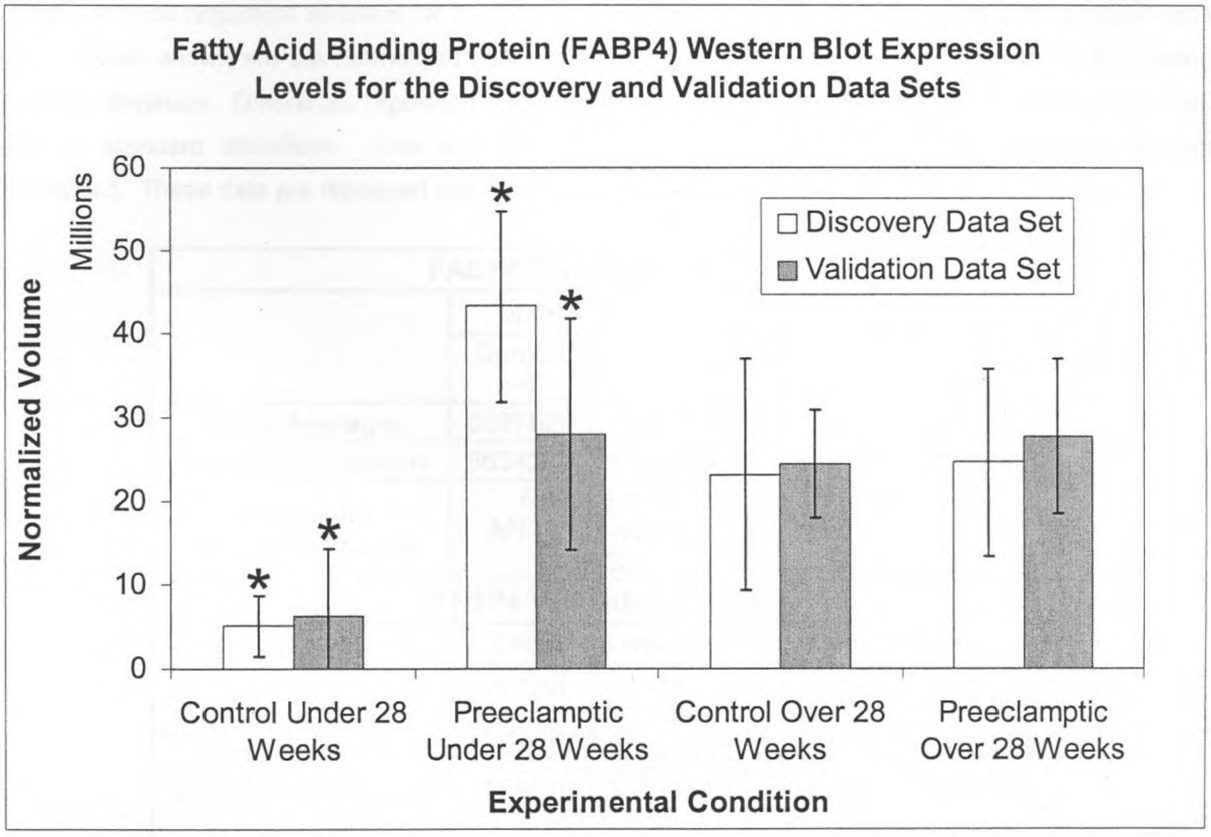

Figure 4.9: Combined results for the fatty acid binding protein (FABP4) western blot protein expression validations in both the discovery and validation data sets. The discovery data set is shown in white while the validation data set is shown in gray. Values are for the average normalized spot volumes for each group. Error bars represent the standard deviation of each test group. Statistically relevant differences are denoted as (*).

Table 4.9: Total regulation statistics for the fatty acid binding protein (FABP4) discovery and validation data sets. Values shown are the normalized spot volume averages for each group as well as the associated standard deviation. Differential regulation values are the average fold difference in the preeclamptic data sets +/- standard deviations. One way ANOVA values are shown to highlight statistically relevant differences. These data are displayed graphically in Figure 2.10.

FABP4 Discovery Data Set				
	Under-28 weeks		Over-28 weeks	
	Control n=5	PE n=5	Control n=6	PE n=6
Group Averages	5097526	43299122	23156783	24705966
Standard Deviations	3624230	11451548	13833129	11174454
Differential Regulation Values	8.49 +/- 6.44 ANOVA p-value = <0.0001		1.06 +/- 0.79 ANOVA p-value = >0.83	
FABP4 Validation Data Set				
	Under-28 weeks		Over-28 weeks	
	Control n=9	PE n=9	Control n=10	PE n=10
Group Averages	6347268	29147290	24438689	27792686
Standard Deviations	8105040	14246549	6510942	9234250
Differential Regulation Values	4.59 +/- 6.27 ANOVA p-value = <0.001		1.13+/- 0.48 ANOVA p-value = > 0.35	

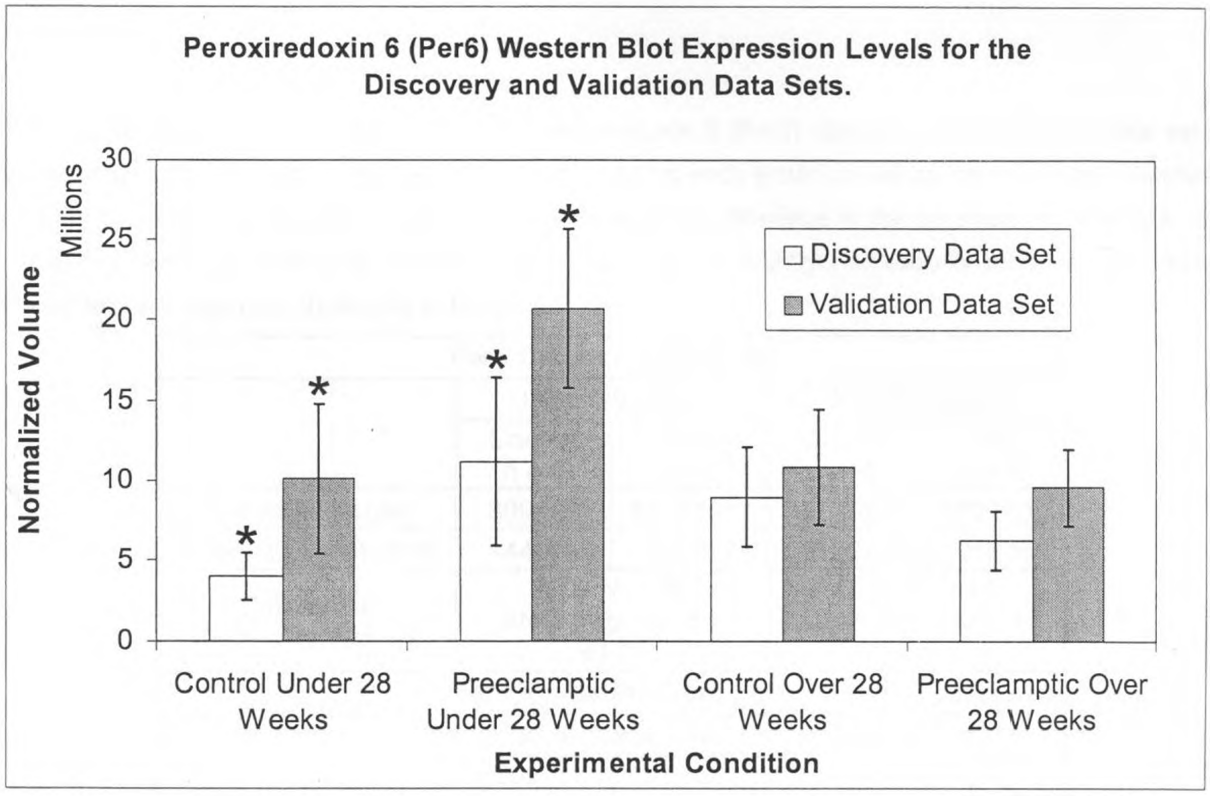

Figure 4.10: Combined results for peroxiredoxin 6 (Per6) western blot protein expression validations in both the discovery and validation data sets. The discovery data set is shown in white while the validation data set is shown in gray. Values are for the average normalized spot volumes for each group. Error bars represent the standard deviation of each test group. Statistically relevant differences are denoted as (*).

Table 4.10: Total regulation statistics for the peroxiredoxin 6 (Per6) discovery and validation data sets. Values shown are the normalized spot volume averages for each group as well as the associated standard deviation. Differential regulation values are the average fold difference in the preeclamptic data sets +/- standard deviations. One way ANOVA values are shown to highlight statistically relevant differences. These data are displayed graphically in Figure 2.11.

Per6 Discovery Data Set				
	Under-28 weeks		Over-28 weeks	
	Control n = 5	PE n = 5	Control n = 6	PE n = 6
Group Averages	3991892	11163517	8939211	6232705
Standard Deviations	1440004	5222873	3122789	1815760
Differential Regulation Values	2.79 +/- 1.65 ANOVA p-value = <0.01		0.69 +/- 0.44 ANOVA p-value = >0.1	
Per6 Validation Data Set				
	Under-28 weeks		Over-28 weeks	
	Control n=9	PE n=9	Control n=10	PE n=10
Group Averages	10095459	20704498	10810546	9574273
Standard Deviations	4679979	4949433	3605970	2400218
Differential Regulation Values	2.05 +/- 1.38 ANOVA p-value = <0.001		0.88 +/- 0.53 ANOVA p-value = >0.39	

Chapter 5
Discussion

5.1 Discussion

5.1.1 Sample Preparation and Extraction

Overall, the isolations, separations, and analyses of proteins from the control and preeclamptic CV samples were successful. As mentioned previously, one of the most significant hurdles overcome in this project was the successful inactivation of endogenous proteases from the samples. Initially, the concentrations of protease inhibitors used in the isolation of sample proteins were not adequate to prevent proteolysis of the sample from occurring; however, an optimized protease inhibitor cocktail was eventually formulated. By increasing the concentration of EDTA in the extraction buffer while holding other protease inhibitor concentrations constant, the unwanted proteolysis of the samples during protein extraction was eliminated. Since an increase in EDTA, a divalent cation chelator, resolved the proteolysis problems seen during the protein extractions, it was postulated (for reasons stated below) that a metalloprotease was the entity responsible for the bulk of the proteolysis observed. It was noted that during protein extraction and 2D gel analysis, the preeclamptic samples were more difficult to extract without the occurrence of the unwanted proteolytic digestion. The high concentrations of EDTA and extensive dialysis required to inhibit proteolysis in these samples may be attributed to the prophylactic treatment of preeclamptic patients with $MgSO_4$ prior to collection of the placenta. In order to prevent maternal seizures associated with eclampsia, $MgSO_4$ is administered to preeclamptic patients in an initial dose of 2-4 grams over 30 min, followed by up to 2 g/h thereafter. It is recognized that the therapeutic concentrations of Mg^{2+} in maternal serum is between 4 - 8 mg/dL or 1.6 - 3.3 mM [70, 71]. This concentration range of Mg^{2+} creates optimal conditions for the high activity of metalloproteases, such as leucine aminopeptidase. Since EDTA exerts its mode of protease inhibition through the binding of divalent cations, such as Mg^{2+} (an essential activator of leucyl aminopeptidase), the presence of high Mg^{2+}

concentrations in maternal and fetal tissues would require a proportional increase in the concentration of EDTA for adequate protease inhibition. Evidence for the presence of a metalloprotease, such as leucyl aminopeptidase and matrix metalloprotease, contributing to the problem of proteolysis is supported by the source data used to compile Figure 4.1. Figure 4.1 illustrates the proportion of intact proteins that were isolated in the initial proteomic analysis of full term CV tissue. The 294 highest abundance proteins visualized after 2D gel analysis were selected from the gel, identified by LC-MS/MS, and the integrity of the proteins was assessed. Of the 270 proteins identified, only 105 proteins were not degraded, among which was leucyl aminopeptidase. Having this proteolytic enzyme present in high concentrations in an un-degraded form, as well as an abundance of Mg^{2+} ions from the $MgSO_4$ prophylactic treatment in preeclamptic patients, may have accounted for the high levels of EDTA and extensive dialysis that were needed to prevent proteolysis of the samples in this study. In order to treat both the control and preeclamptic samples identically the high concentration of EDTA used on the preeclamptic samples was also used on the control samples.

As mentioned previously, considerable effort was invested into the development of a high resolution isoelectric focusing protocol that would allow for the presence of high EDTA concentrations, while still preventing unwanted proteolysis. Because EDTA is an ionic species that could impede the IEF step of the 2D gel analysis, the high concentrations of EDTA in the samples created a considerable problem. Therefore, the development of a sample separation protocol that made high resolution 2D gels possible despite the high, yet necessary, EDTA concentrations, accounted for a substantial portion of the time invested in method development.

5.1.2 Proteins Identified as Being Differentially Expressed

After the successful extraction and 2D gel analysis of the control and preeclamptic samples, 12 proteins were identified with statistical significance as being potential biomarkers of preeclampsia by their differential regulation. These

12 proteins can be divided into five functional groups, including 3 fatty acid metabolism-related proteins, 3 oxidative stress-related proteins, 2 proteins involved with growth regulation and control, 2 proteins involved in the inflammatory response, and 2 proteins with undetermined activity in preeclampsia. Several of the 12 potential preeclamptic biomarkers perform functions that are not fully delineated in preeclamptic pathophysiology and warrant further investigation. While a diverse range of proteins from various functional groups were identified, the majority of the biomarker candidates identified were linked to fatty acid metabolism, or cellular mediators of oxidative stress.

It is well known that in preeclamptic pregnancies, there is a generalized increase in lipids, specifically a buildup of free fatty acids in the maternal blood stream [72, 73]. Several of the differentially regulated proteins identified in this study are directly involved in the metabolism of fatty acids: fatty acid binding protein 4 (FABP4), enoyl-CoA hydratase (ECHS1), and Δ3,5-Δ2,4-dienoyl-CoA isomerase (ECH1). As shown above, FABP4 was validated by western blotting as being differentially expressed in preeclamptic pregnancies. As determined by 2D SDS-PAGE, the 3.7-fold up-regulation of this protein in the preeclamptic CV samples suggests that a maternal excess of free fatty acid exists, which agrees with currently published data [72].

Two additional proteins, ECHS1 and ECH1, were both determined to be down-regulated in preeclampsia by 2.0- and 3.4-fold, respectively. These two proteins were not validated by western blotting since there were no known sources for the antibodies required to do this at the time of writing of this thesis. Both of these proteins are key enzymes required for the β-oxidation of fatty acids [74, 75]. ECHS1 is an essential enzyme in the fatty acid β-oxidation cycle responsible for catalyzing the second step of saturated fatty acid metabolism. [74] Although the β-oxidation cycle requires saturated fatty acids in order to liberate acetyl-CoA through metabolic degradation, not all free fatty acids are saturated. In order for unsaturated fatty acids to enter the β-oxidation cycle, auxiliary isomerization enzymes, such as ECHS1, are needed [75]. It is

important to note that while there is a known free fatty acid increase in preeclampsia, and an increase in FABP4 expression as shown above, it was determined that there is a substantial down-regulation of at least two enzymes that are responsible for the generation of energy through the metabolic degradation of free fatty acids in the preeclamptic samples. The root cause of the free fatty acid buildup in preeclampsia is not fully understood; however, the observation of under-expressed enzymes involved in the β-oxidation of these free fatty acids warrants further investigation of the regulation of this pathway in preeclampsia as a source of potential preeclamptic biomarkers. There is no restriction stating that a preeclamptic biomarker has to be a protein; in fact, specific lipids or oxidized lipids may very well prove to be ideal biomarkers. Since a clinically useful biomarker should be soluble in the maternal blood stream, circulating free fatty acid derivatives could potentially make ideal preeclamptic biomarkers.

In addition to the lipid metabolism defects that are present in preeclampsia, there is also ample evidence that supports that oxidative stress plays a major role in the pathophysiology of preeclampsia [76]. Oxidative stress is characterized by reactive oxygen species (ROS), such as superoxides and hydroperoxides, causing oxidative damage to cellular components and resulting in the production of oxidized proteins, lipid peroxides, and DNA damage [77]. One mechanism of oxidative stress initiation is hypoxia, a condition of low oxygen availability, which is a well characterized physiological condition of preeclampsia [31].

In this study, three differentially regulated proteins related to oxidative stress were identified. Of these proteins, the antioxidant protein Per6 and heat shock protein β-1 (HSP27) are involved in the mediation of oxidative stress. Another protein, stathmin - a microtubule destabilizing protein, is differentially regulated in response to oxidative stress. Per6 and HSP27, proteins largely involved in the limitation of cellular damage in response to oxidative stress [78, 79], are up-regulated in the preeclamptic samples by factors of 2.7 and 2-fold, respectively. Both Per6 and HSP27 have antioxidant activities and have been

shown to reduce lipid and protein peroxides present due to oxidative stress [78, 80-82]. Conversely, stathmin was down-regulated by a factor of 2.1 in preeclampsia, and has been found in other studies to be down-regulated in response to oxidative damage [83]. While Per6 and HSP27 limit the damage done in the cell by oxidative stress, stathmin has been shown to be regulated by oxidized low density lipoprotein (oxLDL), a product of oxidative stress [84]. Recent findings have shown that in response to oxLDL, stathmin expression is down-regulated and the phosphorylated form of stathmin is increased [83]. While the actions of these three proteins may or may not act in a cohesive manner, it has been shown that in response to oxidative stress, these same three proteins are regulated in a nearly identical manner as determined in this study [85]. In the work of Strey and coworkers (2004), a mouse knockout model of superoxide dismutase (SOD) was constructed that lacked the ability to convert superoxides to hydrogen peroxide and oxygen. Upon a proteomic analysis of this mutant, it was found that Per6 and HSP27 were both up-regulated and stathmin was down-regulated in response to oxidative stress [85]. Our study showed that the same three proteins identified as differentially regulated in the oxidative stress mouse mutant [85] are differentially regulated in preeclamptic pregnancies. These results support the hypothesis that Per6, HSP27 and stathmin are all differentially regulated in preeclamptic CV samples in response to oxidative stress.

Preeclampsia produces a diverse range of maternal symptoms. While many discrete physiological events are known to give rise to preeclampsia, there is still no link between the placental defects that are the root of preeclampsia and the widespread maternal symptoms that are observed as this disease progresses. While proteins identified as being involved in lipid metabolism and oxidative stress may be involved in localized imbalances within the placenta, two additional differentially regulated proteins were identified that play a broader role in inflammatory response.

In preeclampsia, it is well known that diverse maternal endothelial damage is present, including general endothelial activation, vascular injury, vasospasm and microthrombosis [86]. Endothelial activation in particular creates a situation

with a vigorous inflammatory response. Two proteins involved in the inflammatory response that were found to be differentially regulated in the preeclamptic CV samples were lipocortin (LPC1) and prostaglandin dehydrogenase 1 (PGDH1). Prostaglandins, which are potent mediators of inflammation, are inactivated by PGDH1 through oxidation of the 15(S) – hydroxyl group. [87] As prostaglandins are produced in response to inflammation, an up-regulation in PDGH1 would assist in reducing prostaglandin activity and hence, prostaglandin-initiated inflammation. In this study, it was determined that PGDH1 is up-regulated by a factor of 2 in the preeclamptic samples. Current research has shown that in preeclamptic pregnancies, there is increased expression of prostaglandins associated with this disease. [88] The up-regulation of this anti-inflammatory protein would assist in the mediation of the maternal inflammatory response, which plays a known role in the pathophysiology of preeclampsia. [29, 89]

In contrast to the up-regulation of PDGH1, LPC1 was determined to be down-regulated by a factor of 2.4 in the preeclamptic samples. The observed down-regulation of LPC1, a potent anti-inflammatory molecule, is disadvantageous in the context of preeclampsia. [90] These findings are contradictory, since an increase in the expression of an anti-inflammatory protein should help mediate the state of inflammation seen in preeclampsia. Why is there a down regulation of LPC1 in a condition where you would expect it to be up-regulated? While this question has yet to be examined, the findings of this study should lead to a further investigation into the role of this molecule in the pathology of preeclampsia, and its possible use as a biomarker of preeclampsia.

Two additional proteins that are differentially expressed in preeclampsia are proliferation-associated protein 2G4 (PA2G4) and estradiol 17-beta-dehydrogenase (HSD17B1). Both of these proteins perform functions that are related to the metabolism of estrogen precursors. PA2G4 is also known to function as a growth regulatory molecule [91, 92]. PA2G4 has not previously been implicated in the pathology of preeclampsia. One of the known functions of PA2G4 is to repress the transcription of estrogen precursors [92]. In this study, it

was found that PA2G4 was down-regulated by 2.7-fold in the preeclamptic samples, which could indicate the potential down-regulation of estrogen precursor transcription in preeclamptic pregnancies. In this study, it was also noted that HSD17B1, a protein responsible for the conversion of estrogen precursors to estradiol, [93] was down-regulated by 2.0-fold in the preeclamptic samples. Again, the down-regulation of these two proteins, which play a role in estrogen biosynthesis, in preeclamptic pregnancies is not currently known, but this finding may provide a starting point for further discovery of preeclamptic biomarkers.

The final two proteins that were identified in this study are human placental growth hormone, or chorionic sommatomammotropin hormone (CSH1), and macrophage capping protein (CAPG). Neither of these proteins have been previously associated with preeclampsia as direct causative agents. However, CSH1 is currently under investigation as a putative preeclamptic biomarker.[28] CSH1 plays a strong role in fetal growth, metabolism, and lactation stimulation in the mother. [94] It has been previously shown that in preeclamptic pregnancies, there is a decrease in CSH1 in the maternal circulation [24]; this finding agrees with the discovery of the 2.5-fold down-regulation of CSH1 in this study. While this protein is a putative preeclamptic biomarker, the exact mechanism of its action in this disease remains to be determined and further research will ultimately prove its efficacy in this application. [28, 45]

After an extensive literature review, it was found that CAPG has not previously been reported as being differentially regulated in preeclampsia. The action of this protein – its binding to the barbed ends of actin filaments - has been previously postulated to play an important role in the correct functioning of macrophages. [95, 96] While this study identified CAPG as being up-regulated in preeclampsia by a factor of 2.2, the exact role of this protein in the onset or progression of preeclampsia remains to be elucidated.

While the significance of several proteins identified in this study have yet to be determined in the context of preeclampsia, many of these differentially expressed proteins have been implicated in preeclamptic pathology. Figure 5.1

illustrates the proteins identified in this study that have been grouped into functional categories based on published data. Many of the proteins that were identified belong to similar metabolic processes and this may provide insight towards further avenues for preeclamptic biomarker discovery. The majority of the proteins identified in this study were from the under-28 week samples, an advantageous finding since putative preeclamptic biomarkers would hold more promise as a clinical tool if they are present in the earliest stages of pregnancy.

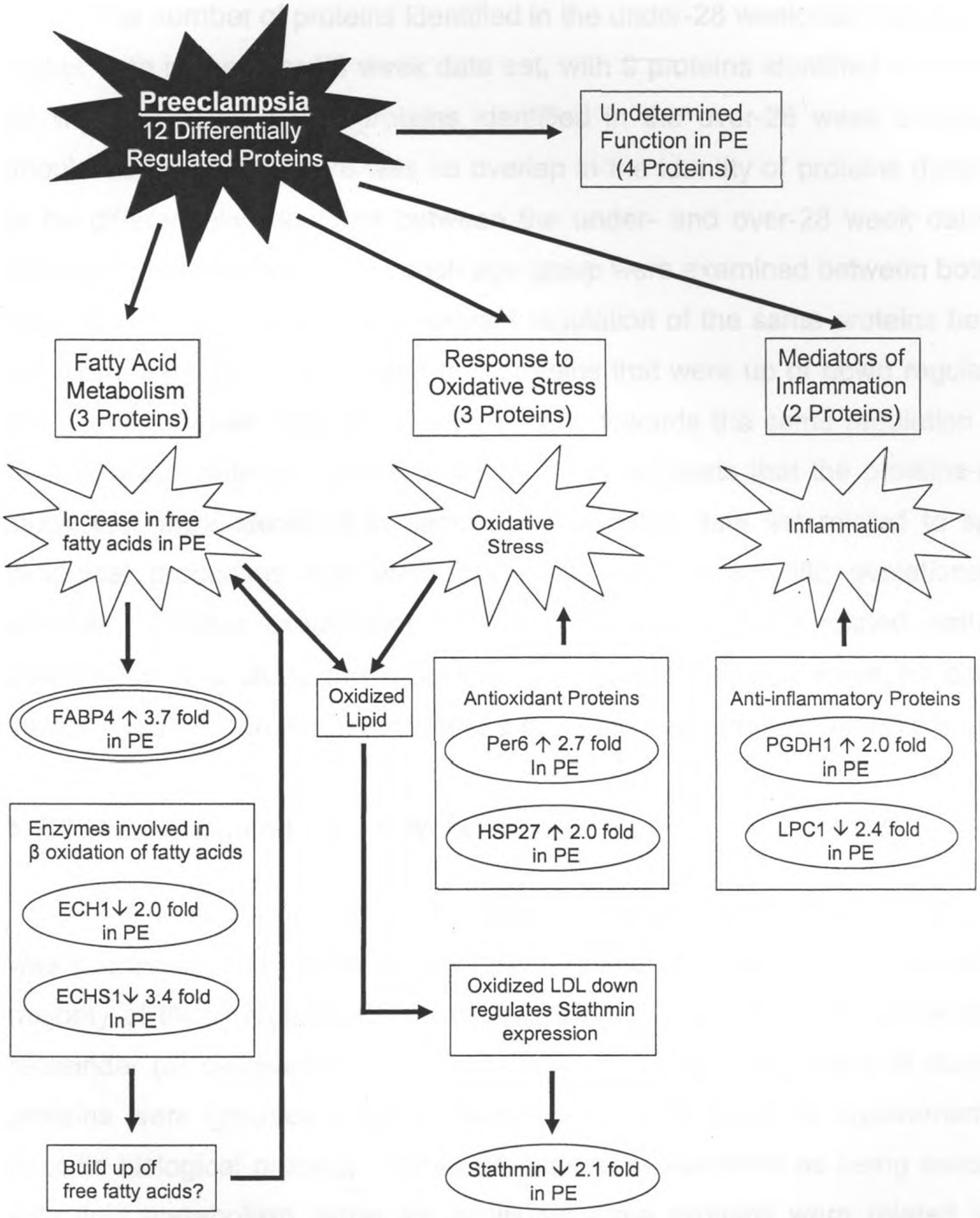

Figure 5.1: Functional groupings of the proteins that were identified as being differentially regulated in preeclampsia

The number of proteins identified in the under-28 week data set was 3-fold higher than in the over-28 week data set, with 9 proteins identified in the under-28 week samples and 3 proteins identified in the over-28 week samples. It should be noted that there was no overlap in the identity of proteins determined to be differentially regulated between the under- and over-28 week data sets. Although proteins identified in each age group were examined between both data sets, there was no statistically relevant regulation of the same proteins between the two data sets. It was noted that proteins that were up or down regulated in the under-28 week data set showed a trend towards the same regulation in the over-28 week data set, and vice versa. This suggests that the proteins in this study that were identified in each age-dependent data set related to specific biological processes that were occurring within a specific gestational age window. Further examination of the proteins (and their related pathways) identified in this study are required. Potentially, they will serve as cohesive starting points in the determination of a panel of preeclamptic biomarkers.

5.2 Conclusions and Future Work

The analysis of control and preeclamptic CV samples by 2D SDS-PAGE was successful and twelve differentially regulated proteins were identified. The majority of these proteins (9) were found in the under-28 week sample set, the remainder (3) discovered in the over-28 week sample set. Several clusters of proteins were grouped together based on their function or involvement in a specific biological process. Three proteins were identified as being associated with lipid metabolism, while an additional three proteins were related to one another with respect to their modulation, or response to oxidative stress.

Further examination of the metabolism of fatty acids, or of fatty acids themselves, could yield clues as to what is initiating the maternal symptoms of preeclampsia and could enhance the discovery of clinically useful preeclamptic biomarkers. Additionally, a comprehensive examination of proteins involved in the modulation of oxidative stress may show a link between the build up of free

fatty acids and the damage that is caused by oxidized lipid and lipid peroxides. Both of these biological processes are suitable candidates for further studies in the causation of preeclampsia and in the biomarker discovery process.

While the analysis of the samples used in this study was performed using the largest format and highest resolution 2D gels available, there are potentially thousands of proteins that are below the detection limit of this technology. Since many of these undetectable proteins could play a role in preeclamptic pathology, additional proteomic technologies will need to replace 2D gel analysis of subsequent sample sets. The sensitivity and quantitation technologies that are currently being developed in the field of MS may allow for a more comprehensive examination of the protein, or alternatively, the lipid constituents in future preeclamptic samples.

Future work to determine the relevance of the identified proteins and putative pathways that have been identified in this study will undoubtedly require the involvement of high resolution, robust, MS-based analyses. Subsequent analyses of control and preeclamptic samples will focus on the differences associated with maternal serum lipid levels and the effects of oxidative stress on the lipid environment.

References

1. MacKay, A.P., C.J. Berg, and H.K. Atrash, *Pregnancy-related mortality from preeclampsia and eclampsia.* Obstet Gynecol, 2001. **97**(4): p. 533-8.
2. Goodwin, A.A. and B.M. Mercer, *Does maternal race or ethnicity affect the expression of severe preeclampsia?* Am J Obstet Gynecol, 2005. **193**(3 Pt 2): p. 973-8.
3. Higgins, J.R. and S.P. Brennecke, *Pre-eclampsia--still a disease of theories?* Curr Opin Obstet Gynecol, 1998. **10**(2): p. 129-33.
4. Myatt, L., *Role of placenta in preeclampsia.* Endocrine, 2002. **19**(1): p. 103-11.
5. Roberts, J.M. and H.S. Gammill, *Preeclampsia: recent insights.* Hypertension, 2005. **46**(6): p. 1243-9.
6. Roberts, J.M., James M.; Pearson, Gail; Cutler, Jeff; Lindheimer, Marshall., *Summary of the NHLBI Working Group on Research on Hypertension During Pregnancy.* Hypertension, 2003. **41**(3): p. 437-45.
7. Levine, R.J., et al., *Circulating angiogenic factors and the risk of preeclampsia.* N Engl J Med, 2004. **350**(7): p. 672-83.
8. Lam, C., K.H. Lim, and S.A. Karumanchi, *Circulating angiogenic factors in the pathogenesis and prediction of preeclampsia.* Hypertension, 2005. **46**(5): p. 1077-85.
9. Moseman, C.P. and S. Shelton, *Permanent blindness as a complication of pregnancy induced hypertension.* Obstet Gynecol, 2002. **100**(5 Pt 1): p. 943-5.
10. Royburt, M., et al., *Neurologic involvement in hypertensive disease of pregnancy.* Obstet Gynecol Surv, 1991. **46**(10): p. 656-64.
11. Kenny, L. and P.N. Baker, *Maternal pathophysiology in pre-eclampsia.* Baillieres Best Pract Res Clin Obstet Gynaecol, 1999. **13**(1): p. 59-75.
12. Stennett, A.K. and R.A. Khalil, *Neurovascular mechanisms of hypertension in pregnancy.* Curr Neurovasc Res, 2006. **3**(2): p. 131-48.
13. Hernandez, C. and F.G. Cunningham, *Eclampsia.* Clin Obstet Gynecol, 1990. **33**(3): p. 460-6.
14. Ramsey, P.S., Van Winter, J. T.Gaffey, T. A.Ramin, K. D., *Eclampsia complicating hydatidiform molar pregnancy with a coexisting, viable fetus. A case report.* J Reprod Med, 1998. **43**(5): p. 456-8.
15. <http://www.fofweb.com/Electronic_Images/onfiles/SciHumAnat9-27c.gif>.
16. Gude, N.M., Roberts, C. T. Kalionis, B. King, R. G., *Growth and function of the normal human placenta.* Thromb Res, 2004. **114**(5-6): p. 397-407.
17. Kaufmann, P., S. Black, and B. Huppertz, *Endovascular trophoblast invasion: implications for the pathogenesis of intrauterine growth retardation and preeclampsia.* Biol Reprod, 2003. **69**(1): p. 1-7.
18. <http://www.bartleby.com/107/pages/page64.html>.
19. Morrish, D.W., J. Dakour, and H. Li, *Functional regulation of human trophoblast differentiation.* J Reprod Immunol, 1998. **39**(1-2): p. 179-95.
20. Malassine, A. and L. Cronier, *Hormones and human trophoblast differentiation: a review.* Endocrine, 2002. **19**(1): p. 3-11.

21. Castellucci, M., Kosanke, G. Verdenelli, F. Huppertz, B. Kaufmann, P., *Villous sprouting: fundamental mechanisms of human placental development.* Hum Reprod Update, 2000. **6**(5): p. 485-94.
22. Goldman-Wohl, D. and S. Yagel, *Regulation of trophoblast invasion: from normal implantation to pre-eclampsia.* Mol Cell Endocrinol, 2002. **187**(1-2): p. 233-8.
23. Myatt, L. and X. Cui, *Oxidative stress in the placenta.* Histochem Cell Biol, 2004. **122**(4): p. 369-82.
24. Bersinger, N.A. and R.A. Odegard, *Second- and third-trimester serum levels of placental proteins in preeclampsia and small-for-gestational age pregnancies.* Acta Obstet Gynecol Scand, 2004. **83**(1): p. 37-45.
25. Bersinger, N.A., et al., *Women with preeclampsia have increased serum levels of pregnancy-associated plasma protein A (PAPP-A), inhibin A, activin A and soluble E-selectin.* Hypertens Pregnancy, 2003. **22**(1): p. 45-55.
26. Budak, E., Madazli, R. Aksu, M. F. Benian, A. Gezer, A. Palit, N. Yildizfer, F., *Vascular cell adhesion molecule-1 (VCAM-1) and leukocyte activation in pre-eclampsia and eclampsia.* Int J Gynaecol Obstet, 1998. **63**(2): p. 115-21.
27. Conrad, K.P. and D.F. Benyo, *Placental cytokines and the pathogenesis of preeclampsia.* Am J Reprod Immunol, 1997. **37**(3): p. 240-9.
28. Smets, E.M., et al., *Novel biomarkers in preeclampsia.* Clin Chim Acta, 2006. **364**(1-2): p. 22-32.
29. Redman, C.W. and I.L. Sargent, *Pre-eclampsia, the placenta and the maternal systemic inflammatory response--a review.* Placenta, 2003. **24 Suppl A**: p. S21-7.
30. Sankaralingam, S., Arenas, I. A. Lalu, M. M. Davidge, S. T., *Preeclampsia: current understanding of the molecular basis of vascular dysfunction.* Expert Rev Mol Med, 2006. **8**(3): p. 1-20.
31. Roberts, J.M. and K.Y. Lain, *Recent Insights into the pathogenesis of pre-eclampsia.* Placenta, 2002. **23**(5): p. 359-72.
32. Mignini, L.E., J. Villar, and K.S. Khan, *Mapping the theories of preeclampsia: the need for systematic reviews of mechanisms of the disease.* Am J Obstet Gynecol, 2006. **194**(2): p. 317-21.
33. Salas, S.P., *What causes pre-eclampsia?* Baillieres Best Pract Res Clin Obstet Gynaecol, 1999. **13**(1): p. 41-57.
34. Carr, D.B., Epplein, M. Johnson, C. O. Easterling, T. R. Critchlow, C. W., *A sister's risk: family history as a predictor of preeclampsia.* Am J Obstet Gynecol, 2005. **193**(3 Pt 2): p. 965-72.
35. Trupin, L.S., L.P. Simon, and B. Eskenazi, *Change in paternity: a risk factor for preeclampsia in multiparas.* Epidemiology, 1996. **7**(3): p. 240-4.
36. Sud, S.S., Gupta, I. Dhaliwal, L. K. Kaur, B. Ganguly, N. K., *Serial plasma fibronectin levels in pre-eclamptic and normotensive women.* Int J Gynaecol Obstet, 1999. **66**(2): p. 123-8.
37. Islami, D., Shoukir, Y. Dupont, P. Campana, A. Bischof, P., *Is cellular fibronectin a biological marker for pre-eclampsia?* Eur J Obstet Gynecol Reprod Biol, 2001. **97**(1): p. 40-5.

38. Conde-Agudelo, A., R. Lede, and J. Belizan, *Evaluation of methods used in the prediction of hypertensive disorders of pregnancy.* Obstet Gynecol Surv, 1994. **49**(3): p. 210-22.
39. Hietala, R., U. Turpeinen, and T. Laatikainen, *Serum homocysteine at 16 weeks and subsequent preeclampsia.* Obstet Gynecol, 2001. **97**(4): p. 527-9.
40. Sorensen, T.K., Williams, M. A. Zingheim, R. W. Clement, S. J. Hickok, D. E., *Elevated second-trimester human chorionic gonadotropin and subsequent pregnancy-induced hypertension.* Am J Obstet Gynecol, 1993. **169**(4): p. 834-8.
41. Lachmeijer, A.M., Arngrimsson, R. Bastiaans, E. J. Pals, G. ten Kate, L. P. de Vries, J. I. Kostense, P. J. Aarnoudse, J. G. Dekker, G. A., *Mutations in the gene for methylenetetrahydrofolate reductase, homocysteine levels, and vitamin status in women with a history of preeclampsia.* Am J Obstet Gynecol, 2001. **184**(3): p. 394-402.
42. Fayyad, A.M. and K.F. Harrington, *Prediction and prevention of preeclampsia and IUGR.* Early Hum Dev, 2005. **81**(11): p. 865-76.
43. Daniel, Y., Kupferminc, M. J. Baram, A. Jaffa, A. J. Fait, G. Wolman, I. Lessing, J. B., *Plasma interleukin-12 is elevated in patients with preeclampsia.* Am J Reprod Immunol, 1998. **39**(6): p. 376-80.
44. Conrad, K.P., T.M. Miles, and D.F. Benyo, *Circulating levels of immunoreactive cytokines in women with preeclampsia.* Am J Reprod Immunol, 1998. **40**(2): p. 102-11.
45. Kupferminc, M.J., Daniel, Y. Englender, T. Baram, A. any, A. Jaffa, A. J. Gull, I. Lessing, J. B., *Vascular endothelial growth factor is increased in patients with preeclampsia.* Am J Reprod Immunol, 1997. **38**(4): p. 302-6.
46. Karumanchi, S.A. and I.E. Stillman, *In vivo rat model of preeclampsia.* Methods Mol Med, 2006. **122**: p. 393-9.
47. Park, C.W., Park, J. S. Shim, S. S. Jun, J. K. Yoon, B. H. Romero, R., *An elevated maternal plasma, but not amniotic fluid, soluble fms-like tyrosine kinase-1 (sFlt-1) at the time of mid-trimester genetic amniocentesis is a risk factor for preeclampsia.* Am J Obstet Gynecol, 2005. **193**(3 Pt 2): p. 984-9.
48. Aebersold, R. and M. Mann, *Mass spectrometry-based proteomics.* Nature, 2003. **422**(6928): p. 198-207.
49. Wolters, D.A., M.P. Washburn, and J.R. Yates, 3rd, *An automated multidimensional protein identification technology for shotgun proteomics.* Anal Chem, 2001. **73**(23): p. 5683-90.
50. Pasa-Tolic, L., Masselon, C. Barry, R. C. Shen, Y. Smith, R. D., *Proteomic analyses using an accurate mass and time tag strategy.* Biotechniques, 2004. **37**(4): p. 621-4, 626-33, 636 passim.
51. Ong, S.E. and M. Mann, *Mass spectrometry-based proteomics turns quantitative.* Nat Chem Biol, 2005. **1**(5): p. 252-62.
52. Gygi, S.P., Rist, B. Gerber, S. A. Turecek, F. Gelb, M. H. Aebersold, R., *Quantitative analysis of complex protein mixtures using isotope-coded affinity tags.* Nat Biotechnol, 1999. **17**(10): p. 994-9.
53. Smolka, M.B., et al., *Optimization of the isotope-coded affinity tag-labeling procedure for quantitative proteome analysis.* Anal Biochem, 2001. **297**(1): p. 25-31.

54. Ong, S.E., Blagoev, B. Kratchmarova, I. Kristensen, D. B. Steen, H. Pandey, A. Mann, M., *Stable isotope labeling by amino acids in cell culture, SILAC, as a simple and accurate approach to expression proteomics.* Mol Cell Proteomics, 2002. **1**(5): p. 376-86.
55. Leitner, A. and W. Lindner, *Current chemical tagging strategies for proteome analysis by mass spectrometry.* J Chromatogr B Analyt Technol Biomed Life Sci, 2004. **813**(1-2): p. 1-26.
56. Thiede, B., Hohenwarter, W. Krah, A. Mattow, J. Schmid, M. Schmidt, F. Jungblut, P. R., *Peptide mass fingerprinting.* Methods, 2005. **35**(3): p. 237-47.
57. Chernushevich, I.V., A.V. Loboda, and B.A. Thomson, *An introduction to quadrupole-time-of-flight mass spectrometry.* J Mass Spectrom, 2001. **36**(8): p. 849-65.
58. Glish, G.L. and R.W. Vachet, *The basics of mass spectrometry in the twenty-first century.* Nat Rev Drug Discov, 2003. **2**(2): p. 140-50.
59. Anderson, N.L. and N.G. Anderson, *The human plasma proteome: history, character, and diagnostic prospects.* Mol Cell Proteomics, 2002. **1**(11): p. 845-67.
60. Gorg, A., Obermaier, C. Boguth, G. Harder, A. Scheibe, B. Wildgruber, R. Weiss, W., *The current state of two-dimensional electrophoresis with immobilized pH gradients.* Electrophoresis, 2000. **21**(6): p. 1037-53.
61. Rabilloud, T., *Solubilization of proteins for electrophoretic analyses.* Electrophoresis, 1996. **17**(5): p. 813-29.
62. Candiano, G., Bruschi, M. Musante, L. Santucci, L. Ghiggeri, G. M. Carnemolla, B. Orecchia, P. Zardi, L. Righetti, P. G., *Blue silver: a very sensitive colloidal Coomassie G-250 staining for proteome analysis.* Electrophoresis, 2004. **25**(9): p. 1327-33.
63. Chevallet, M., Diemer, H. Luche, S. van Dorsselaer, A. Rabilloud, T. Leize-Wagner, E., *Improved mass spectrometry compatibility is afforded by ammoniacal silver staining.* Proteomics, 2006. **6**(8): p. 2350-4.
64. Lee, C., A. Levin, and D. Branton, *Copper staining: a five-minute protein stain for sodium dodecyl sulfate-polyacrylamide gels.* Anal Biochem, 1987. **166**(2): p. 308-12.
65. Lanne, B. and O. Panfilov, *Protein staining influences the quality of mass spectra obtained by peptide mass fingerprinting after separation on 2-d gels. A comparison of staining with coomassie brilliant blue and sypro ruby.* J Proteome Res, 2005. **4**(1): p. 175-9.
66. Chevalier, F., Rofidal, V. Vanova, P. Bergoin, A. Rossignol, M., *Proteomic capacity of recent fluorescent dyes for protein staining.* Phytochemistry, 2004. **65**(11): p. 1499-506.
67. http://www-medlib.med.utah.edu/WebPath/PLACHTML/PLAC032.html.
68. Wheelock, A.M. and A.R. Buckpitt, *Software-induced variance in two-dimensional gel electrophoresis image analysis.* Electrophoresis, 2005. **26**(23): p. 4508-20.
69. Zeeberg, B.R., et al., *GoMiner: a resource for biological interpretation of genomic and proteomic data.* Genome Biol, 2003. **4**(4): p. R28.

70. Mantle, D., B. Lauffart, and A. Gibson, *Purification and characterization of leucyl aminopeptidase and pyroglutamyl aminopeptidase from human skeletal muscle.* Clin Chim Acta, 1991. **197**(1): p. 35-45.
71. Yoshida, M., Matsuda, Y. Akizawa, Y. Ono, E. Ohta, H., *Serum ionized magnesium during magnesium sulfate administration for preterm labor and preeclampsia.* Eur J Obstet Gynecol Reprod Biol, 2005.
72. Hubel, C.A., McLaughlin, M. K. Evans, R. W. Hauth, B. A. Sims, C. J. Roberts, J. M., *Fasting serum triglycerides, free fatty acids, and malondialdehyde are increased in preeclampsia, are positively correlated, and decrease within 48 hours post partum.* Am J Obstet Gynecol, 1996. **174**(3): p. 975-82.
73. Sattar, N., Bendomir, A. Berry, C. Shepherd, J. Greer, I. A. Packard, C. J., *Lipoprotein subfraction concentrations in preeclampsia: pathogenic parallels to atherosclerosis.* Obstet Gynecol, 1997. **89**(3): p. 403-8.
74. Agnihotri, G. and H.W. Liu, *Enoyl-CoA hydratase. reaction, mechanism, and inhibition.* Bioorg Med Chem, 2003. **11**(1): p. 9-20.
75. Hiltunen, J.K., Filppula, S. A. Koivuranta, K. T. Siivari, K. Qin, Y. M. Hayrinen, H. M., *Peroxisomal beta-oxidation and polyunsaturated fatty acids.* Ann N Y Acad Sci, 1996. **804**: p. 116-28.
76. Scholl, T.O., Leskiw, M. Chen, X. Sims, M. Stein, T. P., *Oxidative stress, diet, and the etiology of preeclampsia.* Am J Clin Nutr, 2005. **81**(6): p. 1390-6.
77. Gille, G. and K. Sigler, *Oxidative stress and living cells.* Folia Microbiol (Praha), 1995. **40**(2): p. 131-52.
78. Manevich, Y. and A.B. Fisher, *Peroxiredoxin 6, a 1-Cys peroxiredoxin, functions in antioxidant defense and lung phospholipid metabolism.* Free Radic Biol Med, 2005. **38**(11): p. 1422-32.
79. Papp, E., Nardai, G. Soti, C. Csermely, P., *Molecular chaperones, stress proteins and redox homeostasis.* Biofactors, 2003. **17**(1-4): p. 249-57.
80. Arrigo, A.P., *Hsp27: novel regulator of intracellular redox state.* IUBMB Life, 2001. **52**(6): p. 303-7.
81. Preville, X., Salvemini, F. Giraud, S. Chaufour, S. Paul, C. Stepien, G. Ursini, M. V. Arrigo, A. P., *Mammalian small stress proteins protect against oxidative stress through their ability to increase glucose-6-phosphate dehydrogenase activity and by maintaining optimal cellular detoxifying machinery.* Exp Cell Res, 1999. **247**(1): p. 61-78.
82. Arrigo, A.P., *Small stress proteins: chaperones that act as regulators of intracellular redox state and programmed cell death.* Biol Chem, 1998. **379**(1): p. 19-26.
83. Kinumi, T., Ogawa, Y. Kimata, J. Saito, Y. Yoshida, Y. Niki, E., *Proteomic characterization of oxidative dysfunction in human umbilical vein endothelial cells (HUVEC) induced by exposure to oxidized LDL.* Free Radic Res, 2005. **39**(12): p. 1335-44.
84. Yamashita, H., Nakamura, K. Arai, H. Furumoto, H. Fujimoto, M. Kashiwagi, S. Morimatsu, M., *Electrophoretic studies on the phosphorylation of stathmin and mitogen-activated protein kinases in neuronal cell death induced by oxidized very-low-density lipoprotein with apolipoprotein E.* Electrophoresis, 2002. **23**(7-8): p. 998-1004.

85. Strey, C.W., Spellman, D. Stieber, A. Gonatas, J. O. Wang, X. Lambris, J. D. Gonatas, N. K., *Dysregulation of stathmin, a microtubule-destabilizing protein, and up-regulation of Hsp25, Hsp27, and the antioxidant peroxiredoxin 6 in a mouse model of familial amyotrophic lateral sclerosis.* Am J Pathol, 2004. **165**(5): p. 1701-18.
86. Roberts, J.M., et al., *Preeclampsia: an endothelial cell disorder.* Am J Obstet Gynecol, 1989. **161**(5): p. 1200-4.
87. Tai, H.H., et al., *Prostaglandin catabolizing enzymes.* Prostaglandins Other Lipid Mediat, 2002. **68-69**: p. 483-93.
88. Ishihara, O., et al., *Isoprostanes, prostaglandins and tocopherols in pre-eclampsia, normal pregnancy and non-pregnancy.* Free Radic Res, 2004. **38**(9): p. 913-8.
89. Contreras, F., et al., *Endothelium and hypertensive disorders in pregnancy.* Am J Ther, 2003. **10**(6): p. 415-22.
90. Kamal, A.M., R.J. Flower, and M. Perretti, *An overview of the effects of annexin 1 on cells involved in the inflammatory process.* Mem Inst Oswaldo Cruz, 2005. **100 Suppl 1**: p. 39-47.
91. Yoo, J.Y., et al., *Interaction of the PA2G4 (EBP1) protein with ErbB-3 and regulation of this binding by heregulin.* Br J Cancer, 2000. **82**(3): p. 683-90.
92. Zhang, Y., et al., *Repression of androgen receptor mediated transcription by the ErbB-3 binding protein, Ebp1.* Oncogene, 2002. **21**(36): p. 5609-18.
93. Allan, G.M., et al., *Novel, potent inhibitors of 17beta-hydroxysteroid dehydrogenase type 1.* Mol Cell Endocrinol, 2006. **248**(1-2): p. 204-7.
94. Walsh, S.T. and A.A. Kossiakoff, *Crystal structure and site 1 binding energetics of human placental lactogen.* J Mol Biol, 2006. **358**(3): p. 773-84.
95. Mishra, V.S., et al., *The human actin-regulatory protein cap G: gene structure and chromosome location.* Genomics, 1994. **23**(3): p. 560-5.
96. Witke, W., et al., *Comparisons of CapG and gelsolin-null macrophages: demonstration of a unique role for CapG in receptor-mediated ruffling, phagocytosis, and vesicle rocketing.* J Cell Biol, 2001. **154**(4): p. 775-84.

Appendix 1

Phoretix 2D Expressions Analysis Protocol.

With the exception of having high quality, high resolution 2D gel images to analyze, the most critical step in the determination of differentially expressed proteins between multiple samples separated by 2D gel, is the careful and thorough software based analysis of the gel images. Although most 2D gel analysis software packages state that they are fully automated, rarely, if ever, is a complex analysis of multiple samples devoid of manual manipulations. In this study most of the software based steps in the analysis of the under and over 28 week sample sets were done by hand with the exception of the actual spot detection. As a general rule, 2D gel analysis using Phoretix 2D Expressions™ adheres to the following path of analytical functions. Spots are detected on the gels, noise spots are removed, the background is subtracted from each spot, the images are warped to a master reference gel, spots between all of the gels are matched, individual gels are normalized and comparisons are made to determine differentially expressed proteins. In practice all of these functions are essential; however additional manual manipulations are occasionally required. The entire software based analysis protocol is complex and tedious; however the following describes the actual steps that were taken in the analysis of the 2D gels in this study. The following steps outline the analysis of the under 28 week sample set and it should be noted that the over 28 week sample set was analyzed in an identical manner.

As mentioned previously, high quality gel images were prepared from all of the 2D gels run in this study. Prior to spot detection and differential analysis the gels were separated *in silico* into two groups, one group containing all of the control samples and one group containing all of the preeclamptic samples. From each of these groups a single gel, usually the gel with the highest resolution, was selected to become an *in silico* average of all of the spots present in its respective group. Furthermore, one of the two theoretical averaged gels was selected to be a master reference for all comparisons in the experiment. At this

point the experimental layout for a hypothetical sample set of three control gel and three preeclamptic gels would look like what is shown in figure A1.1.

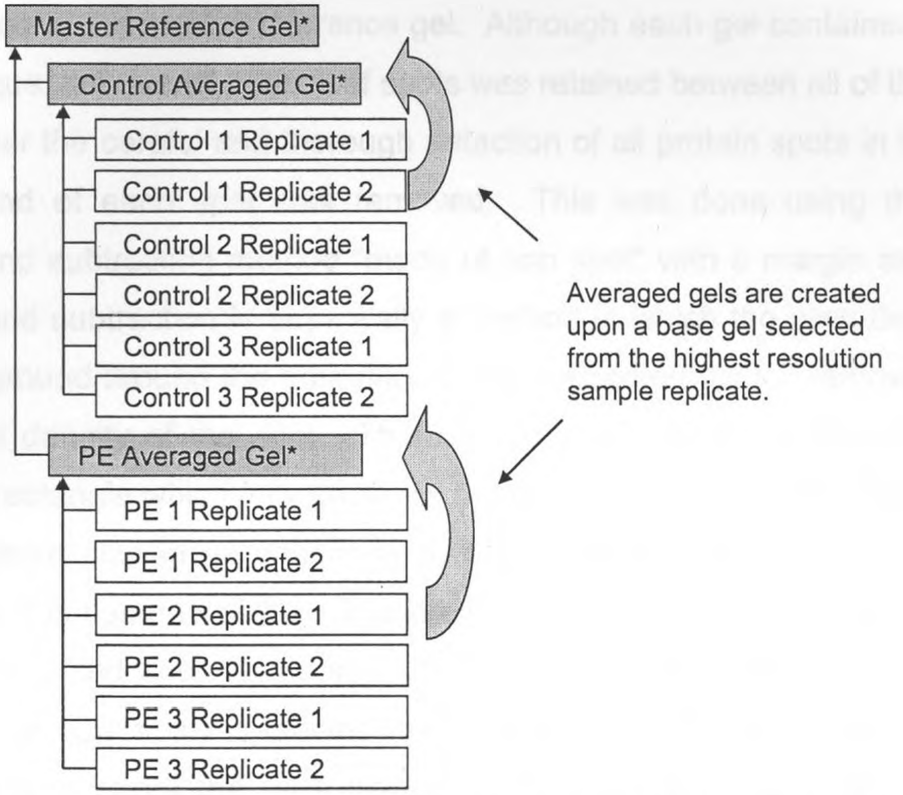

Figure A1.1: The layout of the Phoretix 2D Expressions analysis. Group averages are based upon one of the sample replicates within that group. These averages are based on the averaging parameters applied once all of the spots within a particular group are matched to one another. The master reference gel is based upon one of the two averaged gels and comprised of spots added using identical averaging parameters as in the control and preeclamptic averages. * Note that the shaded boxes represent gels that are not real, but computer generated catalogs of all spots present in a particular group, or in the case of the master reference gel, in the whole experiment.

After the experiment was set up, all gels were subjected to spot detection using the "2005 detection" algorithm supplied with the Phoretix software. Spot detection resulted in all of the protein spots in the gel being encompassed by a boundary that represented the entire volume of the spot in terms of pixel density. This value of the total pixel density within the boundary of the spot is called the spot volume. While this detects all of the protein spots in the gel it also detects noise and artifacts in the gel image. In order to successfully compare protein spots between multiple gels it was essential to remove these artifact spots. The gel that was selected as the master reference was also used as the reference for manual spot editing. The gel in which the reference gel was based upon was

fully edited to contain only spots that represented proteins. Once this gel was satisfactorily edited, all of the other gels in the experiment were edited in the same fashion with an attempt to maintain similar spots, and spot constellations as detected in the master reference gel. Although each gel contained spots that were unique, the overall pattern of spots was retained between all of the gels.

After the careful and thorough detection of all protein spots in the gels the background of each spot was removed. This was done using the supplied background subtraction method "mode of non spot" with a margin setting of 45. Background subtraction is essentially a method in which the pixel density of the gel background around the boundary of each detected spot is removed from the total pixel density of the spot. This is achieved when the software draws the smallest rectangle which fully encloses the entire protein spot and then increases this rectangle size in all directions by the number of pixels set in the margin setting, in this case 45 pixels. The area between the boundary of the rectangle and the detected spot boundary is then examined and the pixel intensity that occurs most commonly is labeled the background of the spot. This pixel value was subtracted from the pixel values present in the detected spot yielding a background subtracted spot volume. This process is repeated for each spot detected in each of the gels in the experiment.

Once the spots were detected and the backgrounds subtracted, the individual images were manually warped to one another to aid in the matching of spots. For each gel in the experiment an individual set of warping parameters was applied to the gel so that it resembled the reference gel in shape and orientation of the spot constellations within the gel. Accurate and careful warping of the gels to the master reference gel is essential in order to obtain successful matching of proteins between the gels.

With the gels warped and aligned properly, spot matching between all of the gels proceeded successfully. Initially all of the spots from the control group were matched to the control average, and all of the spots from the preeclamptic group were matched to the preeclamptic average. These two averages were then matched to one another and all spots that were matched were added to the

computer based master reference gel in order to create an inventory of all spots under consideration in the experiment.

Once all of the spots were matched, the final step before determination of differentially regulated spots in the experiment was the normalization of each gel. Even with careful determination of sample protein concentration prior to loading of the 2D gel, there are still subtle differences in protein loading intensity between the different gels in a given experiment. In order to account for the loading differences between each gel, and in order to make meaningful comparisons between different gels in the experiment, the spots were normalized. Normalization is achieved by adding together the total spot volumes of each spot in a given gel and dividing each spot in that same gel by this value. This new value for the spot volume is typically a very small number so a scaling factor is applied to all spots in the experiment to bring this number back into a manageable range.

The final step of the 2D gel analysis was to compare the averaged gels to one another by applying a difference map filter. A differential regulation threshold value of +/- 2 fold difference was assigned and all of the spots that conformed to this cutoff were examined. Typically hundreds of spots were selected from the initial difference map however due to spurious matches within complex portions of the gel, and spots that are only present in some of the gels and not in others, each of these spots needed to be inspected manually. After manual confirmation of differentially regulated spot presence between all of the gels in the experiment the spots of interest were selected for further analysis by mass spectrometry.

Appendix 2

The raw data and enlarged images of each discovery set sample analyzed for each of the twelve proteins that were identified. Individual normalized spot volumes are shown for each sample as well as the averaged normalized spot volumes for the control and preeclamptic group. All spot detection and densiometric analyses were performed with Phoretix 2D expressions software.

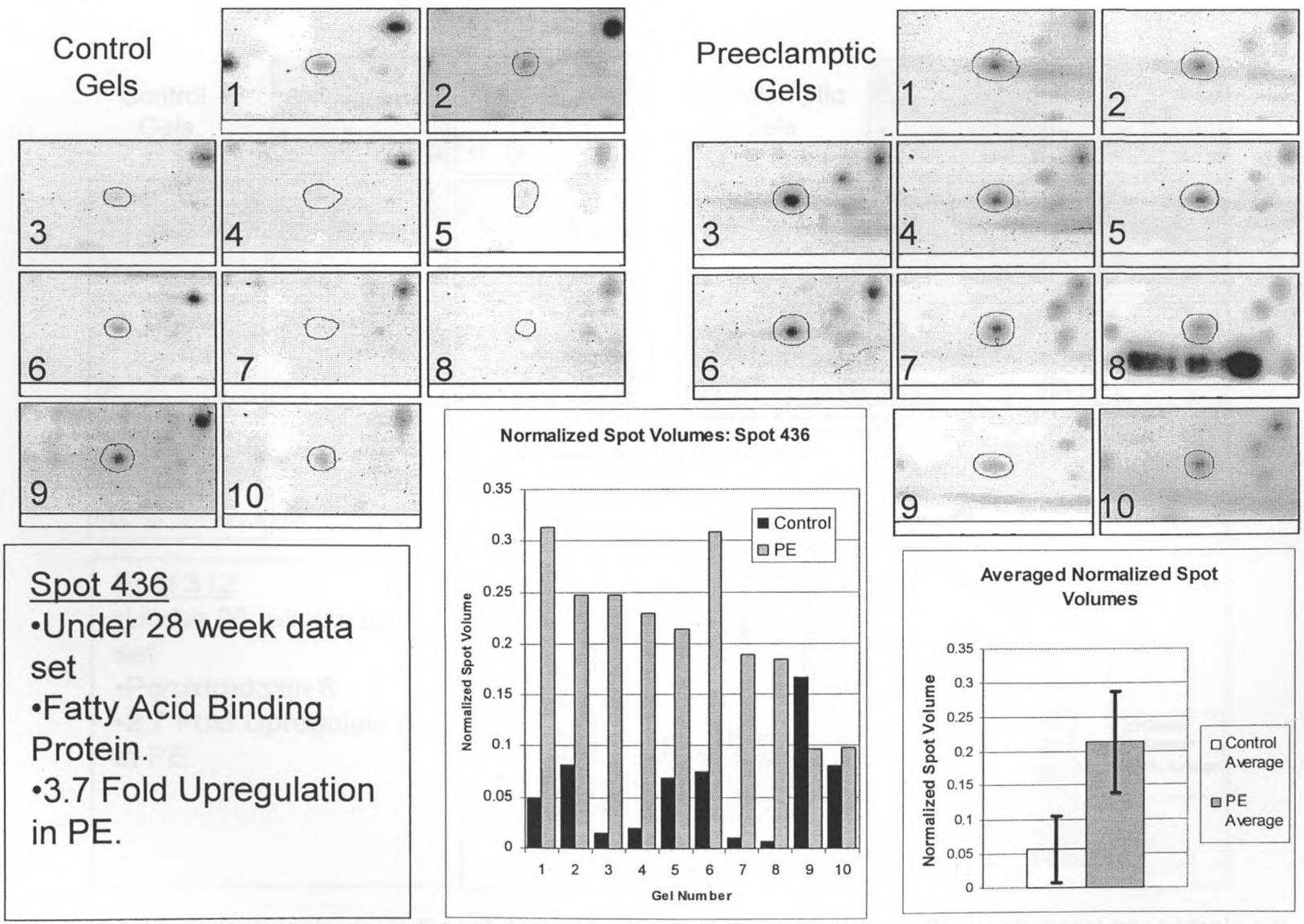

Figure A2.1: Raw fatty acid binding protein 4 spot data from each gel in the less than 28 week discovery sample set.

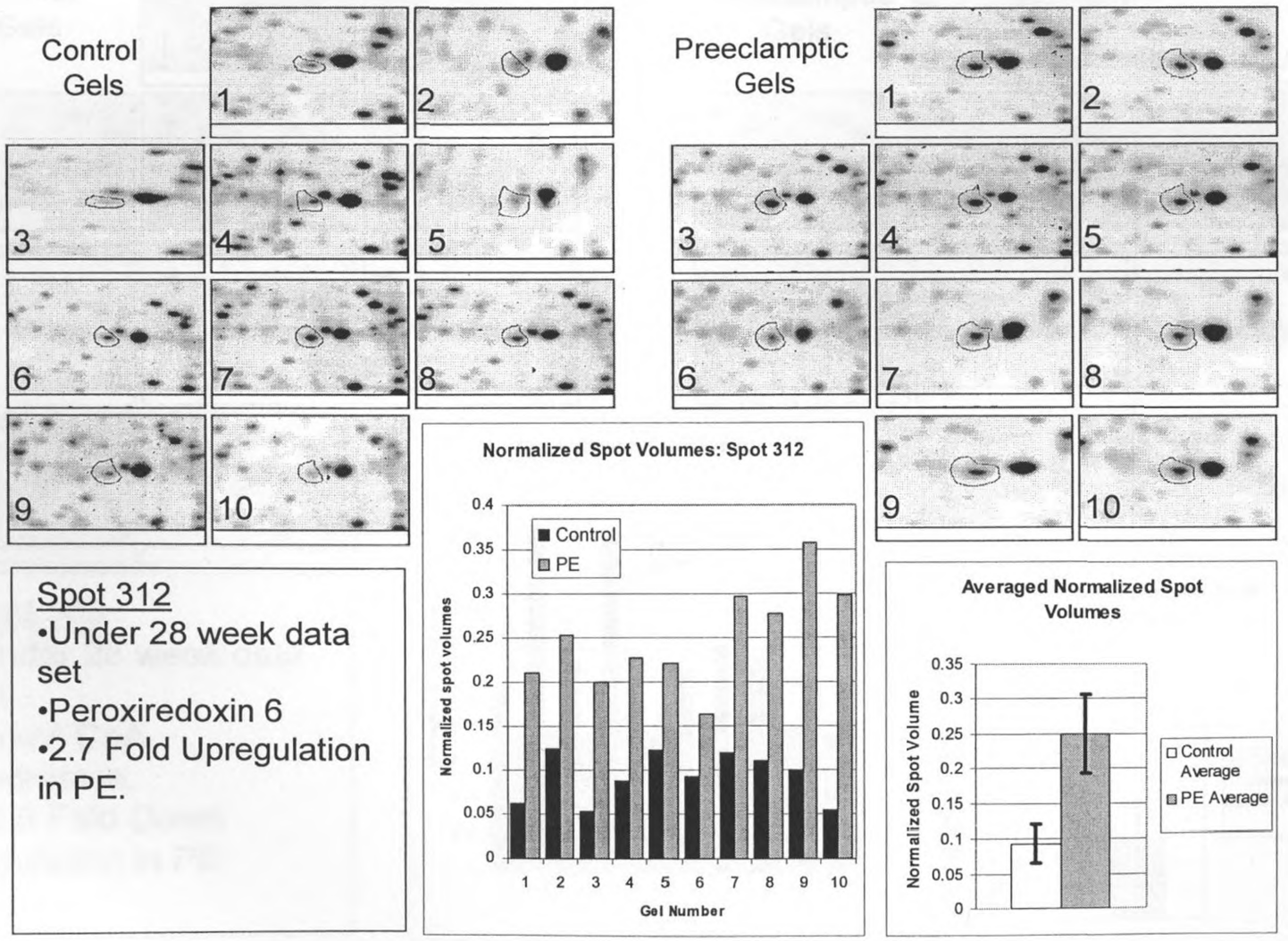

Figure A2.2: Raw peroxiredoxin 6 spot data from each gel in the less than 28 week discovery sample set.

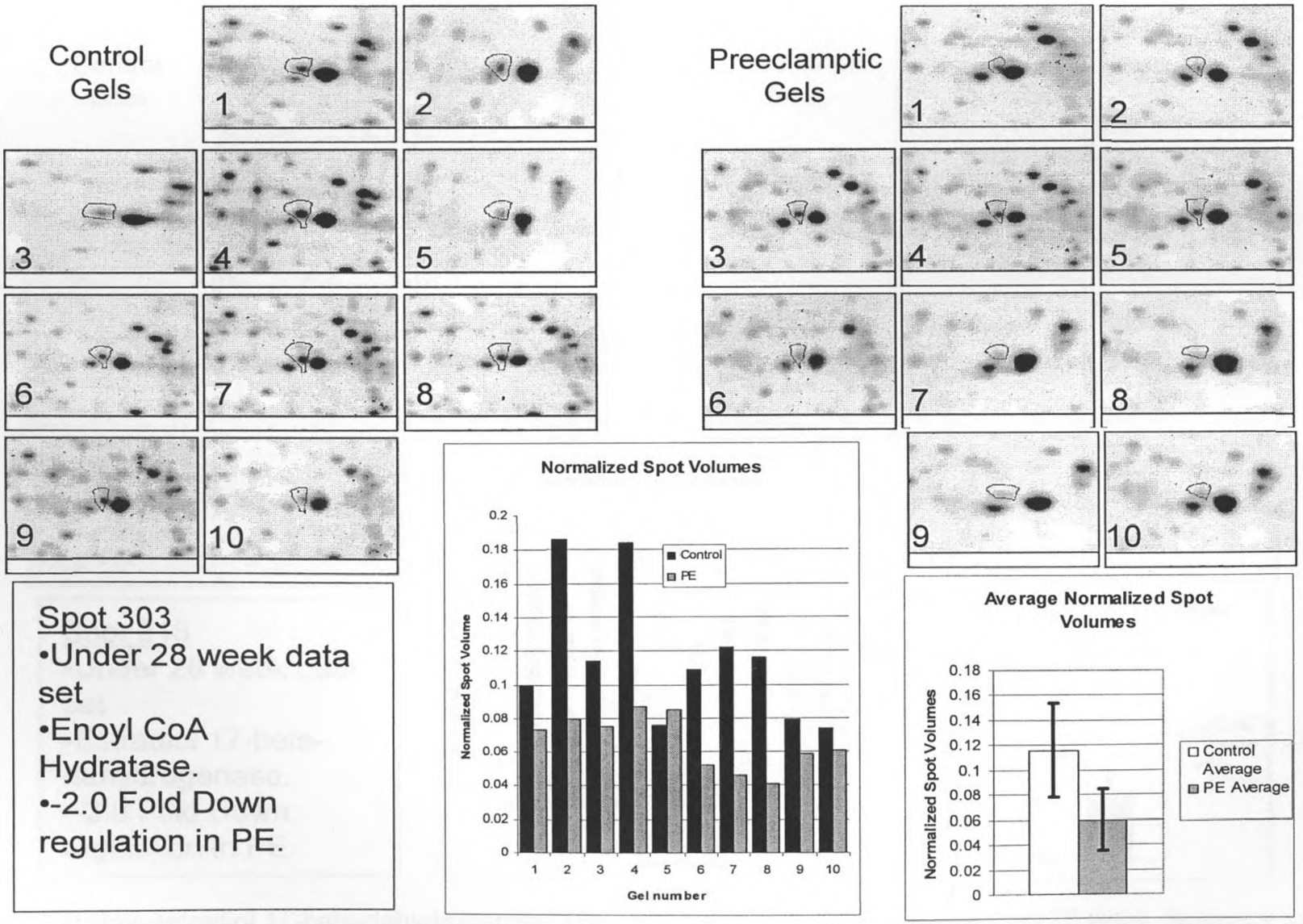

Figure A2.3: Raw enoyl CoA hydratase spot data from each gel in the less than 28 week discovery sample set.

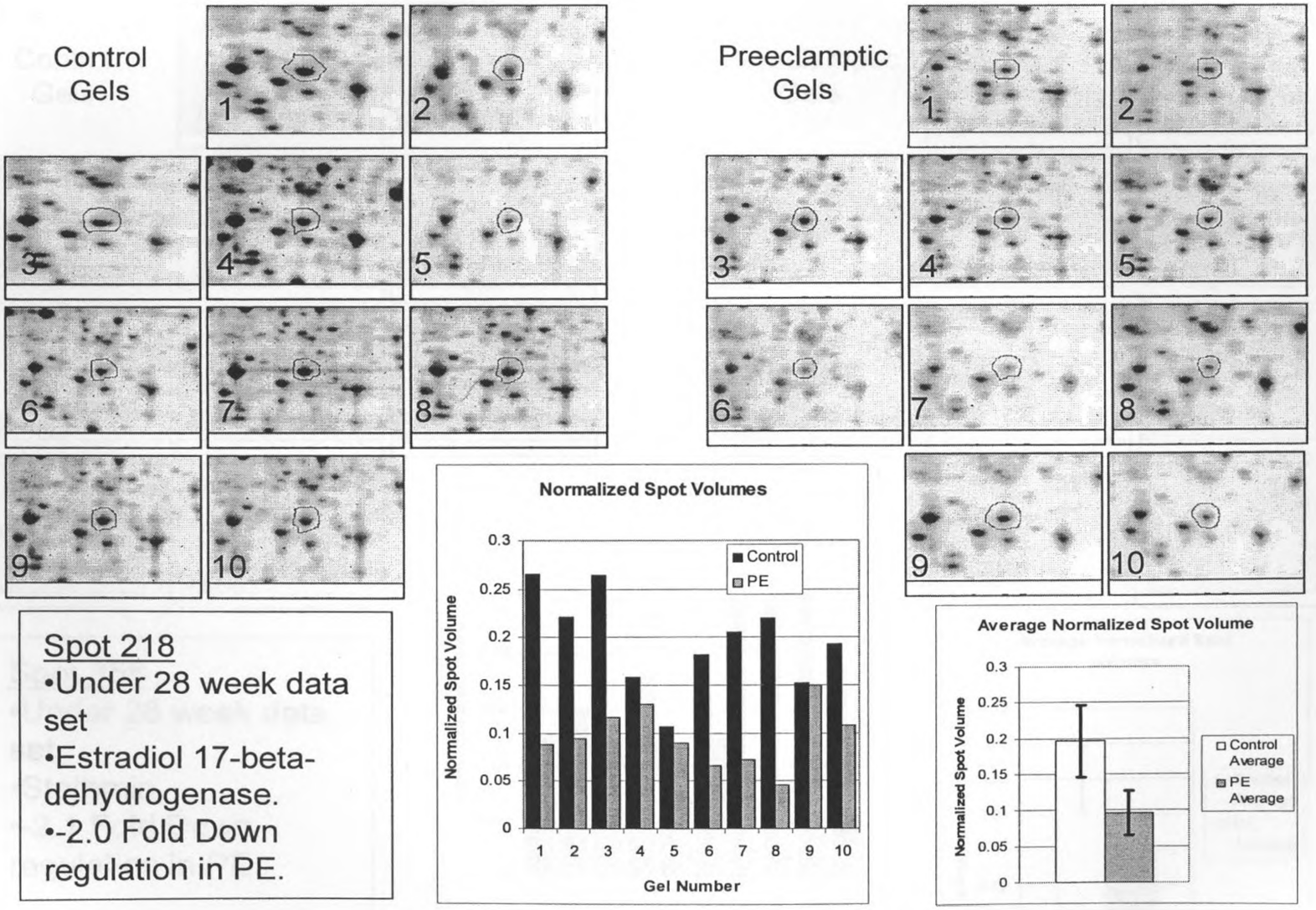

Figure A2.4: Raw estradiol 17-beta-dehydrogenase spot data from each gel in the less than 28 week discovery samples.

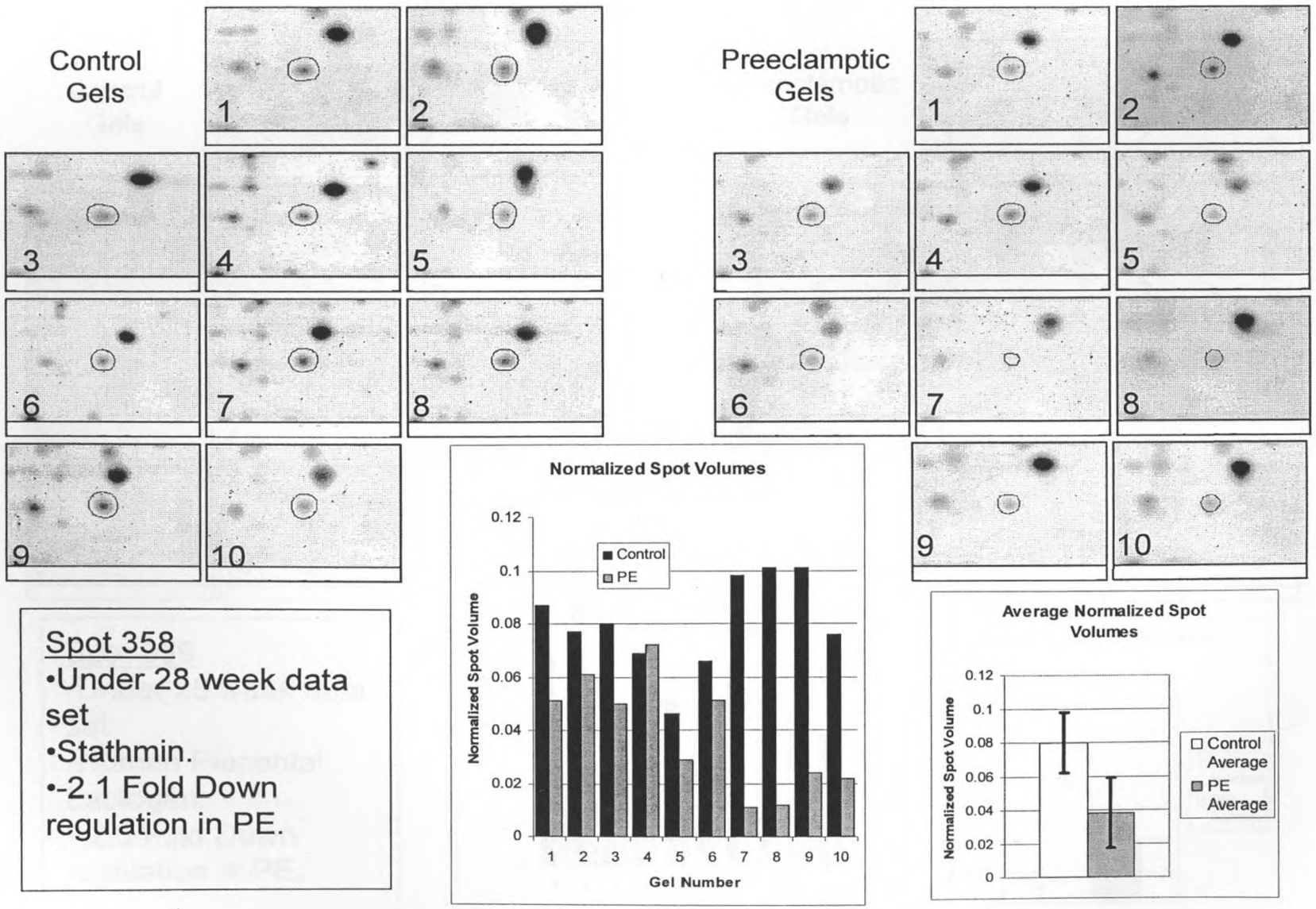

Figure A2.5: Raw stathmin spot data from each gel in the less than 28 week discovery sample set.

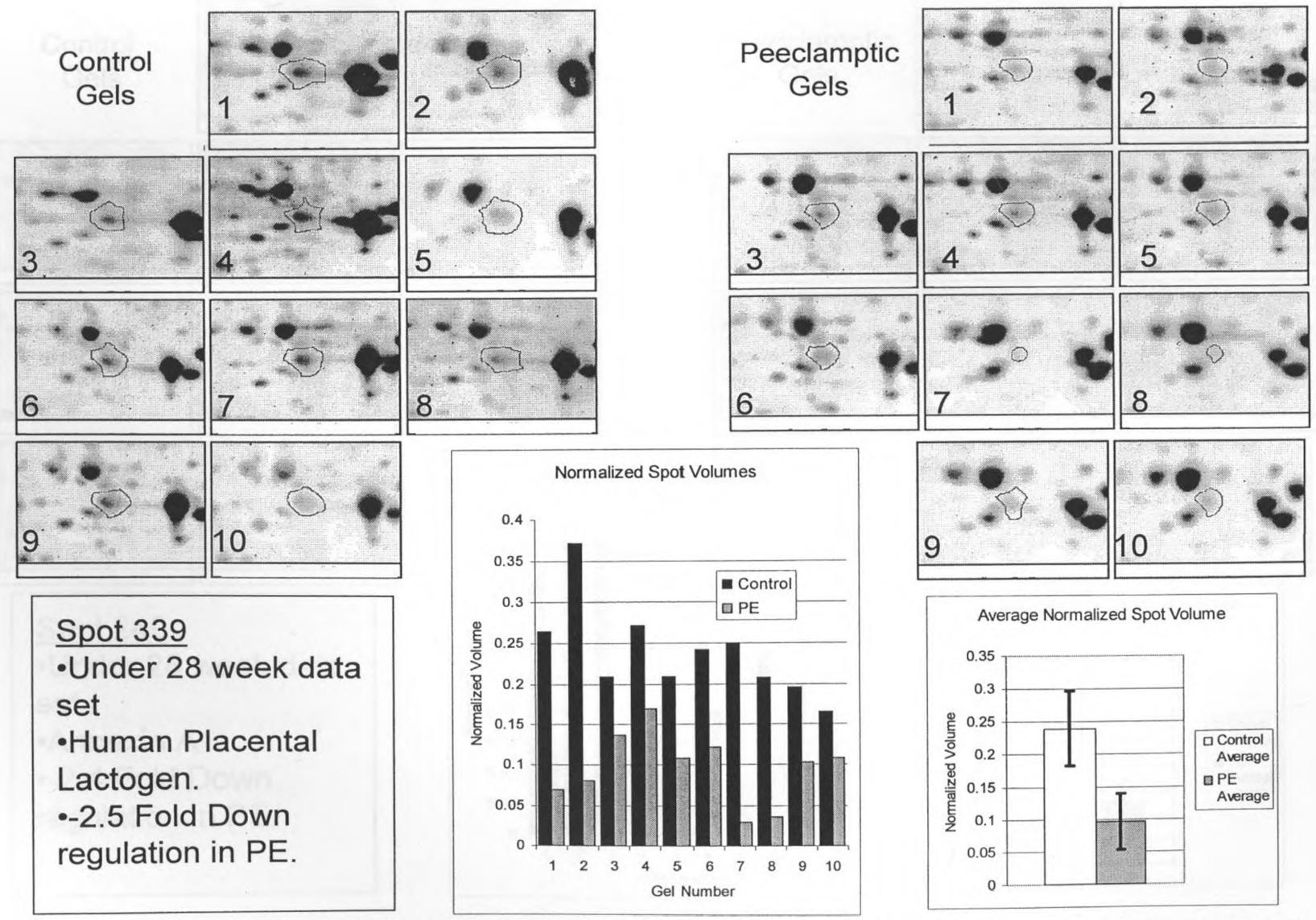

Figure A2.6: Raw human placental lactogen spot data from each gel in the less than 28 week discovery sample set.

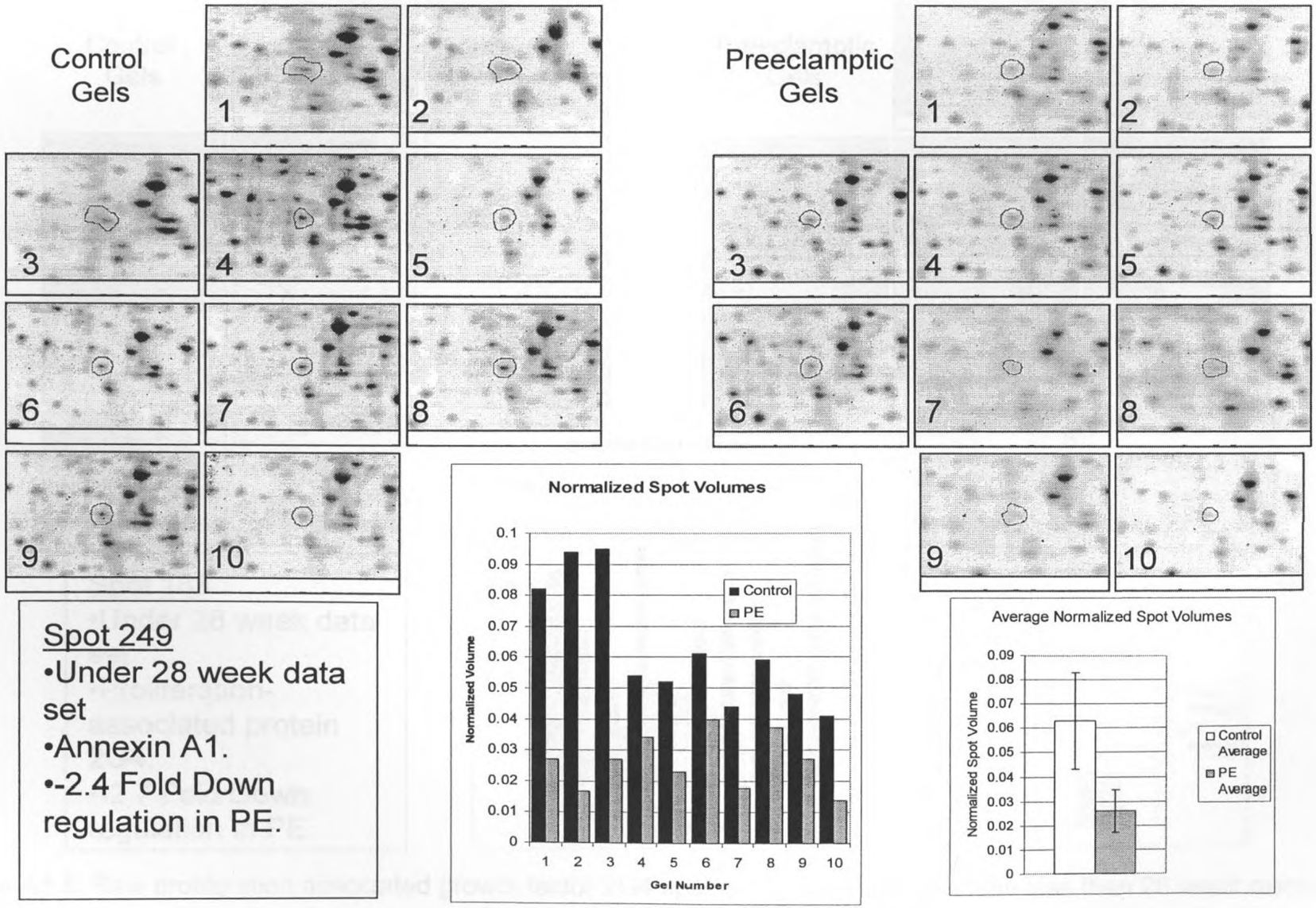

Figure A2.7: Raw lipocortin spot data from each gel in the less than 28 week discovery sample set.

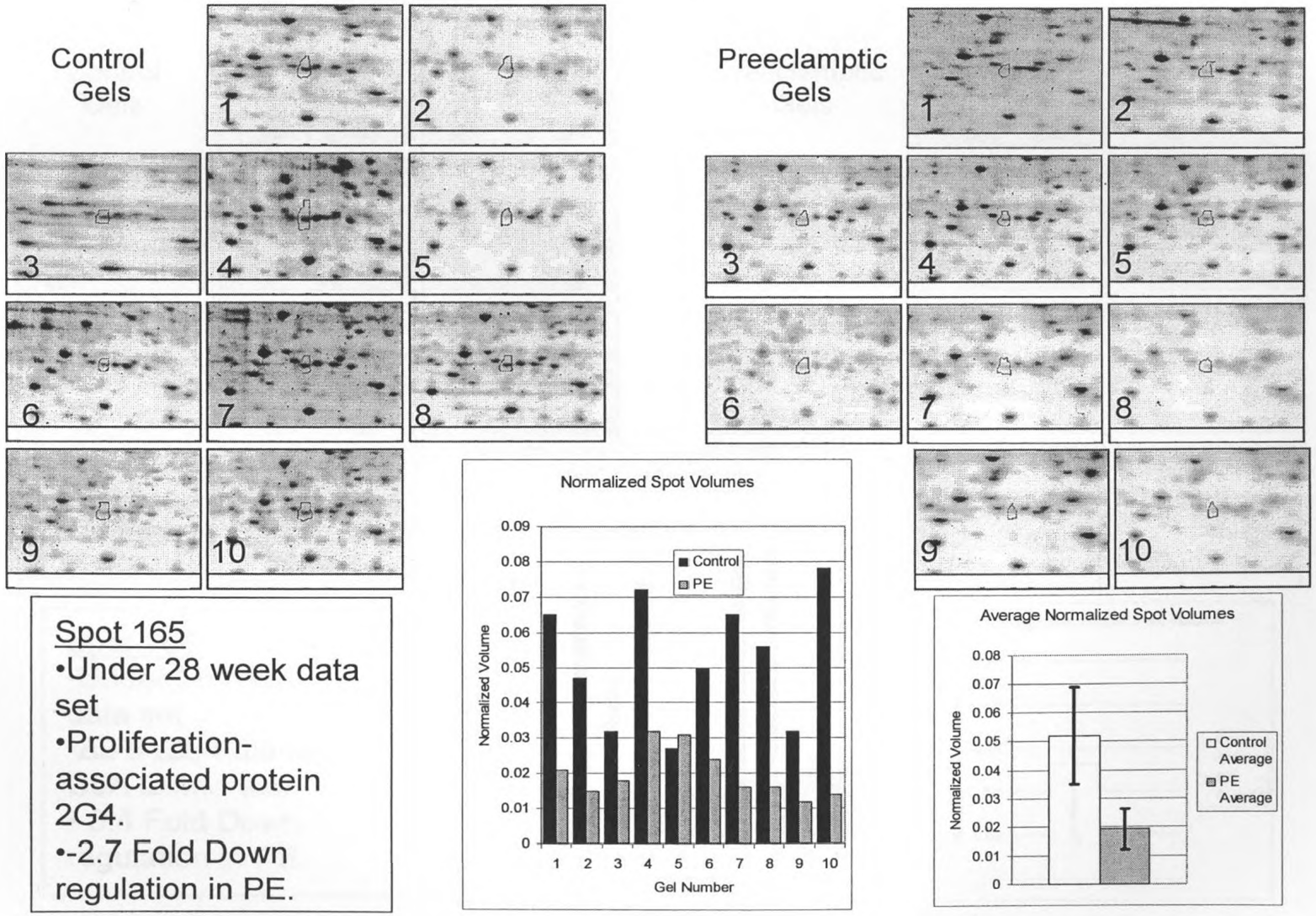

Figure A2.8: Raw proliferation associated growth factor 2G4 spot data from each gel in the less than 28 week discovery sample set.

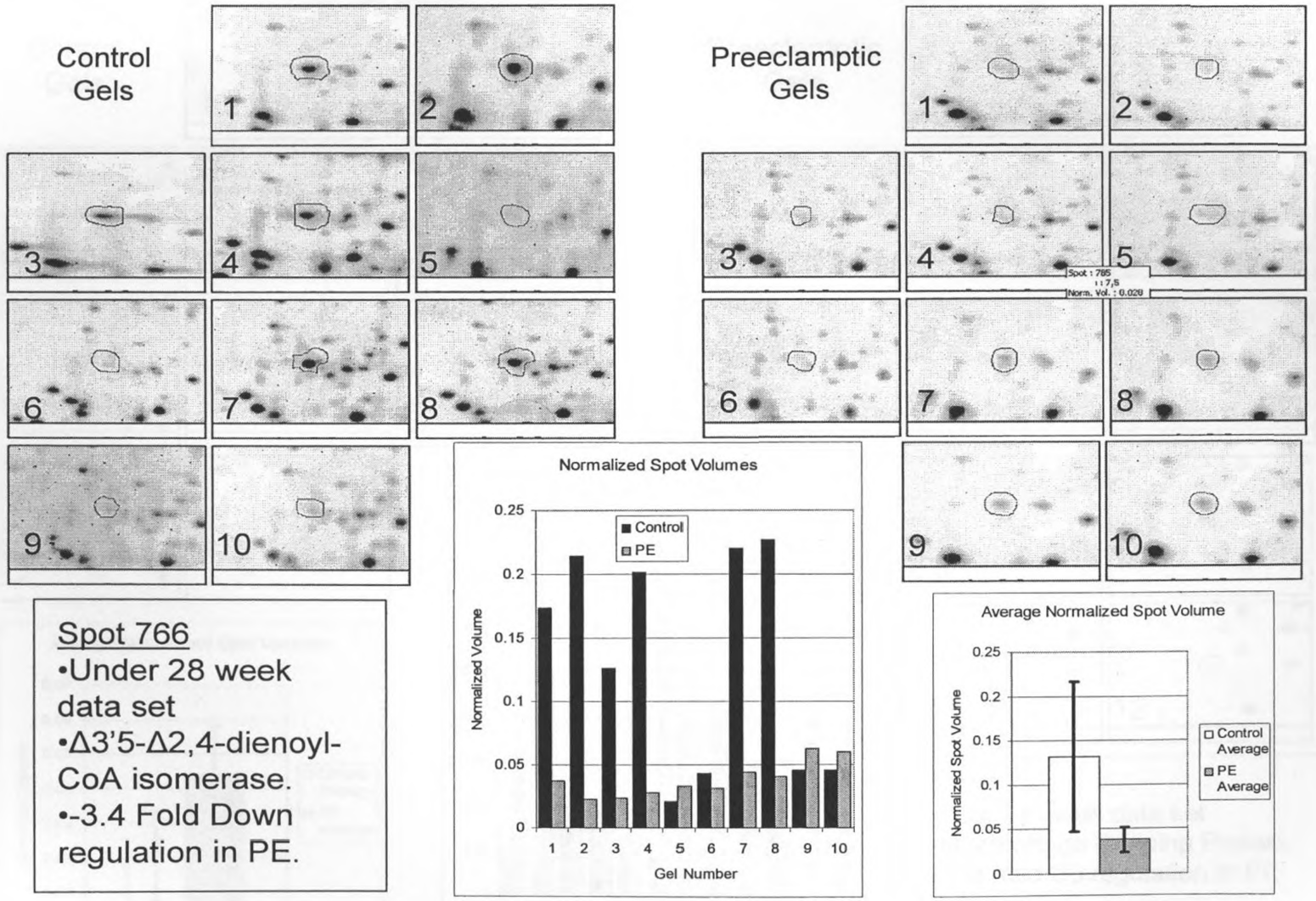

Figure A2.9: Raw Δ3,5-Δ2,4-dienoyl CoA isomerase spot data from each gel in the less than 28 week discovery samples.

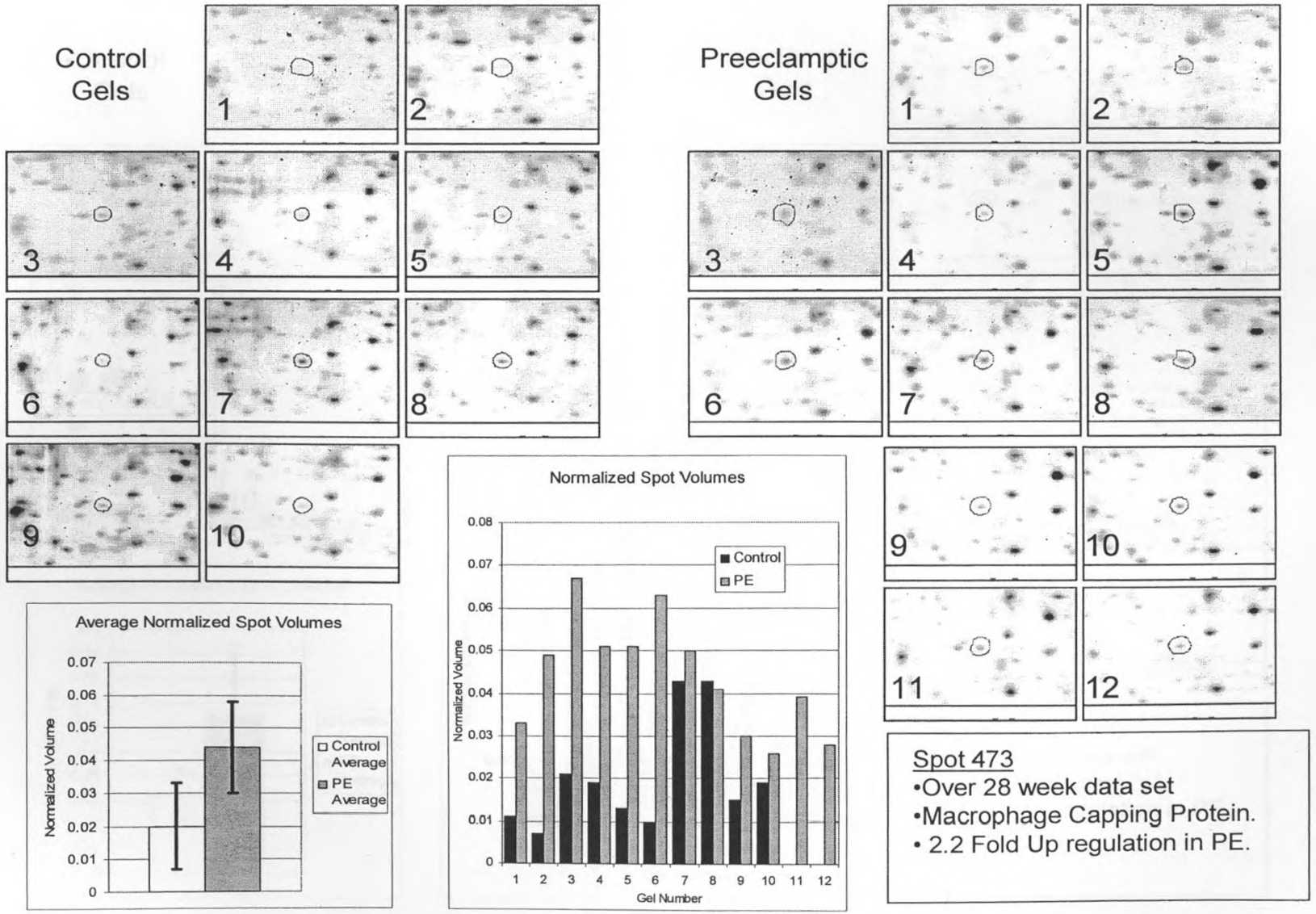

Figure A2.10: Raw macrophage capping protein spot data from each gel in the more than 28 week discovery sample set.

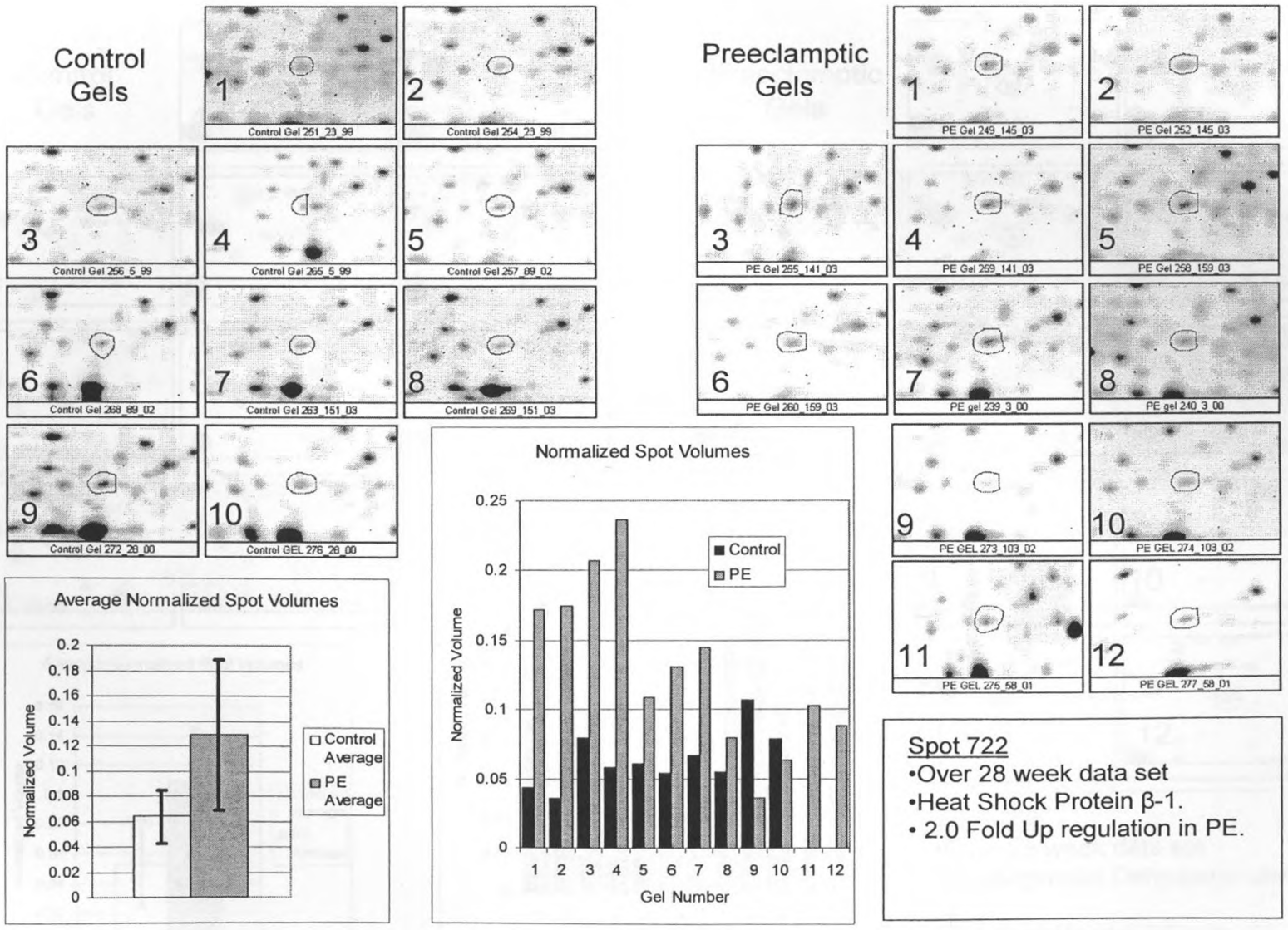

Figure A2.11: Raw heat shock protein 27 spot data from each gel in the more than 28 week discovery sample set.

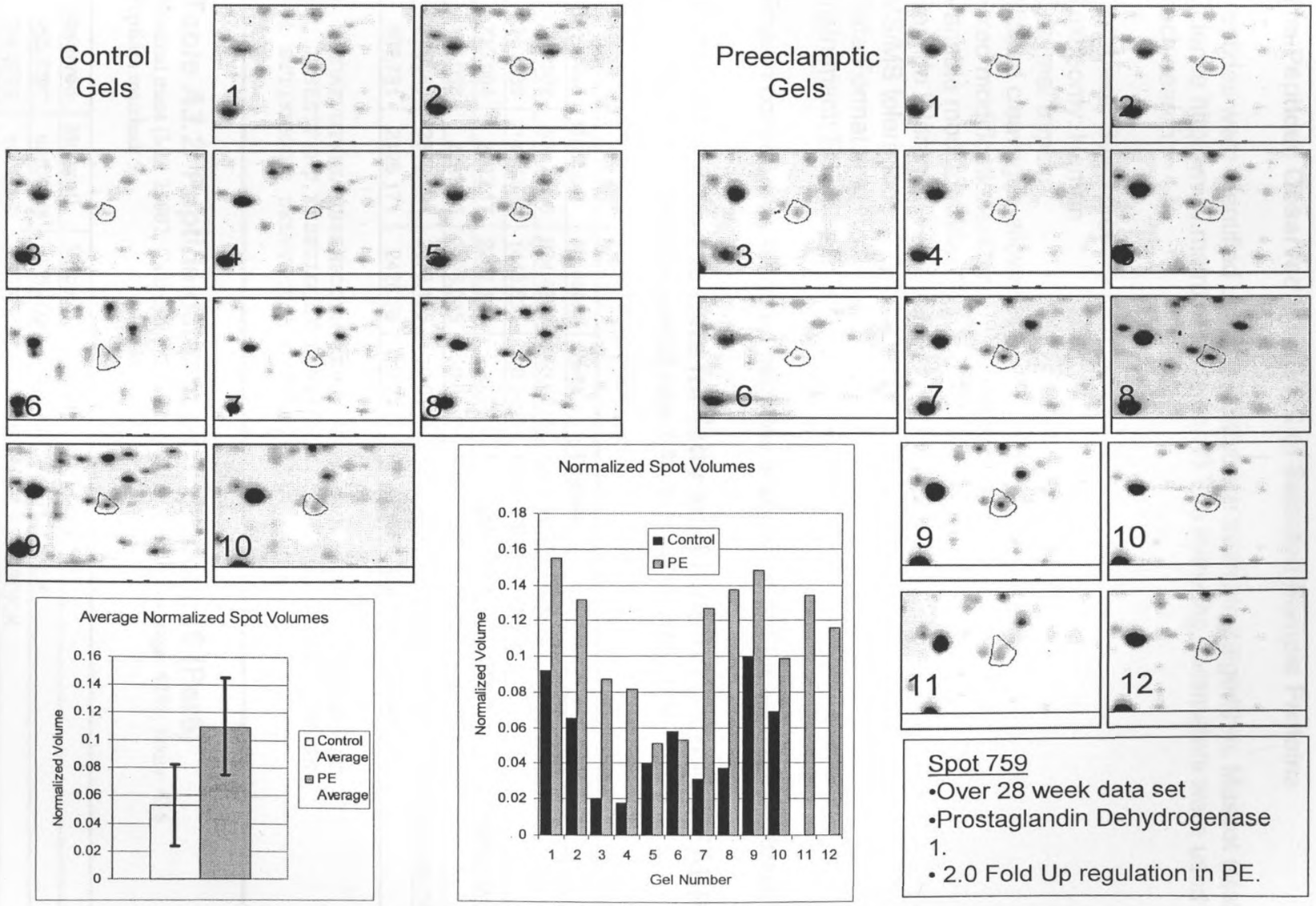

Figure A2.12: Raw prostaglandin dehydrogenase 1 spot data from each gel in the more than 28 week discovery samples.

APPENDIX 3

The Peptides Observed by MS/MS of Selected Sample Proteins

Peptides were identified using the database searching algorithm, Mascot (Matrix Science http://www.matrixscience.com/) The following parameters were used for each search:

Database: Swissprot
Taxonomy: Human
Enzyme: trypsin
Missed cleavages allowed:1
Fixed modifications: Carbamidomethyl (C)
Variable modifications: Oxidation (M)
Peptide tolerance: +/- 0.1 Da
MS/MS tolerance: +/- 0.1 Da
Data Format: .pkl
Instrument: ESI-QUAD-TOF

Protein coverage by detected peptides is shown in red for each protein identified.

Table A3.1: Peptide data for fatty acid-binding protein 4(FABP4)

Nominal mass (M_r): **14692**; Calculated pI value: **6.81**; Sequence Coverage: **48%**; Score: **374**
Peptides matched: **6**

Observed	Mr(expt)	Mr(calc)	Delta	Peptide
468.2502	934.4858	934.4872	-0.0013	K.EVGVGFATR.K
724.3289	1446.643	1446.634	0.0096	K.LVSSENFDDYMK.E
735.064	2202.17	2202.175	-0.005	K.VAGMAKPNMIISVNGDVITIK.S + 2 Oxidation (M)
1150.038	2298.06	2298.065	-0.0047	K.NTEISFILGQEFDEVTADDR.K
794.0386	2379.094	2379.105	-0.0112	K.LVSSENFDDYMKEVGVGFATR.K + Oxidation (M)
809.731	2426.171	2426.16	0.0111	K.NTEISFILGQEFDEVTADDRK.V

```
1   CDAFVGTWKL VSSENFDDYM KEVGVGFATR KVAGMAKPNM IISVNGDVIT
51  IKSESTFKNT EISFILGQEF DEVTADDRKV KSTITLDGGV LVHVQKWDGK
101 STTIKRKRED DKLVVECVMK GVTSTRVYER A
```

Table A3.2: Peptide data for peroxiredoxin 6 (Per6)

Nominal mass (M_r): **25002**; Calculated pI value: **6.02**; Sequence Coverage: **52%**; Score: **416**
Peptides matched: **9**

Observed	Mr(expt)	Mr(calc)	Delta	Peptide
453.7297	905.4448	905.4606	-0.0158	R.NFDEILR.V
504.2792	1006.544	1006.549	-0.0049	R.VVFVFGPDK.K
543.2957	1084.577	1084.592	-0.0148	K.LPFPIIDDR.N
596.3318	1190.649	1190.666	-0.0168	K.LSILYPATTGR.N

698.318	1394.621	1394.65	-0.0285	R.DFTPVCTTELGR.A
764.8864	1527.758	1527.822	-0.0635	R.ELAILLGMLDPAEK.D + Oxidation (M)
791.774	1581.533	1581.662	-0.1282	K.DINAYNCEEPTEK.L
615.9502	1844.829	1844.871	-0.0425	K.DGDSVMVLPTIPEEEAK.K + Oxidation (M)
950.9724	1899.93	1899.986	-0.056	R.ELAILLGMLDPAEKDEK.G + Oxidation (M)

```
1   PGGLLLGDVA PNFEANTTVG RIRFHDFLGD SWGILFSHPR DFTPVCTTEL
51  GRAAKLAPEF AKRNVKLIAL SIDSVEDHLA WSKDINAYNC EEPTEKLPFP
101 IIDDRNRELA ILLGMLDPAE KDEKGMPVTA RVVFVFGPDK KLKLSILYPA
151 TTGRNFDEIL RVVISLQLTA EKRVATPVDW KDGDSVMVLP TIPEEEAKKL
201 FPKGVFTKEL PSGKKYLRYT PQP
```

Table A3.3: Peptide data for enoyl CoA hydratase

Nominal mass (M_r): **31835**; Calculated pI value: **8.34**; Sequence Coverage: **35%**; Score: **345**
Peptides matched: **7**

Observed	Mr(expt)	Mr(calc)	Delta	Peptide
432.2245	862.4344	862.4548	-0.0204	K.AFAAGADIK.E
514.2203	1026.426	1026.469	-0.0431	K.EGMTAFVEK.R + Oxidation (M)
677.7988	1353.583	1353.627	-0.0438	K.SLAMEMVLTGDR.I + 2 Oxidation (M)
865.3672	1728.72	1728.788	-0.0677	K.ESVNAAFEMTLTEGSK.L + Oxidation (M)
610.9801	1829.919	1829.941	-0.0225	K.IFEEDPAVGAIVLTGGDK.A
663.6555	1987.945	1987.959	-0.0147	K.ICPVETLVEEAIQCAEK.I
1063.048	2124.08	2124.133	-0.0522	K.AQFAQPEILIGTIPGAGGTQR.L

```
1   MAALRVLLSC VRGPLRPPVR CPAWRPFASG ANFEYIIAEK RGKNNTVGLI
51  QLNRPKALNA LCDGLIDELN QALKIFEEDP AVGAIVLTGG DKAFAAGADI
101 KEMQNLSFQD CYSSKFLKHW DHLTQVKKPV IAAVNGYAFG GGCELAMMCD
151 IIYAGEKAQF AQPEILIGTI PGAGGTQRLT RAVGKSLAME MVLTGDRISA
201 QDAKQAGLVS KICPVETLVE EAIQCAEKIA SNSKIVVAMA KESVNAAFEM
251 TLTEGSKLEK KLFYSTFATD DRKEGMTAFV EKRKANFKDQ
```

Table A3.4: Peptide data for estradiol 17-beta dehydrogenase

Nominal mass (M_r): **35139**; Calculated pI value: **5.47**; Sequence Coverage: **53%**; Score: **818**
Peptides matched: **14**

Observed	Mr(expt)	Mr(calc)	Delta	Peptide
408.6776	815.3406	815.3813	-0.0407	R.YFTTER.F
481.2478	960.481	960.4916	-0.0105	R.EVFGDVPAK.A
513.7504	1025.4862	1025.5043	-0.018	R.TDIHTFHR.F
540.2679	1078.5212	1078.5295	-0.0082	R.LASDPSQSFK.V
578.7786	1155.5426	1155.5713	-0.0286	R.FYQYLAHSK.Q
607.3192	1212.6238	1212.635	-0.0111	K.VLGSPEEVLDR.T
613.2612	1224.5078	1224.5882	-0.0804	R.MLQAFLPDMK.R + 2 Oxidation (M)

745.8401	1489.6656	1489.7048	-0.0392	R.GAVGDPELGDPPAAPQ.-
560.2391	1677.6955	1677.7417	-0.0462	R.LDDPSGSNYVTAMHR.E + Oxidation (M)
600.5845	1798.7317	1798.7717	-0.04	K.AEAGAEAGGGAGPGAEDEAGR.G
920.4151	1838.8156	1838.956	-0.1403	R.ALACPPGSLETLQLDVR.D
661.292	1980.8542	1980.8782	-0.024	R.MRLDDPSGSNYVTAMHR.E + 2 Oxidation (M)
663.0032	1985.9878	1986.0057	-0.018	R.EAAQNPEEVAEVFLTALR.A
800.7163	2399.1271	2399.1864	-0.0593	R.VLVTGSVGGLMGLPFNDVYCASK.F + Oxidation (M)

```
1   ARTVVLITGC SSGIGLHLAV RLASDPSQSF KVYATLRDLK TQGRLWEAAR
51  ALACPPGSLE TLQLDVRDSK SVAAARERVT EGRVDVLVCN AGLGLLGPLE
101 ALGEDAVASV LDVNVVGTVR MLQAFLPDMK RRGSGRVLVT GSVGGLMGLP
151 FNDVYCASKF ALEGLCESLA VLLLPFGVHL SLIECGPVHT AFMEKVLGSP
201 EEVLDRTDIH TFHRFYQYLA HSKQVFREAA QNPEEVAEVF LTALRAPKPT
251 LRYFTTERFL PLLRMRLDDP SGSNYVTAMH REVFGDVPAK AEAGAEAGGG
301 AGPGAEDEAG RGAVGDPELG DPPAAPQ
```

Table A3.5: Peptide data for stathmin

Nominal mass (M_r): **17161**; Calculated pI value: **5.77**; Sequence Coverage: **28%**; Score: **169**
Peptides matched: **4**

Observed	Mr(expt)	Mr(calc)	Delta	Peptide
473.2456	944.4766	944.4927	-0.016	K.KLEAAEER.R
537.775	1073.535	1073.56	-0.025	K.DLSLEEIQK.K
663.8217	1325.629	1325.687	-0.0578	K.ESVPEFPLSPPK.K
694.8436	1387.673	1387.746	-0.0733	R.ASGQAFELILSPR.S

```
1   ASSDIQVKEL EKRASGQAFE LILSPRSKES VPEFPLSPPK KKDLSLEEIQ
51  KKLEAAEERR KSHEAEVLKQ LAEKREHEKE VLQKAIEENN NFSKMAEEKL
101 THKMEANKEN REAQMAAKLE RLREKDKHIE EVRKNKESKD PADETEAD
```

Table A3.6: Peptide data for human placental lactogen

Nominal mass (M_r): **25289**; Calculated pI value: **5.34**; Sequence Coverage: **29%**; Score: **316**
Peptides matched: **5**

Observed	Mr(expt)	Mr(calc)	Delta	Peptide
603.2839	1204.553	1204.57	-0.0166	K.NYGLLYCFR.K
635.2912	1268.568	1268.607	-0.0392	K.DMDKVETFLR.M + Oxidation (M)
452.2105	1353.61	1353.661	-0.0515	R.LFDHAMLQAHR.A + Oxidation (M)
689.3262	1376.638	1376.661	-0.0227	K.DLEEGIQTLMGR.L + Oxidation (M)
822.0051	2462.994	2463.09	-0.0965	R.SMFANNLVYDTSDSDDYHLLK.D + Oxidation (M)

```
1   MAPGSRTSLL LAFALLCLPW LQEAGAVQTV PLSRLFDHAM LQAHRAHQLA
51  IDTYQEFEET YIPKDQKYSF LHDSQTSFCF SDSIPTPSNM EETQQKSNLE
101 LLRISLLLIE SWLEPVRFLR SMFANNLVYD TSDSDDYHLL KDLEEGIQTL
151 MGRLEDGSRR TGQILKQTYS KFDTNSHNHD ALLKNYGLLY CFRKDMDKVE
201 TFLRMVQCRS VEGSCGF
```

Table A3.7: Peptide data for lipocortin

Nominal mass (M_r): **38787**; Calculated pI value: **6.64**; Sequence Coverage: **21%**; Score: **437**
Peptides matched: **6**

Observed	Mr(expt)	Mr(calc)	Delta	Peptide
694.3574	1386.7	1386.761	-0.0603	K.GVDEATIIDILTK.R
775.8941	1549.774	1549.81	-0.0363	K.GTDVNVFNTILTTR.S
535.9944	1604.961	1604.95	0.0113	K.ALTGHLEEVVLALLK.T
560.307	1677.899	1677.905	-0.0058	R.KGTDVNVFNTILTTR.S
851.9432	1701.872	1701.878	-0.0066	K.GLGTDEDTLIEILASR.T
871.4318	1740.849	1740.843	0.0064	K.MYGISLCQAILDETK.G

```
1   AMVSEFLKQA WFIENEEQEY VQTVKSSKGG PGSAVSPYPT FNPSSDVAAL
51  HKAIMVKGVD EATIIDILTK RNNAQRQQIK AAYLQETGKP LDETLKKALT
101 GHLEEVVLAL LKTPAQFDAD ELRAAMKGLG TDEDTLIEIL ASRTNKEIRD
151 INRVYREELK RDLAKDITSD TSGDFRNALL SLAKGDRSED FGVNEDLADS
201 DARALYEAGE RRKGTDVNVF NTILTTRSYP QLRRVFQKYT KYSKHDMNKV
251 LDLELKGDIE KCLTAIVKCA TSKPAFFAEK LHQAMKGVGT RHKALIRIMV
301 SRSEIDMNDI KAFYQKMYGI SLCQAILDET KGDYEKILVA LCGGN
```

Table A3.8: Peptide data for proliferation associated protein 2G4

Nominal mass (M_r): **43970**; Calculated pI value: **6.13**; Sequence Coverage: **12%**; Score: **186**
Peptides matched: **5**

Observed	Mr(expt)	Mr(calc)	Delta	Peptide
466.7353	931.456	931.5087	-0.0526	K.ALLQSSASR.K
491.2378	980.461	980.4815	-0.0204	K.SDQDYILK.E
607.2471	1212.48	1212.5	-0.0205	K.GDAMIMEETGK.I + 2 Oxidation (M)
643.3267	1284.639	1284.667	-0.0285	K.TIIQNPTDQQK.K
647.7788	1293.543	1293.576	-0.0328	K.SEMEVQDAELK.A + Oxidation (M)

```
1   SGEDEQQEQT IAEDLVVTKY KMGGDIANRV LRSLVEASSS GVSVLSLCEK
51  GDAMIMEETG KIFKKEKEMK KGIAFPTSIS VNNCVCHFSP LKSDQDYILK
101 EGDLVKIDLG VHVDGFIANV AHTFVVDVAQ GTQVTGRKAD VIKAAHLCAE
151 AALRLVKPGN QNTQVTEAWN KVAHSFNCTP IEGMLSHQLK QHVIDGEKTI
201 IQNPTDQQKK DHEKAEFEVH EVYAVDVLVS SGEGKAKDAG QRTTIYKRDP
251 SKQYGLKMKT SRAFFSEVER RFDAMPFTLR AFEDEKKARM GVVECAKHEL
301 LQPFNVLYEK EGEFVAQFKF TVLLMPNGPM RITSGPFEPD LYKSEMEVQD
351 AELKALLQSS ASRKTQKKKK KKASKTAENA TSGETLEENE AGD
```

Table A3.9: Peptide data for Δ3,5-Δ2,4-dienoyl-CoA isomerase

Nominal mass (M_r): **36136**; Calculated pI value: **8.16;** Sequence Coverage: **39%;** Score: **564**
Peptides matched: **12**

Observed	Mr(expt)	Mr(calc)	Delta	Peptide
401.2356	800.4566	800.4755	-0.0189	R.AVVISGAGK.M
419.2209	836.4272	836.4545	-0.0272	R.ISWYLR.D
432.7414	863.4682	863.4865	-0.0182	K.VNLLYSR.D
528.7233	1055.432	1055.442	-0.0095	R.EMVECFNK.I
649.7917	1297.5688	1297.63	-0.0614	R.YQETFNVIER.C
688.793	1375.5714	1375.623	-0.0516	R.YCAQDAFFQVK.E
485.6132	1453.8178	1453.827	-0.0088	K.HVLHVQLNRPNK.R
734.8284	1467.6422	1467.67	-0.0275	K.MMADEALGSGLVSR.V + 2 Oxidation (M)
771.8922	1541.7698	1541.805	-0.035	K.EVDVGLAADVGTLQR.L
532.9248	1595.7526	1595.765	-0.0121	R.KMMADEALGSGLVSR.V + 2 Oxidation (M)
577.9795	1730.9167	1730.932	-0.0148	K.VIGNQSLVNELAFTAR.K
715.6563	2143.9471	2143.984	-0.0369	K.MFTAGIDLMDMASDILQPK.G + 3 Oxidation (M)

```
1   MAAGIVASRR LRDLLTRRLT GSNYPGLSIS LRLTGSSAQE EASGVALGEA
51  PDHSYESLRV TSAQKHVLHV QLNRPNKRNA MNKVFWREMV ECFNKISRDA
101 DCRAVVISGA GKMFTAGIDL MDMASDILQP KGDDVARISW YLRDIITRYQ
151 ETFNVIERCP KPVIAAVHGG CIGGGVDLVT ACDIRYCAQD AFFQVKEVDV
201 GLAADVGTLQ RLPKVIGNQS LVNELAFTAR KMMADEALGS GLVSRVFPDK
251 EVMLDAALAL AAEISSKSPV AVQSTKVNLL YSRDHSVAES LNYVASWNMS
301 MLQTQDLVKS VQATTENKEL KTVTFSKL
```

Table A3.10: Peptide data for macrophage capping protein

Nominal mass (M_r): **38779**; Calculated pI value: **5.88;** Sequence Coverage: **18%;** Score: **242**
Peptides matched: **5**

Observed	Mr(expt)	Mr(calc)	Delta	Peptide
458.743	915.4714	915.5025	-0.0311	K.TSTGAPAAIK.K
640.8074	1279.6002	1279.6078	-0.0075	K.VSDATGQMNLTK.V + Oxidation (M)
659.2851	1316.5556	1316.5732	-0.0175	K.EGNPEEDLTADK.A
695.3617	1388.7088	1388.7412	-0.0323	R.QAALQVAEGFISR.M
930.9593	1859.904	1859.9199	-0.0159	R.MQYAPNTQVEILPQGR.E + Oxidation (M)

```
1   MYTAIPQSGS PFPGSVQDPG LHVWRVEKLK PVPVAQENQG VFFSGDSYLV
51  LHNGPEEVSH LHLWIGQQSS RDEQGACAVL AVHLNTLLGE RPVQHREVQG
101 NESDLFMSYF PRGLKYQEGG VESAFHKTST GAPAAIKKLY QVKGKKNIRA
151 TERALNWDSF NTGDCFILDL GQNIFAWCGG KSNILERNKA RDLALAIRDS
201 ERQGKAQVEI VTDGEEPAEM IQVLGPKPAL KEGNPEEDLT ADKANAQAAA
251 LYKVSDATGQ MNLTKVADSS PFALELLISD DCFVLDNGLC GKIYIWKGRK
301 ANEKERQAAL QVAEGFISRM QYAPNTQVEI LPQGRESPIF KQFFKDWK
```

Table A3.11: Peptide data for heat shock protein β-1

Nominal mass (M_r): **22826**; Calculated pI value: **5.98;** Sequence Coverage: **35%;** Score: **172**
Peptides matched: **6**

Observed	Mr(expt)	Mr(calc)	Delta	Peptides
459.2603	916.506	916.4865	0.0195	K.DGVVEITGK.H
471.248	940.4814	940.4977	-0.0163	R.AQLGGPEAAK.S
538.2837	1074.5528	1074.5669	-0.014	R.QLSSGVSEIR.H
582.3047	1162.5948	1162.6134	-0.0186	R.LFDQAFGLPR.L
595.3182	1782.9328	1782.9152	0.0176	R.VSLDVNHFAPDELTVK.T
953.4852	1904.9558	1904.9843	-0.0285	K.LATQSNEITIPVTFESR.A

```
1   MTERRVPFSL LRGPSWDPFR DWYPHSRLFD QAFGLPRLPE EWSQWLGGSS
51  WPGYVRPLPP AAIESPAVAA PAYSRALSRQ LSSGVSEIRH TADRWRVSLD
101 VNHFAPDELT VKTKDGVVEI TGKHEERQDE HGYISRCFTR KYTLPPGVDP
151 TQVSSSLSPE GTLTVEAPMP KLATQSNEIT IPVTFESRAQ LGGPEAAKSD
201 ETAAK
```

Table A3.12: Peptide data for prostaglandin dehydrogenase 1

Nominal mass (M_r): **29187**; Calculated pI value: **5.56;** Sequence Coverage: **42%;** Score: **535**
Peptides matched: **6**

Observed	Mr(expt)	Mr(calc)	Delta	Peptide
443.7329	885.4512	885.482	-0.0308	K.HGIVGFTR.S
488.2855	974.5564	974.58	-0.0236	R.AFAEALLLK.G
606.8453	1211.676	1211.6985	-0.0225	K.VALVTGAAQGIGR.A
638.2994	1274.5842	1274.6142	-0.03	K.AALDEQFEPQK.T
695.8406	1389.6666	1389.7034	-0.0367	R.SAALAANLMNSGVR.L + Oxidation (M)
756.8662	1511.7178	1511.7943	-0.0764	R.LDILVNNAGVNNEK.N
851.4141	1700.8136	1700.8555	-0.0419	K.VALVDWNLEAGVQCK.A
589.9419	1766.8039	1766.8264	-0.0225	K.GIHFQDYDTTPFQAK.T
612.2953	1833.8641	1833.9043	-0.0402	K.TLFIQCDVADQQQLR.D

```
1   MHVNGKVALV TGAAQGIGRA FAEALLLKGA KVALVDWNLE AGVQCKAALD
51  EQFEPQKTLF IQCDVADQQQ LRDTFRKVVD HFGRLDILVN NAGVNNEKNW
101 EKTLQINLVS VISGTYLGLD YMSKQNGGEG GIIINMSSLA GLMPVAQQPV
151 YCASKHGIVG FTRSAALAAN LMNSGVRLNA ICPGFVNTAI LESIEKEENM
201 GQYIEYKDHI KDMIKYYGIL DPPLIANGLI TLIEDDALNG AIMKITTSKG
251 IHFQDYDTTP FQAKTQ
```

Appendix 4

Raw Data and Computational Details of Protein Expression Validation

Expression values for each sample detected by western blot were determined by densiometric analysis with the Phoretix 2D Expressions software package. Since actin was used as a loading control, the initial protein expression values were corrected for by using a scaling factor determined by the actin expression values. The loading correction values were arrived at in the following manner:

1. For each validation experiment the individual values for each actin loading control were summed.
2. The average was calculated for the actin values within that experiment.
3. Each actin value was divided by the average actin value obtained to give a loading control correction value.
4. The loading control correction value was then multiplied by the original FABP4 or Per6 expression values to arrive at the loading control corrected values.
5. The expression level of a particular group was determined by the numerical average of the corrected values within that group.
6. Standard deviations (σ) were calculated for each average expression level based on the following formula:

$$\sigma = \sqrt{\frac{\Sigma\ [x - \overline{x}]^2}{n - 1}}$$

σ = lower case sigma
Σ = capital sigma
$\overline{x}$ = x bar

Where σ is the standard deviation, X is the measured value, X bar is the mean, and n is the number of values.
(http://www.gcseguide.co.uk/standard_deviation.htm)

7. When calculating the fold regulation values by division of the average expression values, the standard deviation was calculated as follows. If x = y / z , and x is the expression value of the protein, then the standard deviation of x is:

$$\sigma_x = x\sqrt{\frac{\sigma_y^2}{y^2} + \frac{\sigma_z^2}{z^2}}$$

(http://www.who.int/tb/surveillanceworkshop/math_and_excel_functions/measures_of_uncertainty.htm)

8. ANOVA P-values were calculated using the One-Way Analysis of Variance program found at http://faculty.vassar.edu/lowry/anova1u.html

Table A4.1: The raw and calculated expression values for FABP4 in the discovery sample set.

FABP4	Western Blot Sample Number	Placental Sample ID	Raw FABP Expression Levels	Raw Actin Expression Levels	Loading Control Correction Value	Corrected FABP values
Control Under 28 Weeks	1	21-99	794317	12319925	0.69	551501
	2	59-01	7709043	12999885	0.73	5647874
	3	188-04	7476494	12292383	0.69	5179396
	4	46-01	7734059	14012970	0.78	6107771
	5	118-02	12397975	15730948	0.88	10991342
	6	87-02	2172146	17214177	0.97	2107270
		Average Expression Level = 5097526				
		Standard Deviation Of Expression Level = 3624230				
Control Over 28 Weeks	7	28-00	28558599	17739908	0.99	28551790
	8	89-02	35745388	20836523	1.17	41974966
	9	23-99	3759538	18663264	1.05	3954277
	10	5-99	9348856	20404496	1.14	10750519
	11	151-03	35149832	15288768	0.86	30285924
	12	34-01	22264438	18667658	1.05	23423223
		Average Expression Level = 23156783				
		Standard Deviation Of Expression Level = 13833129				
PE Under 28 Weeks	13	39-01	25501879	19345477	1.09	27803323
	14	17-99	33740184	24840157	1.39	47233146
	15	117-02	33364166	32256753	1.81	60652124
	16	174-04	29352038	29566991	1.66	48909191
	17	137-03	33266536	20651020	1.16	38716329
	18	189-04	29352038	22053567	1.24	36480618
		Average Expression Level = 43299122				
		Standard Deviation Of Expression Level = 11451548				
PE Over 28 Weeks	19	3-00	33604013	21309272	1.20	40355696
	20	159-03	35155884	13862039	0.78	27464407
	21	145-03	40910017	14214822	0.80	32772998
	22	141-03	29230444	13429085	0.75	22122129
	23	58-01	29944138	9166149	0.51	15468343
	24	103-02	19833929	8993076	0.50	10052222
		Average Expression Level = 24705966				
		Standard Deviation Of Expression Level = 11174454				

Table A4.2: The raw and calculated expression values for Per6 in the discovery sample set.

Per6	Western Blot Sample Number	Placental Sample ID	Raw Per6 Expression Levels	Raw Actin Expression Levels	Loading Control Correction Value	Corrected Per6 values
PE Under 28 Weeks	1	21-99	14202960	12648028	1.42	20209282
	2	59-01	7709043	9524563	1.07	12005855
	3	188-04	7476494	9929802	1.11	7749313
	4	46-01	7734059	7653465	0.86	5646477
	5	118-02	12397975	11364757	1.27	13062515
	6	87-02	2172146	8936539	1.00	8307658
		Average Expression Level = 11163517				
		Standard Deviation Of Expression Level = 5222873				
PE Over 28 Weeks	7	28-00	6036003	10844188	1.21	7363693
	8	89-02	7668849	8100940	0.91	6988996
	9	23-99	8269850	7554189	0.84	7028047
	10	5-99	7669346	9375726	1.05	8089328
	11	151-03	5718706	6711635	0.75	4317927
	12	34-01	4793816	6690594	0.75	3608238
		Average Expression Level =6232705				
		Standard Deviation Of Expression Level = 1815760				
Control Under 28 Weeks	13	39-01	3943966	5761822	0.64	2556478
	14	17-99	5775690	8142367	0.91	5290585
	15	117-02	7452793	6907372	0.77	5791367
	16	174-04	5622978	4274738	0.48	2704114
	17	137-03	6199263	4150971	0.46	2894936
	18	189-04	8130873	5153371	0.57	4713872
		Average Expression Level = 3991892				
		Standard Deviation Of Expression Level = 1440004				
ControlOver 28 Weeks	19	3-00	6206170	9066249	1.01	6329953
	20	159-03	6422475	10284735	1.15	7430956
	21	145-03	5908594	13092421	1.47	8702686
	22	141-03	5818354	12214687	1.37	7995243
	23	58-01	7168608	10012058	1.12	8074346
	24	103-02	8985547	14939743	1.68	15102083
		Average Expression Level = 8939211				
		Standard Deviation Of Expression Level = 3122789				

Table A4.3: The raw and calculated expression values for FABP4 control samples in the validation sample set.

FABP4 Control Samples Under 28 weeks					
Western Blot Sample Number	**Placental Sample ID**	**Raw FABP Expression Levels**	**Raw Actin Expression Levels**	**Loading Control Correction Value**	**Corrected FABP values**
25	203-04	Not Detected	46870739	0	0
26	101-02A	2579272	39701309	1.74	4500998
27	206-04	9670230	36456888	1.60	15496133
28	250-05	1093170	38116181	1.67	1831487
29	149-03	Not Detected	41151794	0	0
30	219-04	Not Detected	42862978	0	0
31	19-98	15887876	24052987	1.05	16797389
32	238-04	11971214	35157072	1.54	18499408
33	229-04	Not Detected	34896353	0	0
	Average Expression Level = 6347268				
	Standard Deviation Of Expression Level = 8105040				

FABP4 Control Samples Over 28 weeks					
Western Blot Sample Number	**Placental Sample ID**	**Raw FABP Expression Levels**	**Raw Actin Expression Levels**	**Loading Control Correction Value**	**Corrected FABP values**
34	260-03	18731645	32686278	1.43	26912145
35	232-04A	21988138	20238856	0.89	19560563
36	278-06	24201885	20722141	0.91	22044017
37	199-04	27133846	22237533	0.97	26521916
38	152-03A	24505355	23303497	1.02	25100885
39	213-04	28039485	18244759	0.80	22486149
40	211-04	16231398	19416582	0.85	13852738
41	261-05	24498376	18469738	0.81	19888634
42	73-01	30833360	22685956	0.99	30745734
43	256-05	35303813	24020313	1.05	37274104
	Average Expression Level = 24438689				
	Standard Deviation Of Expression Level = 6510942				

Table A4.4: The raw and calculated expression values for FABP4 preeclamptic samples in the validation sample set.

FABP4 Preeclamptic Samples Under 28 Weeks					
Western Blot Sample Number	**Placental Sample ID**	**Raw FABP Expression Levels**	**Raw Actin Expression Levels**	**Loading Control Correction Value**	**Corrected FABP values**
44	236-04	8617758	20115470	0.88	7619586
45	135-03	28466456	20384569	0.89	25505971
46	202-04	32742574	24188054	1.06	34811335
47	241-05	40802110	27775816	1.22	49814570
48	39-01	29289092	20160996	0.88	25955226
49	90-02	30914162	24005761	1.05	32619694
50	17-96	11002118	18065733	0.79	8736527
51	82-01	31397372	19244836	0.84	26559167
52	225-05	40292650	22913948	1.00	40581929
	Average Expression Level = 28022667				
	Standard Deviation Of Expression Level = 13696859				
FABP4 Preeclamptic Samples Over 28 weeks					
Western Blot Sample Number	**Placental Sample ID**	**Raw FABP Expression Levels**	**Raw Actin Expression Levels**	**Loading Control Correction Value**	**Corrected FABP values**
53	57-01	16381377	21723884	0.95	15642091
54	16-00	23434868	20269426	0.89	20879057
55	83-01	29162114	20885978	0.91	26771996
56	91-02	48142502	19427392	0.85	41110248
57	215-04	45223035	18336302	0.80	36448393
58	49-01	40401350	16779765	0.73	29798107
59	163-03	34897976	15522224	0.68	23810094
60	142-03A	Omited Due to Degradation			
61	12-00	48336881	8238763	0.36	17504413
62	25-99	50425535	17221151	0.75	38169777
	Average Expression Level = 27792686				
	Standard Deviation Of Expression Level = 9234250				

Table A4.5: The raw and calculated expression values for Per6 control samples in the validation sample set.

Per6 Control Samples Under 28 weeks					
Western Blot Sample Number	**Placental Sample ID**	**Raw FABP Expression Levels**	**Raw Actin Expression Levels**	**Loading Control Correction Value**	**Corrected FABP values**
25	203-04	14506908	20115470	0.81	11780118
26	101-02A	13167867	20384569	0.82	10835814
27	206-04	12319350	24188054	0.97	12029105
28	250-05	17946745	27775816	1.12	20123203
29	149-03	7571788	20160996	0.81	6162473
30	219-04	6849944	24005761	0.96	6638150
31	19-98	5972356	18065733	0.72	4355578
32	238-04	9887209	19244836	0.77	7681261
33	229-04	12165794	22913948	0.92	11253431
	Average Expression Level = 10095460				
	Standard Deviation Of Expression Level = 4679980				
Per6 Control Samples Over 28 weeks					
Western Blot Sample Number	**Placental Sample ID**	**Raw FABP Expression Levels**	**Raw Actin Expression Levels**	**Loading Control Correction Value**	**Corrected FABP values**
34	260-03	15062216	32686278	1.31	19874625
35	232-04A	11390865	20238856	0.81	9306519
36	278-06	11677976	20722141	0.83	9768925
37	199-04	8194885	22237533	0.89	7356548
38	152-03A	11374113	23303497	0.94	10699986
39	213-04	10440391	18244759	0.73	7689524
40	211-04	12884074	19416582	0.78	10098819
41	261-05	13131315	18469738	0.74	9790695
42	73-01	10874052	22685956	0.91	9958480
43	256-05	13985545	24020313	0.96	13561341
	Average Expression Level = 10810547				
	Standard Deviation Of Expression Level = 3605971				

Table A4.6: The raw and calculated expression values for Per6 preeclamptic samples in the validation sample set.

Per6 Preeclamptic Samples Under 28 Weeks					
Western Blot Sample Number	**Placental Sample ID**	**Raw FABP Expression Levels**	**Raw Actin Expression Levels**	**Loading Control Correction Value**	**Corrected FABP values**
44	236-04	15661989	46870739	1.89	29634207
45	135-03	14654290	39701309	1.60	23486278
46	202-04	12013941	36456888	1.47	17681116
47	241-05	14522254	38116181	1.53	22345393
48	39-01	12952768	41151794	1.66	21517705
49	90-02	13775390	42862978	1.73	23835861
50	17-96	13048240	24052987	0.97	12669677
51	82-01	13125711	35157072	1.41	18628596
52	225-05	11742328	34896353	1.40	16541651
	Average Expression Level = 20704499				
	Standard Deviation Of Expression Level = 4949434				
Per6 Preeclamptic Samples Over 28 weeks					
Western Blot Sample Number	**Placental Sample ID**	**Raw FABP Expression Levels**	**Raw Actin Expression Levels**	**Loading Control Correction Value**	**Corrected FABP values**
53	57-01	12639336	21723884	0.87	11084250
54	16-00	10530376	20269426	0.81	8616480
55	83-01	11647882	20885978	0.84	9820789
56	91-02	14893091	19427392	0.78	11680029
57	215-04	13831364	18336302	0.74	10238147
58	49-01	10107118	16779765	0.67	6846329
59	163-03	14218145	15522224	0.62	8909257
60	142-03A	Omited Due to Degradation			
61	12-00	16867692	8238763	0.33	5609992
62	25-99	19222200	17221151	0.69	13363181
	Average Expression Level = 9574273				
	Standard Deviation Of Expression Level = 2400218				